Identification and Characterization of the Enzymes Involved in Biosynthesis of FAD and Tetrahydromethanopterin in *Methanocaldococcus jannaschii*

Zahra Mashhadi

Dissertation submitted to the faculty of the Virginia Polytechnic Institute and State University in partial fulfillment of the requirements for the degree of

Doctor of Philosophy

In

Biochemistry

Robert H. White, Ph.D. Chairperson
Dennis R. Dean, Ph.D.
Pablo Sobrado, Ph.D.
Marcy Hernick, Ph.D.
Florian D. Schubot, Ph.D.

June 30, 2010

Blacksburg, Virginia

Keywords: *Methanocaldococcus jannaschii*, tetrahydromethanopterin, riboflavin kinase, FAD synthetase

Identification and characterization of the enzymes involved in biosynthesis of FAD and tetrahydromethanopterin in Archaea

Zahra Mashhadi

ABSTRACT

Methanogens belong to the archaeal domain, are anaerobes and produce methane from CO_2 or other simple carbon compounds. Methanogenesis is a key process of the global carbon cycle and methanogens produce about 75-85% of all methane emissions.

Besides the universally occurring coenzymes that are needed in normal metabolic pathways, such as biotin, coenzyme A, thiamine, FAD, PLP, etc.; methanogens need six additional coenzymes that are involved in the methane production pathway: methanofuran, tetrahydromethanopterin, coenzyme F_{420}, coenzyme M, coenzyme B, and coenzyme F_{430}. Although now it is known that some non-methanogenic archaea and bacteria have several of these coenzymes, they are named methanogenic coenzymes since these six coenzymes were first isolated and identified from methanogens.

We are using *Methanocaldococcus jannaschii* as a model organism of methanogens to understand and investigate pathways of coenzymes biosynthesis. Our laboratory is involved in establishing the chemical functions of hypothetical proteins that function in targeted biochemical pathways leading to coenzyme production within the euryarchaeon *M. jannaschii* and identifying their corresponding genes. While there are many coenzymes present in this organism, my focus is on the biosynthetic pathways of tetrahydromethanopterin and FAD.

7,8-Dihydro-D-neopterin 2',3'-cyclic phosphate (H_2N-cP) is the first intermediate in the biosynthesis of the pterin portion of tetrahydromethanopterin (H_4MPT), a C_1 carrier coenzyme. This intermediate is produced from GTP by MptA (MJ0775 gene product), a new class of GTP cyclohydrolase I. An Fe(II)-dependent cyclic phosphodiesterase (MptB, MJ0837 gene product) hydrolyzes the cyclic phosphate of H_2N-cP to a mixture of 7,8-dihydro-D-neopterin 2'-monophosphate and 7,8-dihydro-D-neopterin 3'-monophosphate. MptB requires Fe^{2+} for activity, the same as observed for MptA. Thus the first two enzymes involved in H_4MPT biosynthesis in the Archaea are Fe^{2+} dependent.

In the FAD biosynthetic pathway, the conversion of riboflavin first into FMN and then to FAD is catalyzed by a bifunctional enzyme (RibF) that first acts as a kinase converting riboflavin to FMN in the presence of ATP and then acts as a nucleotidyl transferase using a second ATP to convert the FMN to FAD. Identification of the archaeal CTP-dependent riboflavin kinase, RibK (MJ0056 gene product) led us to identify a archaeal monofunctional FAD synthetase, RibL (MJ1179 gene product). RibL is the only air-sensitive FAD synthetase identified.

ACKNOWLEDGMENTS

I owe my deepest gratitude to my advisor Dr. Robert White for the continuous support of my Ph.D study and research, for his patience, motivation, enthusiasm, and immense knowledge. This dissertation would also not have been possible without the contributions of my laboratory colleagues: Dr. Laura Grochowski and Huimin Xu. I would also like to thank my graduate committee: Drs. Dennis Dean, Pablo Sobrado, Marcy Hernick, Florian Schubot who have been especially helpful and approachable through out my graduate career. Many thanks to Kim Harick and Dr. Keith Ray for their help with protein and compound identification by mass spectroscopy.

In conclusion, I'd like to thank my husband, Hojat Ghandi, and my son, Sina Ghandi, for their great support and sacrificing to a great extent. I'd like to thank my parents Zohreh Faezi and Hossein Mashhadi for valuing education above all else and sacrificing to a great extent that I could have one. Lastly my brother, Mostafa Mashhadi, and many dear friends including, Maryam Kamali, Somayesadat Badieyan, Leyla Nazhandali, Masood Agah and Reza Sohrabi, have been like a family for me and a source of constant support and encouragement.

TABLE OF CONTENTS

TABLE OF FIGURES

CHAPTER 1

CHAPTER 2

CHAPTER 3

CHAPTER 4

CHAPTER 5

CHAPTER 6

TABLE OF TABLES

CHAPTER 2

CHAPTER 4

CHAPTER 5

ABBREVIATIONS

H_2N-cP	7,8-dihydro-D-neopterin 2',3'-cyclic phosphate
H_2N-2'-P	7,8-dihydro-D-neopterin 2'-phosphate
H_2N-3'-P	7,8-dihydro-D-neopterin 3'-phosphate
GTP	guanosine 5'-triphosphate
2',3'-cAMP	adenosine 2',3'-cyclic phosphate
PDE	phosphodiesterase
bis-pNPP	bis(4-nitrophenyl)phosphate
pNPPC	4-nitrophenylphosphoryl choline
TES	*N*-tris(hydroxymethyl)methyl-2-aminoethanesulfonic acid
ICPES	inductively coupled plasma emission spectrophotometry
HEPES	*N*-(2-hydroxyethyl)piperazine-*N*-(2-ethanesulfonic acid)
PAP	purple acid phosphatase
CTP	cytidine 5'-triphosphate
ATP	adenosine 5'-triphosphate
DTT	dithiothreitol
FMN	flavin mononucleotide
FAD	flavin adenine dinucleotide
ES-MS	electrospray mass spectroscopy
EDTA	ethylene diamine tetraacetic acid
AMP	adenosine 5'-monophosphate
PPi	pyrophosphate
FCD	flavin cytidine dinucleotide
GCT	glycerol-3-phosphate cytidylyltransferase
LC-ES-MS	liquid chromatography electrospray mass spectroscopy
TFAA	trifluoroacetic anhydride
TLC	thin layer chromatography
IAA	iodoacetamide
H_2neopterin	7,8-dihydro-D-neopterin
H_2HMP	6-hydroxymethyl-7,8-dihydropterin

cFMN	riboflavin-4,5-cyclic phosphate
TEM	Transmission Electron Microscopy

CHAPTER 1

Methanogens and biosynthesis of methanogenic coenzymes

Life on Earth can be placed into three domains, Archaea, Eukarya, and Bacteria. Prior to 1990 Archaea were classified as a group of Bacteria and were named Archaebacteria. In 1977 Carl Woese claimed that Archaebacteria had a different evolutionary history from other forms of life, which was revealed from a phylogenetic tree based on their ribosomal RNA (rRNA) sequences (*1*). He proposed the three-domain classification of life and put the Archaebacteria in a separate domain, Archaea (*2*). Archaea are single cell organisms that do not have a nucleus or other organelles. Although Archaea and Bacteria differ biochemically and genetically, most of the archaeons have similar size and shape to bacteria and they cannot be differentiated under the microscope. Besides their different rRNA sequence, the differences between Archaea, Bacteria, and Eukarya also include their cell membrane composition. Archaeal cell membranes contain isoprenoids lipids with ether linkages to L-glycerol (*3*) while Bacteria and Eukarya have fatty acids with ester linkage to D-glycerol. Unlike bacteria, archaea do not have peptidoglycan in their cell wall (*4*). Although archaeons are prokaryotes, their replication, transcription, and translation proteins are more similar to eukaryotes than bacteria (*5-7*). Like bacteria, archaea have one RNA polymerase but the protein assemblies and its function in transcription is similar to the Eukaryotic RNA polymerase II (Fig. 1.1) (*8*). The archaeal DNA replication machinery is very similar to that of eukaryotes. Even several structures of components of archaeal replication factors brings important insights for eukaryotic DNA replication mechanism (*9*). All archaeal genome sequences revealed that they have many unique genes not found in other organisms (*6, 10, 11*).

The domain of Archaea presently has five taxonomic phyla, Crenarchaeota, Euryarchaeota, Korarchaeota, Nanoarchaeota, and the recently proposed Thaumarchaeota (*12*). Crenarchaeota and Euryarchaeota are the two main phyla of this domain and contain the most intensively studied organisms. Crenarchaea, thermophilic and thermoacetophilic archaea, are most abundant in marine environments. Euryarchaeota, which includes methanogenic, extremely

halophilic, and some extreme thermophilic archaea, exist in different habitats from hypertermophilic vents to ruminant intestinal tracts.

1.1-Methanogens, biological generators of methane

Methanogenesis, the anaerobic production of methane from CO_2 or other simple carbon compounds such as acetate, is a key process of the global carbon cycle. Methanogens produce about 75-85% of all methane emissions (*13*). The production of methane as a major catabolite is unique to methanogens. The major portion (60-90%) of methane produced by methanogens escapes to the atmosphere and contributes to the greenhouse effect, while the reminder is used by methanotrophs as a carbon and energy source. Archaeons and particularly methanogens are not pathogens (*14*) and they are resistant to most antibiotics (*15*).

Methanogens can be found in many different anaerobic habitats including intestinal tracts of ruminants and termites, marine and freshwater sediments, geothermal areas, and rice field soil. Methanogens have great diversity in both salinity and temperature requirements for growth. There are some methanogens in the *Methanohalophilus* genus that grow well in up to 2.5 M salt concentration (*16*). In contrast some methanogens live in freshwater. Methanogens are anaerobes and they do not grow or produce methane in presence of oxygen. A study of oxygen toxicity in methanogens, including *Methanococcus voltae* and *Methanobacterium thermoautotrophicum*, revealed after they are exposed to O_2 they die within several hours (*17*). There is some evidence of oxygen adaptively in some methanogens. For instance, several studies revealed that some methanogens possess small amount of superoxide dismutases (*18, 19*). Also, it has been shown that when *M. thermoautotrophicum* is exposed to O_2, AMP or GMP binds to the 8-hydroxy of the deazoflavin ring of coenzyme F_{420}, the hydride transfer coenzyme, via a phosphoester linkage and forms F_{390}. This reaction is catalyzed by F_{390} synthetase (*20*), which causes the maximum absorbance of this coenzyme to shift from 420 nm to 390 nm. This factor 390 is not able to react with the F_{420}-dependent dehydrogenase, which is involved in methanogenesis. It is proposed that it is a signal for methanogen cells exposed to oxygen (*21*).

Production of methane by methanogens can occur by three different catabolic pathways: CO_2 reducing pathway, methylotrophic pathway and aceticlastic pathway (Fig. 1.2). The CO_2-

reducing pathway includes four steps of two-electron reductions to convert CO_2 to methane (Fig. 1.2 A) (*22*). The methylotrophic pathway uses compounds that contain methyl groups such as methanol and trimethylamine to produce methane (Fig. 1.2 B). For instance, in absence of H_2 the methylotrophic methanogens use one mole of methanol and oxidize its methyl group to CO_2 and produce six reducing equivalent ([H]). These 6[H] then are used to reduce 3 moles of methanol to 3 moles of methane. The aceticlastic pathway is the acetate degradation pathway (Fig. 1.2 C). In this pathway acetate splits and its carboxyl group is oxidized to CO_2 and its methyl group is reduced to methane. In all of these cases the final formation of methane is catalyzed by methylCoM reductase.

Most methanogens use H_2 as electron source through the activity of hydrogenases, either F_{420}-dependent dehydrogenase or non-F_{420}-dependent dehydrogenase. Methanogens can use either geologically available H_2 or, more commonly, hydrogen produced by other organisms. Some methanogens are able to use formate instead of H_2 (*23, 24*). Most methanogens can only use one or two carbon sources however some strains of *Methanosarcina* can utilize up to seven different substrates.

1.2-Introduction to Methanocaldococcus jannaschii

Methanocaldococcus jannaschii belongs to *Methanocaldococcaceae* family, which are methanogens, in phylum of Euryarchaeota. *M. jannaschii* was originally isolated from a white smoke hydrothermal vent in the bottom of the pacific ocean (*25*). *M. jannaschii* is an hyperthermophile that grows in the temperature range of 48° to 94°C with the optimum growth temperature at 85°C and under the pressure more than 200 atm (*25*). *M. jannaschii* is autotroph and can grow on mineral media supplied with CO_2 and H_2. This methanogen reduces CO_2 to methane by using H_2 as an electron source and uses the energy produced in this process for its growth. This organism uses ammonium and elemental sulfur as nitrogen and sulfur source, respectively. *M. jannaschii* can only use carbon dioxide as carbon source for its methane production. *M. jannaschii* was the first archaea to have its genome sequenced (*26*).

The *M. jannaschii* genome consists of three distinct elements: a main circular chromosome, a large circular extrachromosomal element (ECE) and small ECE. The main circular chromosome, large and small ECEs are predicted to have 1682, 44, and 12 open reading

frames, respectively. According to TIGR database, about 58% of the *M. jannaschii* genes are annotated as hypothetical.

1.3-Unique coenzymes required in methanogesis

Methanogens possess unique coenzymes that are involved in methane production. Methanogenesis requires two sets of coenzymes: C1 carrier coenzymes, which bind to C1-intermediates and electron transferring coenzymes, which transfer electrons to the C1-intermediates in the CO_2 reduction pathway to methane. C1 carrier coenzymes include methanofuran, tetrahydromethanopterin (H_4MPT), factor III (modified B_{12}), coenzyme F_{430}, and coenzyme M (CoM). Electron transferring cofactors include coenzyme F_{420}, *N-7*-mercaptoheptanoyl-O-phospho-L-threonine (H-S-HTP or CoB), and coenzyme F_{430}. The structures of these coenzymes are shown in Figure 1.3. Although it is now known that even some non-methanogenic archaea and bacteria have several of these coenzymes, since these six coenzymes were first isolated and identified from methanogens they are referred to as methanogenic coenzymes. The methanogenic coenzymes were described fifteen years after discovery of the first methanogens (*27*). CoM was discovered and isolated from *Methanobacterium* strain M. O. H. (*28*). The coenzyme F_{420} was first isolated from *Methanobacterium* strain M. O. H. (*29*). In 1978, coenzymes F_{430} and F_{342} (later known as methanopterin) were reported for the first time (*30*). The existence of coenzyme B (CoB) first was notice in *Methanobacterium thermoautotrophicum* and later it was purified from the same organism and its structure was proposed (*31, 32*). Methanofuran was discovered as a formyl carrier in methanogens (*33*). Besides these unique methanogenic coenzymes there are other coenzymes involved in this pathway, such as FMN, FAD, and Coα-[α-(5-hydroxybenzimidazolyl]-cobamide (factor III), which is a B_{12} analog.

In addition to the methanogenic coenzymes, several transition metals such as iron, nickel, cobalt, molybdenum, and tungsten are required by methanogens. These metals are essential for the activity of some enzymes involved in methanogenic pathway (*34, 35*). For instance, methanogens contain several hydrogenases that activate molecular H_2. F_{420}-reducing hydrogenase catalyzes the reduction of F_{420} by transferring a hydride from molecular hydrogen to F_{420}. This F_{420}-reducing hydrogenase is a nickel and iron dependent enzyme (*36*).

1.4-Methanogenic pathway

The methanogenic pathway elucidated by CO_2-reducing methanogens for instance *M. jannaschii* involves six methanogenic coenzyme and distinct enzymes in nine chemical steps. Formylmethanofuran dehydrogenase, the first enzyme acting in methanogenesis pathway catalyzes reversible addition of CO_2 to methanofuran forming a formamide derivative of methanofuran (reaction #1, Fig. 1.3) (*37*). Free formate can not be used by methanogens and in order to utilize formate it should first be oxidized to CO_2 (*38*). The formyl group is then transferred from formylmethanofuran to N^5- of tetrahydromethanopterin (H_4MPT), the second C1 carrier cofactor involved in this pathway. This reaction, reaction #2 shown in Figure 1.3, is catalyzed by formylmethanofuran:H_4MPT formyltransferase and forms methanofuran and N^5-formylH_4MPT (*39*). N^5-Formyltetrahydromethanopterin then undergoes a cyclization to make N^5,N^{10}-methenyltetrahydromethanopterin catalyzed by N^5,N^{10}-methenyltetrahydromethanopterin cyclohydrolase (*40*). The reversible reduction of N^5,N^{10}-methenyltetrahydromethanopterin to N^5,N^{10}-methylenetetrahydromethanopterin, shown in reaction #4, Fig. 1.3, is catalyzed by an F_{420}-dependent methylene-H_4MPT dehydrogenase (*41*). This reduction requires a reduced F_{420} (H_2F_{420}) as a hydride transfer coenzyme. The reduction of oxidized F_{420} generated in this step to the active form of the coenzyme is catalyzed by F_{420}-reducing hydrogenase. There is another non-F_{420}-dependent hydrogenase identified in methanogens, which catalyzes this reversible reduction of reaction #4 (*42*). The next step, the conversion of N^5,N^{10}-methylentetrahydromethanopterin to N^5-methyl-H_4MPT (reaction #5, Fig. 1.3), is catalyzed by F_{420}-dependent methylene-H_4MPT reductase (*43*). This reaction consists of transferring a hydride from H_2F_{420} to N^5,N^{10}-methylene-H_4MPT. The methyl group from the product, methyl-H_4MPT, will then be transferred first to corrionoid factor III (reaction #6, Fig. 1.3) and then to coenzyme M (CoM) (reaction #7, Fig.1.3) (*44, 45*). This methyl transfer chain is coupled with a sodium ion transporting system. The electrochemical sodium ion gradient produced in this step is coupled to a proton gradient, which further drives synthesis of ATP. Methyl-CoM reductase catalyzes the last step of methane production (reaction #8, Fig. 1.3), by reducing the methyl-CoM with CoB to form methane with concurrent formation of a heterodisulfide linkage between CoM and CoB (*46*). There are three unique coenzymes (CoM, CoB, F_{430}) involved in this step. Coenzyme F_{430} is another methanogenic specific coenzyme, which is a nickel porphinoid. For activation of

molecular hydrogen in this step, the cell uses F_{420}-non-reducing hydrogenase. Heterodisulfide reductase then reduces the disulfide bond between CoM and CoB to regenerate the two coenzymes (*47*).

As my Ph.D. project I focused on biosynthesis of two coenzymes in *M. jannaschii*. One methanogenic coenzyme, tetrahydromethanopterin, and one well distributed coenzyme, FAD. Below, I summarized the chemical steps and some gene products known to be involved in biosynthesis of these two coenzymes.

1.5-Biosynthesis of methanopterin

Tetrahydromethanopterin (H_4MPT) is the C1 carrier coenzyme involved in the second through sixth steps of methanogenesis, at the methenyl, methylene, and methyl level (*48*). This coenzyme carries the formyl group, derived from CO_2, through the reduction reactions to get to the methyl group (Fig. 1.3). In methanogens, H_4MPT also serves as a substitute cofactor for many of the enzymes where the canonical C1 carrier coenzyme, folate, would function since most methanogens do not have folate (*49-51*). The one known exception to this rule is *Methanosarcina barkeri* that possesses several gene products, which are tetrahydrofolate-specific enzymes (*52*).

Methanopterin was first reported as factor F_{342} (*53*) and was later identified as a pterin derivative (*54*). In 1984 the structure of methanopterin was established (*55*). Homologs of first established methanopterin structure are known with several modifications including methylation of different sites of the pterin ring or different modifications of the coenzymes side chain (*56*).

The biosynthesis of H_4MPT starts with GTP, which serves as precursor for the formation of the pterin ring. 4-Aminobenzoic acid is a precursor to the arylamine (5-(4-aminophenyl)-1,2,3,4-tetrahydroxypentane) portion of the final structure (Fig. 1.4). By condensation of the products of these separate pathways the functional portion of this coenzyme is generated (*57*). A final series of reactions then form the biologically active coenzyme, H_4MPT. The structure of the H_4MPT, especially in the functional portion, is similar to that of 5,6,7,8-tetrahydrofolate (H_4folate). Both of these coenzymes are active in their reduced form, H_4MPT and H_4folate (Fig. 5.1), and the C-6 of the reduced pterin ring in both has the same stereochemistry (*58, 59*).

1.6-Formation of the Pterin ring of tetrahydromethanopterin

Despite the fact that the structure of folate and methanopterin are similar and the cell extracts of methanogens readily converted GTP to 6-hydroxy-7,8-dihydropterin, as occurs in the bacterial biosynthetic pathway of the pterin portion of folates, methanogenic archaea do not possess the homologs for the genes of folate biosynthetic enzymes. Although the precursor, GTP, and the final product of the pathways, 6-hydroxymethyl dihydropterin pyrophosphate, are the same for both folate and methanopterin pathways the intermediates and genes producing the enzymes involved in these pathways are different. For example, unlike the bacterial pathway for biosynthesis of folate that has 7,8-dihydroneopterin 3'-triphosphate as the first intermediate, 7,8-dihydroneopterin 2'3'-cyclic phosphate (H_2neopterin-cP) serves as the first intermediate in archaeal pterin biosynthesis (*60*). Also, archaea do not have homologs of *E. coli* genes, *fol*E, *fol*B, and *fol*K, responsible to produce GTP cyclohydrolase I, dihydroneoptedin aldolase, and 6-hydroxymethyldihydroneopterin pyrophosphokinase, respectively. These enzymes are involved in the formation of 6-hydroxydihydropterin pyrophosphate (Fig. 5.2).

The first enzyme involved in the archaeal methanopterin biosynthetic pathway is MptA, coded by the MJ0775 gene in *M. jannaschii*, which is a new type of GTP cyclohydrolase (*61*). MptA catalyzes the conversion of GTP to H_2neopterin-cP while the GTP cyclohydrolase I (GTPCHI) that is found in bacteria produces 7,8-dihydroneopterin 3'-triphosphate. Unlike bacterial GTPCHI as well as other GTP cylohydrolases that require Zn^{2+} for activity, MptA requires Fe^{2+}.

The H_2neopterin-cP is subsequently hydrolyzed to either 7,8-dihydroneopterin 2'-phosphate (H_2N-2'P) or 7,8-dihydroneopterin 3'-phosphate (H_2N-3'P) by the activity of MptB, coded by MJ0837 gene in *M. jannaschii* (Fig. 1.4) (*62*). *M. jannaschii* cell free extracts readily converts both H_2N-2'P and H_2N-3'P to 7,8-dihydroneopterin (H_2neopterin). The utilization of Fe^{2+} by the anaerobic methanogens and not by the aerobic analogs of this enzyme likely relates to the availability of the soluble, reduced form of iron present in methanogen habitats. Based on a chemical speciation study, Fe^{2+} concentration in the hydrothermal vents is about 700 μM (*63*). We currently have no genomic leads for the non-orthologous replacements for H_2neopterin aldolase (FolB) (*64*) and 6-hydroxymethyldihydropterin pyrophosphokinase (FolK) catalyzing

two consecutive reactions to produce 6-hydroxymethyl H_2pterin and 6-hydroxymethyl H_2pterin pyrophosphate (Fig. 1.4).

1.7-Early steps in riboflavin biosynthetic pathways to form 5-amino-6-ribitylamino-2,4(1H,3H)-pyrimidinedione (ARP)

Like in H_4MPT biosynthesis, GTP serves as the precursor for making riboflavinand F_{420}. In this section biosynthesis of 5-amino-6-ribitylamino-2,4(*1H*,3*H*)-pyrimidinedione (ARP), which is an intermediate in riboflavin biosynthetic pathway and also a precursor for the coenzyme F_{420} will be briefly reviewed. RibA, GTP cyclohydrolase II, is the first enzyme involved in the established riboflavin biosynthetic pathway in bacteria (reaction #11, Fig. 1.5). Analysis of archaeal genomes has generally shown the absence of *rib*A. In archaea conversion of GTP to compound 3 (Fig. 1.5) is done in two consecutive reactions catalyze by ArfA and ArfB (reactions #1 and #2). ArfA, archaeal GTP cyclohydrolase III, is coded by the MJ0145 gene in *M. jannaschii* and converts GTP to 2-amino-5-formylamino-6-ribosylamino-4(3*H*)-pyrimidinone 5'-monophosphate (FAPy). In the next reaction FAPy is converted to compound 3 by activity of ArfB, coded by the MJ0116 gene in *M. jannaschii*. The deamination (reaction 12) and the dehydrogenation (reaction 13) steps, which convert compound 3 to compound 5, are catalyzed by a bifunctional enzyme (RibD) in bacteria (blue arrows route, Fig. 1.5) (*65*) and by two separate enzymes in plants (*66, 67*). It has been shown that some bacteria have a monofunctional reductase as well as a bifunctional enzyme. But in fungi and archaea these two steps occur in the reverse order and are catalyzed by two separate enzymes (*68*). ArfC, coded by the MJ0671 in *M. jannaschii*, is the archaeal enzyme that catalyzes the reduction of the ribose ring of compound 3 to compound 4 (*69*). ArfC and its homologs in other archaea have good sequence similarity with the N-terminal section of RibD that contains the reductase active site (*66*). Compound 4 is then converted into 5-amino-6-ribitylamino-2,4(1H,3H)-pyrimidinedione (ARP, compound 6 in Fig. 1.5) by the sequential action of a deaminase at C-2 of the pyrimidine to produce 5-amino-6-ribitylamino-2,4(1*H*,3*H*)-pyrimidinedione (compound 5, Fig. 1.5) and a phosphatase. These two steps are like eukaryotic pathway (*67*). However there are no homologs of C-terminal, deaminase portion, of RibD in the archaea and the enzymes involved in these last two steps have not yet been identified.

1.8-Pathway for conversion APR to riboflavin

This part of the pathway starts by converting the ribulose 5-phosphate (compound 7) to formate and 3,4-dihydroxy-2-butanone 4-phosphate (compound 8, Fig. 1.5) catalyzed by RibB, coded by MJ0055 in *M. jannaschii* (White, R. H., unpublished results). Condensation of compound 8 and ARP is catalyzed by RibE and its archaeal homologs, the gene product of MJ0303 in *M. jannaschii*, to form 6,7-dimethyl-8-ribityllumazine (compound 9, Fig. 1.5). Riboflavin synthase, RibC, and it is archaeal homologs (MJ1184 gene product in *M. jannaschii*) use two molecules of compound 9 to produce one molecule of riboflavin and also one molecule of ARP. There is a fundamental difference in the stereochemistry of the pentacyclic intermediate involved in this latter step in archaeal pathway compare to established pathway in other organisms (*70*).

Riboflavin is converted finally to FMN and FAD via consecutive phosphorylation and adenylation. Two different groups of enzymes are known to be involved in the conversion of riboflavin first to FMN and then to FAD. In one group, the conversion of riboflavin to FMN, the phosphorylation reaction, and then to FAD, the adenylation reaction, is catalyzed by a bifunctional enzyme (RibF) (*71, 72*). In the other group, these reactions are catalyzed by two separate enzymes, riboflavin kinase also refer to as RibR, flavokinase, or FMN1 (*73, 74*) and FAD synthetase (FAD1 in yeast) (*75*). In both cases ATP serves as the phosphoryl and adenylyl donor. There are no homologus genes encoding for any of these enzyme in the archaea. There are, however, two monofunctional enzymes in the archaea that catalyzed these consecutive reactions first forming FMN and then FAD. RibK is the archaeal riboflavin kinase and is unique due to using CTP as phosphate donor (*76*). The structure of this protein is similar to the other riboflavin kinases but its primary sequence is more similar to some transcription factors (*77*).

1.8-Conclusion

Genomic projects aim to determine the complete genome sequence of an organism. It is often reported that the goal of sequencing a genome is to obtain information about the complete set of genes in any particular genome. Knowing the genes in any genome organism without knowing their particular function is not very helpful. Identifying the exact biochemical function of each gene product is an important scientific endeavor in this post genomics age. The metabolic diversity present in organisms of all three domains of life can be concluded after identification of how the many unknown gene products function. Defining function of every gene, no matter from which organism, has a significant advantage.

As a member of Dr. Robert White laboratory, I focused on biosynthetic reactions in a methanogenic archaeon, *M. jannaschii*, to identify and characterize genes involved in coenzyme biosynthesis. Knowledge about function of gene products in *M. jannaschii* as a methanogen can be applied to a diverse range of disciplines from reducing greenhouse gas emission to efficiently producing methane energy sources from anthropogenic wastes. Worldwide, methanogenic archaea produce more than 400 million tones of the greenhouse gas, methane, each year as an essential part of the global carbon cycle (*78*). Consequently, an understanding of the chemistry and biochemistry of methanogenic coenzymes is essential for our understanding of global carbon flux.

Study of the functional genomics of *M. jannaschii* is also very productive because of the following reasons. Because *M. jannaschii* is an autotrophic and lithotrophic microorganism—able to grow on only hydrogen, CO_2, and mineral ions—its genome includes the genetic information needed to sustain life using only inorganic precursors. *M. jannaschii* can be grown to high cell densities to supply cell extracts necessary for biochemical analyses (*79*). Since *M. jannaschii* is a hyperthermophile (*25*), purification of its heterologously produced proteins that are typically stable to heating at temperatures that denature most native *E. coli* enzymes (>70 °C), facilitating purification, activity assays, and X-ray structural analysis.

The metabolism of *M. jannaschii,* as well as that of other methanogens has not been studied as extensively as that of other organisms. Based on my search of the TIGR database about 58% of the *M. jannaschii* genes are annotated as hypothetical. The *M. jannaschii* genome sequence revealed that about 19% of the encoded proteins, mostly involved in biosynthesis of the

methanogenic coenzymes, are archaeal specific. Identifying and characterizing these genes may lead to the discovery of new pathways and new biological functions different from what is already known.

1.9 FIGURES

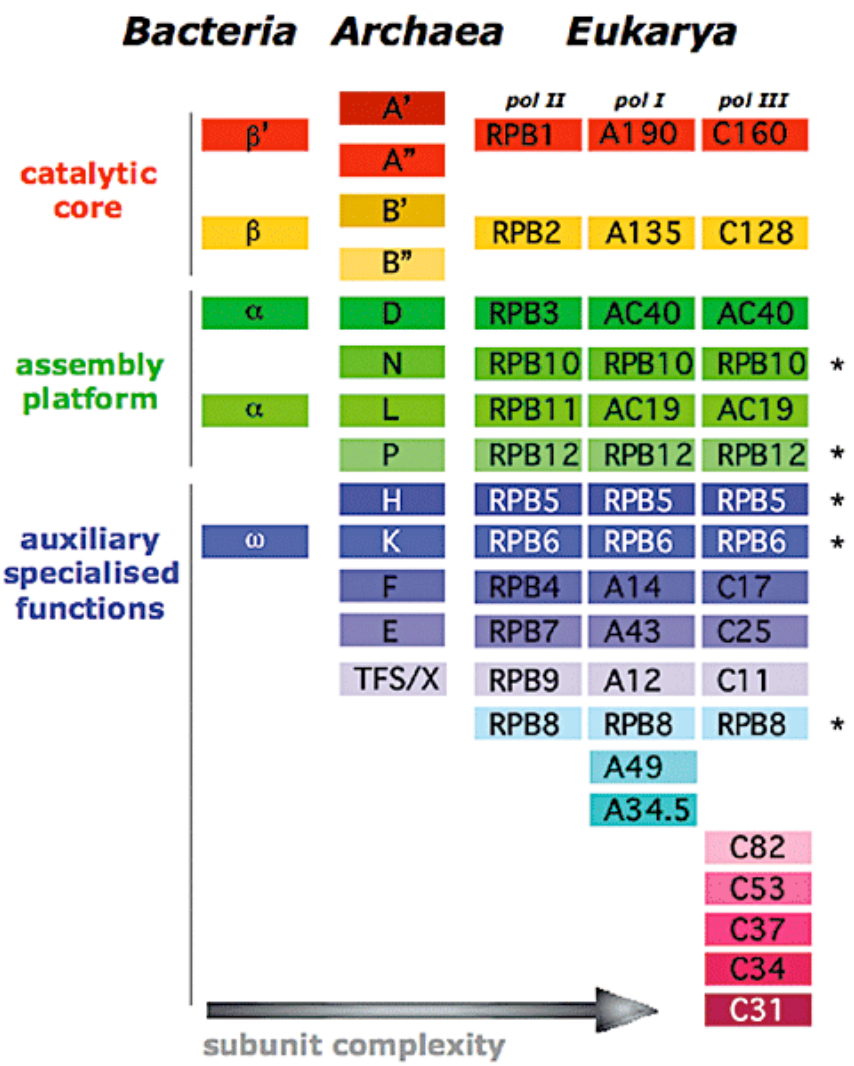

Figure 1.1 Subunits of RNA polymerase in the three domains of life.

The closer the colors match, the higher the homology. Conservation of the subunits throughout the three eukaryotic RNA polymerases is shown with an asterisk. Reprinted with permission from John Wiley and Sons (Werner Finn, 2007).

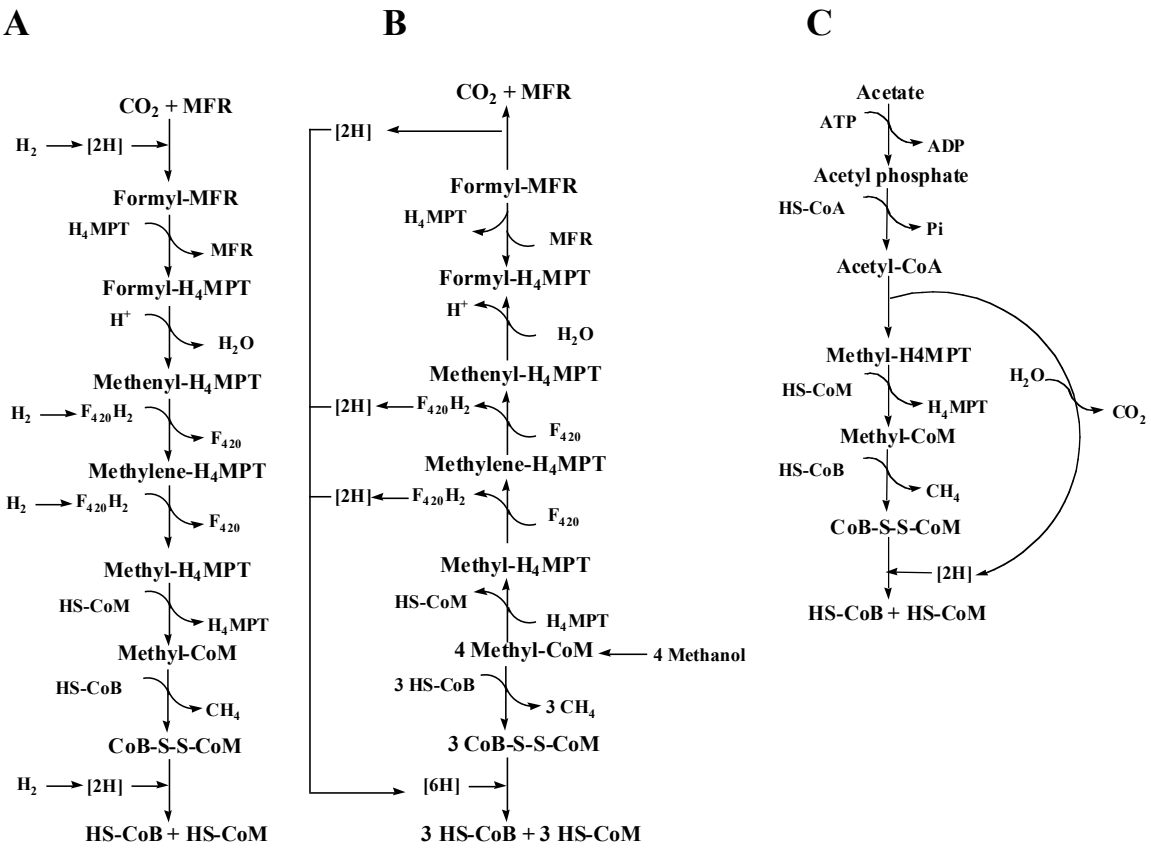

Figure 1.2 Different methanogenic pathways.

A) The pathway used by CO_2-reducing methanogens. B) The pathway used by methylotrophic methanogens. C) The pathway used by aceticlastic methanogens.

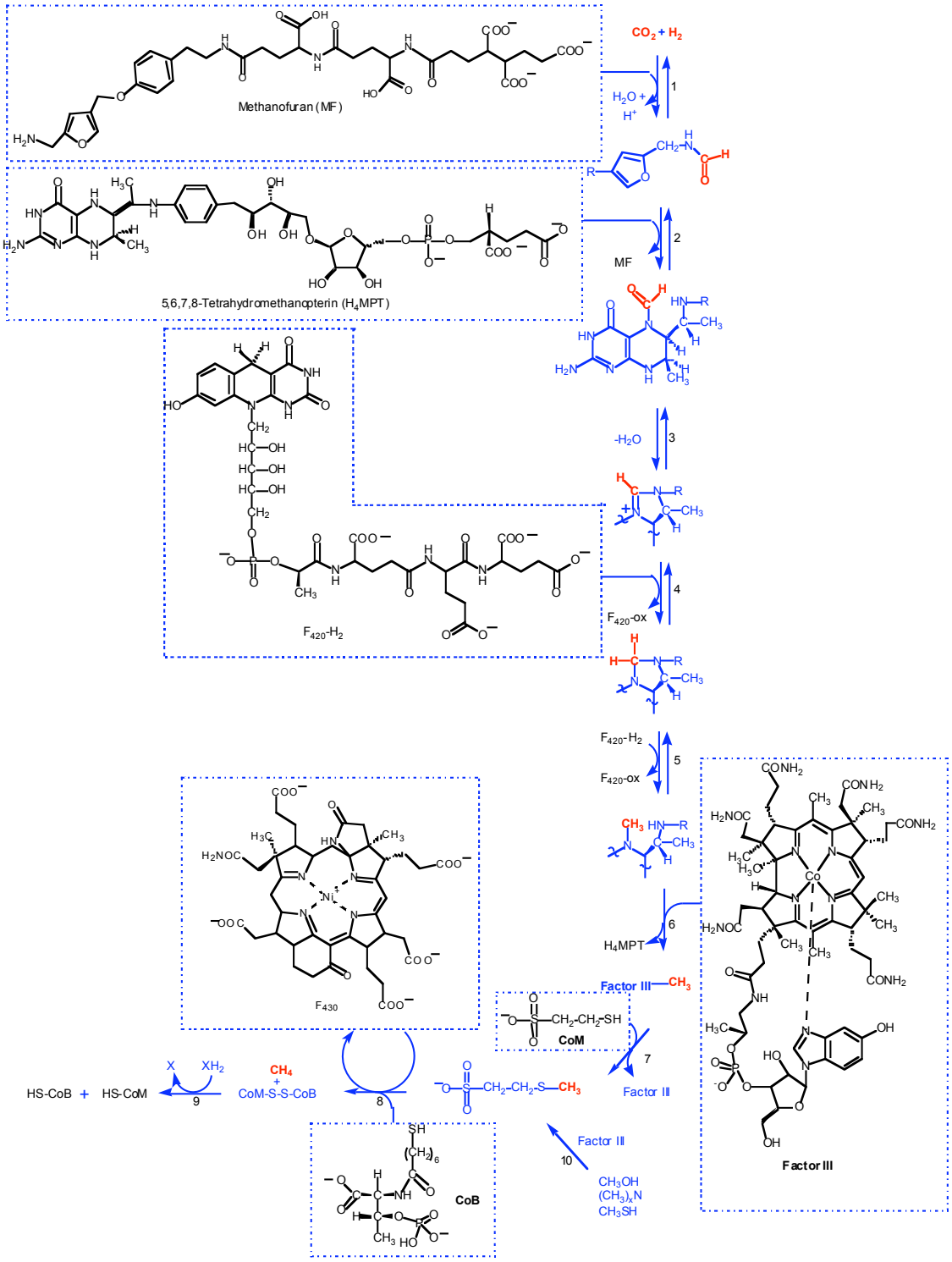

Figure 1.3 The methanogenic pathway and the structures of the coenzymes involved.

The pathway is shown in blue and coenzymes involved in the pathway are boxed.

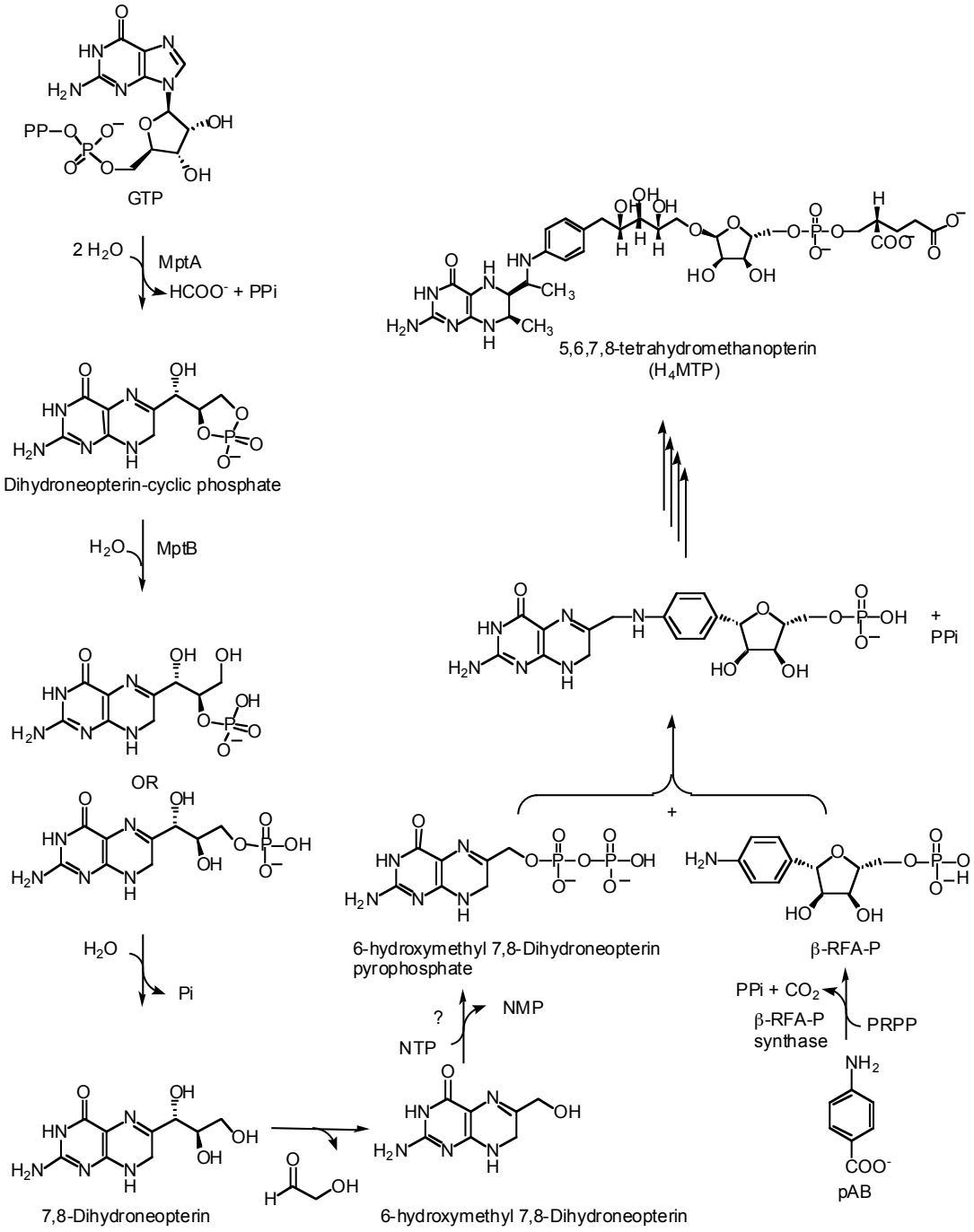

Figure 1.4 Proposed pathway for biosynthesis of the tetrahydromethanopterin

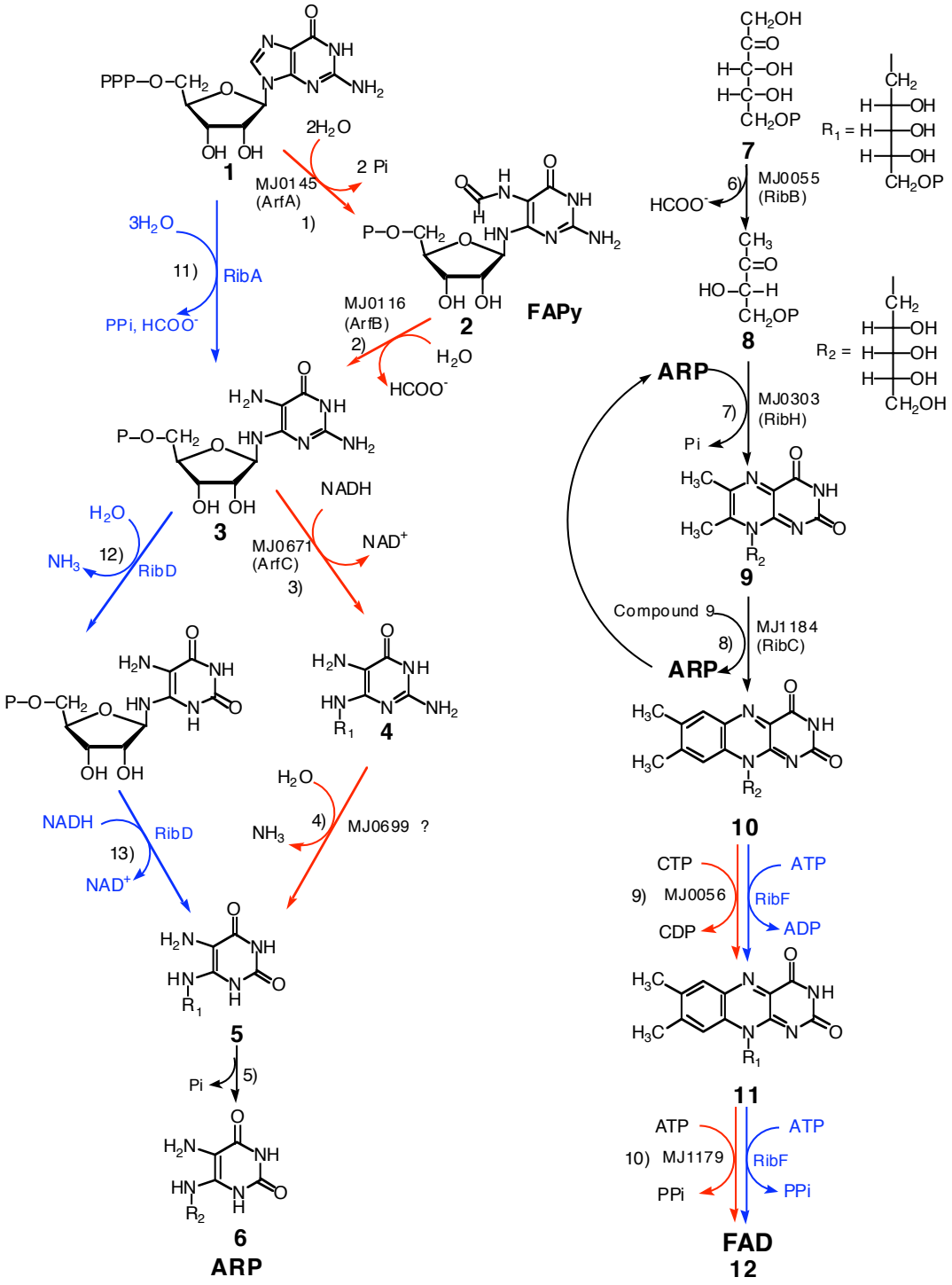

Figure 1.5 Biosynthetic pathway of FAD.

Blue arrows indicate the bacterial route and red arrows indicate archaeal route.

REFERENCES

(1) Woese, C. R., and Fox, G. E. (1977) Phylogenetic structure of the prokaryotic domain: the primary kingdoms. *Proc. Natl. Acad. Sci. U. S. A. 74*, 5088-90.

(2) Woese, C. R., Kandler, O., and Wheelis, M. L. (1990) Towards a natural system of organisms: proposal for the domains Archaea, Bacteria, and Eucarya. *Proc. Natl. Acad. Sci. U. S. A. 87*, 4576-9.

(3) De Rosa, M., Gambacorta, A., and Gliozzi, A. (1986) Structure, biosynthesis, and physicochemical properties of archaebacterial lipids. *Microbiol. Rev. 50*, 70-80.

(4) Kandler, O., and Konig, H. (1998) Cell wall polymers in Archaea (Archaebacteria). *Cell. Mol. Life Sci. 54*, 305-8.

(5) Cann, I. K., and Ishino, Y. (1999) Archaeal DNA replication: identifying the pieces to solve a puzzle. *Genetics 152*, 1249-67.

(6) Andrade, M. A., Ouzounis, C., Sander, C., Tamames, J., and Valencia, A. (1999) Functional classes in the three domains of life. *J. Mol. Evol. 49*, 551-7.

(7) Kyrpides, N. C., and Ouzounis, C. A. (1999) Transcription in archaea. *Proc. Natl. Acad. Sci. U S A 96*, 8545-50.

(8) Werner, F. (2007) Structure and function of archaeal RNA polymerases. *Mol. Microbiol. 65*, 1395-404.

(9) Barry, E. R., and Bell, S. D. (2006) DNA replication in the archaea. *Microbiol. Mol. Biol. Rev. 70*, 876-87.

(10) Glansdorff, N. (1999) On the origin of operons and their possible role in evolution toward thermophily. *J. Mol. Evol. 49*, 432-8.

(11) Kyrpides, N., Overbeek, R., and Ouzounis, C. (1999) Universal protein families and the functional content of the last universal common ancestor. *J. Mol. Evol. 49*, 413-23.

(12) Brochier-Armanet, C., Boussau, B., Gribaldo, S., and Forterre, P. (2008) Mesophilic Crenarchaeota: proposal for a third archaeal phylum, the Thaumarchaeota. *Nat. Rev. Microbiol. 6*, 245-52.

(13) T. Fenchel, G. M. K., and T.H. Blackburn. (1998) Bacterial biogeochemistry : the ecophysiology of mineral cycling, pp 307, Academic Press, San Diego.

(14) Scanlan, P. D., Shanahan, F., and Marchesi, J. R. (2008) Human methanogen diversity and incidence in healthy and diseased colonic groups using *mcrA* gene analysis. *BMC Microbiol. 8*, 79.

(15) Amils, R., Cammarano, P., and Londei, P. (1993) Translation in archaea, in *The Biochemistry of Archaea (Archaebacteria)* (Kates, M., Kushner, D.J., Matheson A.T., Ed.) pp 393-438, Esevier.

(16) Paterek, J. R., Smith, P. H. (1988) *Methanohalophilus mahii* gen. nov., sp. nov., a methylotrophic halophilic methanogen. *Int. J. Syst. Bacteriol. 38*, 122–123.

(17) Kiener, A., and Leisinger, T.,. (1983) Oxygen sensitivity of methanogenic bacteria. *Syst. Appl. Microbiol.*, 305-312.

(18) Kirby, T. W., Lancaster, J. R., Jr., and Fridovich, I. (1981) Isolation and characterization of the iron-containing superoxide dismutase of *Methanobacterium bryantii*. *Arch. Biochem. Biophys. 210*, 140-8.

(19) Brioukhanov, A., Netrusov, A., Sordel, M., Thauer, R.K., and Shima S. (2000) Protection of *Methanosarcina barkeri* against oxidative stress: identification and characterization of an iron superoxide dismutase.
. *Arch. Microbiol. 174*, 213-216.
(20) Vermeij, P., van der Steen, R. J., Keltjens, J. T., Vogels, G. D., and Leisinger, T. (1996) Coenzyme F_{390} synthetase from *Methanobacterium thermoautotrophicum* Marburg belongs to the superfamily of adenylate-forming enzymes. *J. Bacteriol. 178*, 505-10.
(21) Hausinger, R. P., Orme-Johnson, W. H., and Walsh, C. (1985) Factor 390 chromophores: phosphodiester between AMP or GMP and methanogen factor 420. *Biochemistry 24*, 1629-33.
(22) Rouviere, P. E., and Wolfe, R. S. (1988) Novel biochemistry of methanogenesis. *J. Biol. Chem. 263*, 7913-6.
(23) Boone, D. R., Johnson, R. L., and Liu, Y. (1989) Diffusion of the Interspecies Electron Carriers H_2 and Formate in Methanogenic Ecosystems and Its Implications in the Measurement of K_m for H_2 or Formate Uptake. *Appl. Environ. Microbiol. 55*, 1735-1741.
(24) Thiele, J. H., and Zeikus, J. G. (1988) Control of Interspecies Electron Flow during Anaerobic Digestion: Significance of Formate Transfer versus Hydrogen Transfer during Syntrophic Methanogenesis in Flocs. *Appl. Environ. Microbiol. 54*, 20-29.
(25) Jones, W. J., Leigh, J. A., Mayer, F., Woese, C. R., and Wolfe, R. S. (1983) *Methanococcus jannaschii* sp. nov., an extremely thermophilic methanogen from a submarine hydrothermal vent. *Arch. Microbiol. 136*, 254-261.
(26) Bult, C. J., White, O., Olsen, G. J., Zhou, L., Fleischmann, R. D., Sutton, G. G., Blake, J. A., FitzGerald, L. M., Clayton, R. A., Gocayne, J. D., Kerlavage, A. R., Dougherty, B. A., Tomb, J. F., Adams, M. D., Reich, C. I., Overbeek, R., Kirkness, E. F., Weinstock, K. G., Merrick, J. M., Glodek, A., Scott, J. L., Geoghagen, N. S., and Venter, J. C. (1996) Complete genome sequence of the methanogenic archaeon, *Methanococcus jannaschii*. *Science 273*, 1058-73.
(27) Schnellen, C. G. T. P. (1947) Onderzoekingen over der methaangisting. *Thesis, Technical University, Delf*.
(28) McBride, B. C., and Wolfe, R. S. (1971) A new coenzyme of methyl transfer, coenzyme M. *Biochemistry 10*, 2317-24.
(29) Cheeseman, P., Toms-Wood, A., and Wolfe, R. S. (1972) Isolation and properties of a fluorescent compound, factor 420 , from Methanobacterium strain M.o.H. *J. Bacteriol. 112*, 527-31.
(30) Daniels, L., and Zeikus, J. G. (1978) One-carbon metabolism in methanogenic bacteria: analysis of short-term fixation products of $^{14}CO_2$ and $^{14}CH_3OH$ incorporated into whole cells. *J. Bacteriol. 136*, 75-84.
(31) Gunsalus, R. P., and Wolfe, R. S. (1980) Methyl coenzyme M reductase from *Methanobacterium thermoautotrophicum*. Resolution and properties of the components. *J. Biol. Chem. 255*, 1891-5.
(32) Noll, K. M., Rinehart, Jr, K. L., Tanner, R. S., and Wolfe, R. S, . (1986) Structure of component B (7-mercaptoheptanoylthreonine phosphate) of the methylcoenzyme M methylreductase system of *Methanobacterium thermoautotrophicum*. *Proc. Natl. Acad. Sci. U S A 83*, 4238–4242.

(33) Leigh, J. A., Rinehart, K. L., Jr., and Wolfe, R. S. (1985) Methanofuran (carbon dioxide reduction factor), a formyl carrier in methane production from carbon dioxide in Methanobacterium. *Biochemistry 24*, 995-9.
(34) Schonheit, P., Moll, J., and Thauer, R. K. (1979) Nickel, cobalt, and molybdenum requirement for growth of *Methanobacterium thermoautotrophicum*. *Arch. Microbiol. 123*, 105-7.
(35) Winter, J., Lerp, C., Zabel, H. P., Wildnauer, F. X., Konig, H., and Schindler, F. . (1984) *Methanobacterium wolfei*, sp. nov., a new tungsten-requiring, thermophilic, autotrophic methanogen. *System. Appl. Microbiol.*, 457-466.
(36) Fox, J. A., Livingston, D. J., Orme-Johnson, W. H., and Walsh, C. T. (1987) 8-Hydroxy-5-deazaflavin-reducing hydrogenase from *Methanobacterium thermoautotrophicum*: 1. Purification and characterization. *Biochemistry 26*, 4219-27.
(37) Karrasch, M., Borner, G., Enssle, M., and Thauer, R. K. (1989) Formylmethanofuran dehydrogenase from methanogenic bacteria, a molybdoenzyme. *FEBS Lett. 253*, 226-30.
(38) Sparling, R., and Daniels, L. (1986) Source of carbon and hydrogen in methane produced from formate by *Methanococcus thermolithotrophicus*. *J. Bacteriol. 168*, 1402-7.
(39) Donnelly, M. I., and Wolfe, R. S. (1986) The role of formylmethanofuran: tetrahydromethanopterin formyltransferase in methanogenesis from carbon dioxide. *J. Biol. Chem. 261*, 16653-9.
(40) Donnelly, M. I., Escalante-Semerena, J. C., Rinehart, K. L., Jr., and Wolfe, R. S. (1985) Methenyl-tetrahydromethanopterin cyclohydrolase in cell extracts of Methanobacterium. *Arch. Biochem. Biophys. 242*, 430-9.
(41) Schwörer, B. a. R. K., Thauer (1991) Activities of formylmethanofuran dehydrogenase, methylenetetrahydromethanopterin dehydrogenase, methylenetetrahydromethanopterin reductase, and heterodisulfide reductase in methanogenic bacteria. *Arch. Microbiol. 155*, 459-465.
(42) McGlynn, S. E., Boyd, E. S., Shepard, E. M., Lange, R. K., Gerlach, R., Broderick, J. B., and Peters, J. W. (2010) Identification and characterization of a novel member of the radical AdoMet enzyme superfamily and implications for the biosynthesis of the Hmd hydrogenase active site cofactor. *J. Bacteriol. 192*, 595-8.
(43) te Brömmelstroet, B. W., Hensgens, C. M., Keltjens, J. T., van der Drift, C. and Vogels, G. D. . (1990) Purification and properties of 5,10-methylenetetrahydromethanopterin reductase, a coenzyme F_{420}-dependent enzyme, from *Methanobacterium thermoautotrophicum* strain _H. *J. Biol. Chem. 265*, 1852-1857.
(44) Chris M. Poirot, S. M. K., Erik Valk, Jan T. Keltjens, Chris Drift, Godfried D. Vogels. (1987) Formation of methylcoenzyme M from formaldehyde by cell-free extracts of *Methanobacterium thermoautotrophicum*. Evidence for the involvement of a corrinoid-containing methyltransferase. *FEMS Microbiol. Lett. 40*, 7-13.
(45) Kengen, S. W., Daas, P. J., Duits, E. F., Keltjens, J. T., van der Drift, C., and Vogels, G. D. (1992) Isolation of a 5-hydroxybenzimidazolyl cobamide-containing enzyme involved in the methyltetrahydromethanopterin: coenzyme M methyltransferase reaction in *Methanobacterium thermoautotrophicum*. *Biochim. Biophys. Acta 1118*, 249-60.
(46) Ellermann, J., Rospert, S., Thauer, R. K., Bokranz, M., Klein, A., Voges, M., and Berkessel, A. (1989) Methyl-coenzyme-M reductase from *Methanobacterium thermoautotrophicum* (strain Marburg). Purity, activity and novel inhibitors. *Eur. J. Biochem. 184*, 63-8.

(47) Metcalf, N. R. B. a. W. W. (2009) Methanogenesis by Methanosarcina acetivorans involves two structurally and functionally distinct classes of heterodisulfide reductase. *Mol. Microbiol. 75*, 843 - 853.
(48) Escalante-Semerena, J. C., Rinehart, K. L., Jr., and Wolfe, R. S. (1984) Tetrahydromethanopterin, a carbon carrier in methanogenesis. *J. Biol. Chem. 259*, 9447-55.
(49) Worrell, V. E., and Nagle, D. P., Jr. (1988) Folic acid and pteroylpolyglutamate contents of archaebacteria. *J. Bacteriol. 170*, 4420-3.
(50) White, R. H. (1993) Structures of the modified folates in the thermophilic archaebacteria *Pyrococcus furiosus*. *Biochemistry 32*, 745-53.
(51) Delle Fratte, S., White, R. H., Maras, B., Bossa, F., and Schirch, V. (1997) Purification and properties of serine hydroxymethyltransferase from *Sulfolobus solfataricus*. *J. Bacteriol. 179*, 7456-7461.
(52) Buchenau, B., and Thauer, R. K. (2004) Tetrahydrofolate-specific enzymes in *Methanosarcina barker*i and growth dependence of this methanogenic archaeon on folic acid or *p*-aminobenzoic acid. *Arch. Microbiol. 182*, 313-25.
(53) Gunsalus, R. P. W. R. S. (1978) Chromophoric factors F342 and F430 of Methanobacterium thermoautotrophicum. *FEMS Microbiol. Lett. 3*, 191-193.
(54) Keltjens, J. T., Huberts, M. J., Laarhoven, W. H., Vogels, G. D. . (1983) Structural Elements of Methanopterin, a Novel Pterin : Present in *Methanobacterium thermoautotrophicum*. *Eur. J. Biochem. 130*, 537-544.
(55) Patrick BEELEN, A. P. M. S., Johannes W. G. BOSCH, Godfried D. VOGELS, Willem GUIJT, Cornelis A. G. HAASNOOT. (1984) Elucidation of the structure of methanopterin, a coenzyme from *Methanobacterium thermoautotrophicum*, using two-dimensional nuclear-magnetic-resonance techniques. *Eur. J. Biochem. 138*, 563-571.
(56) White, R. H. (1997) Structural characterization of modified folates in Archaea. *methods in enzymology 281*, 391-401.
(57) Xu, H., Aurora, R., Rose. G.D., and White, R.H. (1999) Identifying two ancient enzymes in Archaea using predicted secondary structure alignment. *Nature Structural Biology 6*, 750-754.
(58) White, R. (1996) Absolute stereochemistry of methanopterin and 5,6,7,8-tetrahydromethanopterin *Chirality 8*, 332-340.
(59) Schleucher, J., Schwörer, B., Zirngibl, C., Koch, U., Weber, W., Egert, E., Thauer, R. K., Griesinger, C. (1992) Determination of the relative configuration of 5,6,7,8-tetrahydromethanopterin by two-dimensional NMR spectroscopy. *FEBS Lett. 314*, 440-444.
(60) Howell, D. M., and White, R. H. (1997) D-*erythro*-neopterin biosynthesis in the methanogenic archaea *Methanococcus thermophila* and *Methanobacterium thermoautotrophicum* ΔH. *J. Bacteriol. 179*, 5165-70.
(61) Grochowski, L. L., Xu, H., Leung, K., and White, R. H. (2007) Characterization of an Fe^{2+}-dependent archaeal-specific GTP cyclohydrolase, MptA, from *Methanocaldococcus jannaschii*. *Biochemistry 46*, 6658-67.
(62) Mashhadi, Z., Xu, H., and White, R. H. (2009) An Fe^{2+}-dependent cyclic phosphodiesterase catalyzes the hydrolysis of 7,8-dihydro-D-neopterin 2',3'-cyclic phosphate in methanopterin biosynthesis. *Biochemistry 48*, 9384-92.

(63) Luther, G. W., 3rd, Rozan, T. F., Taillefert, M., Nuzzio, D. B., Di Meo, C., Shank, T. M., Lutz, R. A., and Cary, S. C. (2001) Chemical speciation drives hydrothermal vent ecology. *Nature 410*, 813-6.
(64) Wang, Y., Li, Y., and Yan, H. (2006) Mechanism of dihydroneopterin aldolase: functional roles of the conserved active site glutamate and lysine residues. *Biochemistry 45*, 15232-9.
(65) Magalhaes, M. L., Argyrou, A., Cahill, S. M., and Blanchard, J. S. (2008) Kinetic and mechanistic analysis of the *Escherichia coli* ribD-encoded bifunctional deaminase-reductase involved in riboflavin biosynthesis. *Biochemistry 47*, 6499-507.
(66) Fischer, M., Romisch, W., Saller, S., Illarionov, B., Richter, G., Rohdich, F., Eisenreich, W., and Bacher, A. (2004) Evolution of vitamin B_2 biosynthesis: structural and functional similarity between pyrimidine deaminases of eubacterial and plant origin. *J. Biol. Chem. 279*, 36299-308.
(67) Graupner, M., Xu, H., and White, R. H. (2002) The pyrimidine nucleotide reductase step in riboflavin and F_{420} biosynthesis in archaea proceeds by the eukaryotic route to riboflavin. *J. Bacteriol. 184*, 1952-7.
(68) Romisch-Margl, W., Eisenreich, W., Haase, I., Bacher, A., and Fischer, M. (2008) 2,5-diamino-6-ribitylamino-4(3H)-pyrimidinone 5'-phosphate synthases of fungi and archaea. *Febs J. 275*, 4403-14.
(69) Chatwell, L., Krojer, T., Fidler, A., Romisch, W., Eisenreich, W., Bacher, A., Huber, R., and Fischer, M. (2006) Biosynthesis of riboflavin: structure and properties of 2,5-diamino-6-ribosylamino-4(3H)-pyrimidinone 5'-phosphate reductase of *Methanocaldococcus jannaschii*. *J. Mol. Biol. 359*, 1334-51.
(70) Illarionov, B., Eisenreich, W., Schramek, N., Bacher, A., and Fischer, M. (2005) Biosynthesis of vitamin B_2: diastereomeric reaction intermediates of archaeal and non-archaeal riboflavin synthases. *J. Biol. Chem. 280*, 28541-6.
(71) Manstein, D. J., and Pai, E. F. (1986) Purification and characterization of FAD synthetase from *Brevibacterium ammoniagenes*. *J. Biol. Chem. 261*, 16169-73.
(72) Efimov, I., Kuusk, V., Zhang, X., and McIntire, W. S. (1998) Proposed steady-state kinetic mechanism for *Corynebacterium ammoniagenes* FAD synthetase produced by *Escherichia coli*. *Biochemistry 37*, 9716-23.
(73) Santos, M. A., Jimenez, A., and Revuelta, J. L. (2000) Molecular characterization of FMN1, the structural gene for the monofunctional flavokinase of *Saccharomyces cerevisiae*. *J. Biol. Chem. 275*, 28618-24.
(74) Solovieva, I. M., Kreneva, R. A., Leak, D. J., and Perumov, D. A. (1999) The *ribR* gene encodes a monofunctional riboflavin kinase which is involved in regulation of the *Bacillus subtilis* riboflavin operon. *Microbiology 145 (Pt 1)*, 67-73.
(75) Wu, M., Repetto, B., Glerum, D. M., and Tzagoloff, A. (1995) Cloning and characterization of FAD1, the structural gene for flavin adenine dinucleotide synthetase of *Saccharomyces cerevisiae*. *Mol. Cell Biol. 15*, 264-71.
(76) Mashhadi, Z., Zhang, H., Xu, H., and White, R. H. (2008) Identification and characterization of an archaeon-specific riboflavin kinase. *J. Bacteriol. 190*, 2615-8.
(77) Ammelburg, M., Hartmann, M. D., Djuranovic, S., Alva, V., Koretke, K. K., Martin, J., Sauer, G., Truffault, V., Zeth, K., Lupas, A. N., and Coles, M. (2007) A CTP-dependent archaeal riboflavin kinase forms a bridge in the evolution of cradle-loop barrels. *Structure 15*, 1577-90.

(78) Neue, H. (1993) methane emissions from rice fields. *BioScience 43*, 466-476.
(79) Mukhopadhyay, B., Johnson, E. F., and Wolfe, R. S. (1999) Reactor-scale cultivation of the hyperthermophilic methanarchaeon *Methanococcus jannaschii* to high cell densities. *Appl. Environ. Microbiol. 65*, 5059-65.

CHAPTER 2

An Fe^{2+} Dependent Cyclic Phosphodiesterase Catalyzes the Hydrolysis of 7,8-Dihydro-D-neopterin 2', 3'-cyclic phosphate in Methanopterin Biosynthesis

Minimally modified version of the paper published in: *Biochemistry*. 48: 9384 –9392 (2009).

Zahra Mashhadi, Huimin Xu, Robert H. White

As first author I designed and performed experiments, prepared the figures and the manuscript. Huimin Xu did all cloning and protein expression.

Department of Biochemistry, Virginia Tech, Blacksburg, VA, 24061

2.1 ABSTRACT

7,8-Dihydro-D-neopterin 2',3'-cyclic phosphate (H_2N-cP) is the first intermediate in biosynthesis of the pterin portion of tetrahydromethanopterin (H_4MPT), a C_1 carrier coenzyme first identified in the methanogenic archaea. This intermediate is produced from GTP by MptA (MJ0775 gene product), a new class of GTP cyclohydrolase I. Here we report the identification of a cyclic phosphodiesterase that hydrolyzes the cyclic phosphate of H_2N-cP and converts it to a mixture of 7,8-dihydro-D-neopterin 2'-monophosphate and 7,8-dihydro-D-neopterin 3'-monophosphate. The enzyme from *Methanocaldococcus jannachii* is designated MptB (MJ0837 gene product) to indicate that it catalyzes the second step of the biosynthesis of methanopterin. MptB is a member of the HD domain superfamily of enzymes, which require divalent metals for activity. Direct metal analysis of the recombinant enzyme demonstrated that MptB contained 1.0 mole of zinc and 0.8 mole of iron per protomer. MptB requires Fe^{2+} for activity, the same as observed for MptA. Thus the first two enzymes involved in H_4MPT biosynthesis in the Archaea are Fe^{2+} dependent.

2.2 INTRODUCTION

Methanopterin is one of a series of coenzymes that serve as C_1 carrier coenzymes in methanogenesis—the conversion of CO_2 and acetate to methane (*1*). In addition to its functioning in the methanogens in methane production, it also serves as a substitute cofactor for many of the enzymes where the canonical C_1 carrier coenzyme folate would function (*2-4*). This cofactor substitution is required because folate is not found in most methanogenic archaea (*3*). The one known exception is the confirmed presence of tetrahydrofolate dependent enzymes in *Methanosarcia barkeri* (*5*). GTP is known to be the precursor for the synthesis of the pterin portions of both of these coenzymes.

A review of fully sequenced and annotated genomes of methanogenic archaea revealed that homologs of the genes of folate biosynthetic enzymes were absent in the methanogens despite the fact that cell extracts of methanogens readily converted GTP to 6-hydroxymethyl-7,8-

dihydropterin with 7,8-dihydro-D-neopterin 2'3'-cyclic phosphate (H_2N-cP) and 7,8-dihydro-D-neopterin (H_2N) serving as intermediates (*6, 7*). A bioinformatic analysis of the different archaea genomes identified several genes that may be involved in archaeal pterin biosynthesis (*8*). Using this information it was established that the first enzyme in the archaeal pterin pathway is a new type of GTP cyclohydrolase, MptA, coded by the MJ0775 gene in *Methanocaldococcus jannaschii* (*9*). Unlike the analogous GTP cyclohydrolase I enzymes found in bacteria where the product is 7,8-dihydroneopterin 3'-triphosphate, the product of the *M. jannaschii* enzyme is H_2N-cP. All other known GTP cyclohydrolases have been characterized as Zn^{2+} dependent enzymes (*10*), but MptA was found to be unique in its Fe^{2+} requirement for activity. To process the H_2N-cP product of MptA to 7,8-dihydro-D-neopterin, the cyclic phosphodiester must be hydrolyzed. Here we report the identification of a cyclic phosphodiesterase in *M. jannaschii*, MptB, coded by the MJ0837 gene that hydrolyzes this 5-member cyclic phosphodiester to produce both 7,8-dihydro-D-neopterin 2'-phosphate (H_2N-2'-P) and 7,8-dihydro-D-neopterin 3'-phosphate (H_2N-3'-P) (Fig. 2.1). The MJ0837 gene product is named MptB because it catalyzes the second step in the methanopterin biosynthetic pathway.

2.3 MATERIALS AND METHODS

Chemicals. Diammonium D-neopterin 3'-phosphate, 7,8-dihydro-D-neopterin 3'-phosphate and other pterins were obtained from Schircks Laboratories, Jona, Switzerland. GTP, ATP, 2',3'-cAMP, 3',5'-cAMP, 3',5'-cGMP, bis(4-nitrophenyl)phosphate, *O*-(4-nitrophenylphosphoryl)choline; and all other chemicals were obtained from Sigma. 4',5'-cFMN was prepared as previously described (*11*), briefly, 10 mM FAD was incubated in 50 mM Tris-HCl pH 8.8 in presence of 10 mM $MnCl_2$ for 3 h at 37 °C followed by centrifugation.

Cloning and Recombinant Expression of MptB. The MJ0837 gene which encodes the protein identified by Swiss-Prot accession number Q58247 (*12*) was amplified by PCR from genomic DNA using oligonuculeotide primers synthesized by Invitrogen. Primer MJ0837Fwd, 5'-GGTCATATGGAGAGGTTAATAAAATTG-3' introduced an *Nde*I restriction site at the 5'-end of amplified DNA and MJ0837Rev, 5'-GCTGGATCCTTAATTGGATTCTTTATTTTC-3'

introduced an *Bam*HI restriction site at the 5'-end. PCRs were consist of 1× GeneAmp PCR buffer (Invitrogen), 1 μM each primer, 200 μM each dNTP, 1 μg of *M. jannaschii* chromosomal DNA, and 5 units of AmpliTaq LD DNA polymerase (Invitrogen) in a total volume of 100 μL. MJ0837 was amplified during 35 cycles, and each cycle include incubation at 95 °C for 1 min, 55 °C for 2 min, and 72 °C for 3 min. PCR product was purified using a QIA spin column (QIAGEN Inc.). Purified PCR product was digested with *Nde*I and *Bam*HI restriction enzymes (Invitrogen). DNA fragments were ligated into compatible sites in plasmid pT7-7 (*13*) using bacteriophage T4 DNA ligase. Recombinant plasmid, pMJ0837, was transformed into *Escherichia coli* strain BL21-Codon Plus (DE3)-RIL (Stratagene). Plasmid DNA sequence was verified by dye terminator cycle sequencing at University of Iowa, DNA Facility.

Transformed *E. coli* cells were grown in Luria-Bertani/Miller broth (200 mL) supplemented with 200 mg ampicillin. Cultures were shaken at 37 °C and 250 rpm until they reached an absorbance of 1.0 at 600 nm. Expression of MJ0837 was then induced with 27 mM D-(+)-lactose. After an additional 4 h incubation with shacking at 37 °C, the cells were harvested by centrifugation (6000 × *g,* 10 min). The harvested cells were stored at –20 °C, Induction of MJ0837 was confirmed by SDS-PAGE analysis of the cellular proteins.

Generation of Site-directed Mutants. Three mutants of MptB (H61N, H96N, and D167N) were generated using the QuikChange site-directed mutagenesis kit (Stratagene) using template pMJ0837. The H61N primers were: 5'-GAAGGTGGGTTAATAGAAAATACAATACAATATCAGTAAC-3' (forward) and 5'-GTTACTGAT- ATTGTATTTTCTATTAACCCACCTTC-3' (reverse). The H96N primers were: 5'- CGCTGGAGCTTTATTAAATGATATTATGAAGCCATAC-3' (forward) and 5'-GTATGGCTTCATAATATCATTTAATAAAGCTCCAGCG-3' (reverse). The D167N primers were: 5'-CATATATTGTCCATTATGCTAATGAAGCAGATTCAAAG-3' (forward) and 5'-CTTTGAATCTGCTTCATTAGCATAATGGACAATATATG-3' (reverse). Expression of the mutants was the same as with the wild-type. The mutations were confirmed by sequencing of plasmid inserts.

Purification of Recombinant MptB and its Mutants. The frozen *E. coli* cell pellet (~0.5 g wet weight) was suspended in 3 mL of extraction buffer (50 mM *N*-tris(hydroxymethyl)methyl-2-aminoethanesulfonic acid (TES), pH 7.0, 10 mM $MgCl_2$, 20 mM DTT) and lysed by sonication using Heat Systems Ultrasonics/W-385 (3 min with 5 sec pause). MptB and its mutants were

found to remain soluble after heating the cell extracts for 10 min at 80 ^{o}C. This process allowed for their purification from the majority of *E. coli* proteins, which denature and precipitate under these conditions. In the second step of purification, MptB and its mutants were purified by anion-exchange chromatography of the 80 ^{o}C soluble fraction on a MonoQ HR column (1 × 8 cm; Amersham Bioscience) using a linear gradient of NaCl from 0 to 1 M in 25 mM TES buffer, pH 7.5 over 55 mL at one mL/min flow rate. MptB elutes at about 0.5 M NaCl. All protein concentrations were determined by Bradford analysis (*14*).

Measurement of Native Molecular Weight of MptB. The native molecular weight of MptB was determined by size exclusion chromatography on a Superose 12HR column (10 mm x 300 mm) separated with aerobic buffer containing 50 mM HEPES pH 7.2, and 50 mM NaCl at 0.5 mL/min with detection at 280 nm. Protein standards used to calibrate the column included apoferritin (443 kDa), alcohol dehydrogenase (150 kDa), bovine serum albumin (66 kDa), carbonic anhydrase (29 kDa), and cytochrome c (12.4 kDa).

Transmission Electron Microscopy (TEM) of MptB. A MptB sample was sent to Purdue University for TEM analysis. The MptB sample was purified by MonoQ, and was 3 mg/ml MptB in 25 mM TES, pH 7.0 with 470 mM NaCl. Formvar (400 mesh) with carbon coated grids were used. Formvar was partially removed by placing grids on dichloroethane soaked filter paper for 20 min. Grids were glow discharged to make them hydrophobic prior to use. Samples were imaged in a Philipe CM-100 TEM (FEI Corporation, Hillsdale, Oregon) using 80 kV accelerating voltage. Magnification used was 105 K and 145 K read-out. There were further calibration using asbestos lattice to 102,200 and 147,000x.

Metal Ion Analysis of MptB and its Mutants. Metal analysis of MptB and its mutants was performed at the Virginia Tech Soil Testing Laboratory using inductively coupled plasma emission spectrophotometry (ICPES). The ICPES was a Spectro CirOS VISION (Spectro Analytical Instruments) equipped with a Crossflow nebulizer with a Modified Scott spray chamber. A 50 mg/L yttrium internal standard was introduced by peristaltic pump. Protein solutions, which were eluted from MonoQ, were diluted in elution buffer to give a final calculated metal concentration of 0.5 ppm, assuming one equivalent of metal per protomer. Samples were analyzed for iron, manganese, zinc, magnesium and nickel.

Analysis of Enzymatic Activity of MptB. The standard HPLC assay for MptB with H_2N-cP as substrate was performed in two steps. The first step includes the incubation of 3 μg of MptA in

39 mM TES (K^+) buffer containing 15 mM DTT, pH 7.2, 1.4 mM $Fe(NH_4)_2(SO_4)_2$, and 2.4 mM GTP in total volume of 42 µL under Ar gas at 70 ˚C for 30 min to make the H_2N-cP substrate for MptB. As the second step, the assay was continued by adding 12 µg of MptB and incubating at 70 ˚C for 30 min. 60 µL methanol was added to stop the reaction. The dihydropterin reaction products were oxidized to pterins by the addition of 5 µL iodine in MeOH (50 mg/mL) and the samples were incubated for 30 min at room temperature. $NaHSO_3$ (5 µL, 1 M) was added to reduce excess iodine. HPLC analysis of the reaction mixtures is described below.

The standard spectrophotometric assay for MptB was performed by incubation of 8.4 µg of MptB in 11 mM TES buffer, pH 7.2, 0.75 mM $MnCl_2$ and 1.5 mM of bis-pNPP in total volume of 134 µL at 70 ˚C for 10 min. The incubation was quenched at the end of incubation by adding 1 ml of 0.02 M NaOH. UV-Vis absorption with λ_{max} of 405 nm was used to detect the generated 4-nitrophenolate using a Shimadzu UV-1601 UV-Visible spectrophotometer.

Testing Alternative Substrates. MptB was tested for hydrolysis of alternative substrates such as ATP; 2',3'-cAMP; 3',5'-cAMP; GTP and 3',5'-cGMP by incubation of 13 µg of MptB in 29 mM TES buffer pH 7.0, 5.8 mM $MnCl_2$ and 8.8 mM of each substrate in total volume of 17 µL at 70 ˚C for 10 min. Thin-layer chromatography was used for product analysis as described below.

4',5'-cFMN was also tested as an alternative substrate. The assay for the hydrolysis of phosphodiester bond of 4',5'-cFMN was performed by incubation of 34 mM TES buffer, pH 7.0, 13 µg of MptB, 2.3 mM $MnCl_2$ and ~3 mM of cFMN in total volume of 44 µL at 70 ˚C for 20 min. The HPLC method was used to separate and detect FMN, FAD, and 4',5'-cFMN.

The standard spectrophotometric assay condition was used for the hydrolysis of 4-nitrophenylphosphoryl choline (pNPPC) phosphodiester bond.

HPLC Analysis of Products. A Shimadzu HPLC System with a C18 reverse-phase column (Varian PursuitXRs, 4.6 × 250 mm, 5 µm particle size) was used for analysis of products when either H_2N-cP or cFMN were used as substrate. The elution profile included 95% sodium acetate buffer (25 mM, pH 6.0, 0.02% NaN_3) and 5% MeOH for 5 min followed by a linear gradient to 20% sodium acetate buffer and 80% MeOH over 40 min. The flow rate was 0.5 mL/min. In all assays using HPLC analysis, 80 µL of methanol was added to the assay mixture at the end of the incubation to precipitate the proteins. After centrifugation (14000*g*, 10 min), 600 µL H_2O was added to the supernatant for HPLC analysis.

Pterins were detected by fluorescence using an excitation wavelength of 356 nm and an emission wavelength of 450 nm. Under these conditions, pterins were eluted in the following order and indicated retention times: neopterin 3'-phosphate, 6.2 min; neopterin 2'-phosphate, 6.8 min; D-neopterin 2',3'-cyclic phosphate, 7.9 min; neopterin, 10.8 min. Flavins were detected by fluorescence using λ_{max} of excitation of 450 nm and λ_{max} emission of 520 nm. The flavins were eluted in the following order: FAD 26.5 min, cFMN 28 min and FMN 29 min.

Thin-layer Chromatography Analysis. In studies using cyclic nucleotides as substrates, products were separated on silica plates with a solvent system consisting of 0.2 M ammonium bicarbonate in 70% ethanol. This solvent system was used previously to separate the cyclic nucleotides from tri-, di- and monophospho nucleotides (*15*). Under this condition the retention factor (R_f) are as follow: ATP, 0.11; ADP, 0.35; 5'-AMP, 0.44; 2',3'-cAMP, 0.84; GTP, 0.038; 5'GMP, 0.36; 3',5'-cGMP, 0.78. Also cellulose plates eluted with a solvent system consisting of saturated ammonium sulfate, 3 M sodium acetate and isopropanol (80:6:2 vol/vol/vol) was used to separate 2'- from 3'-NMPs (*16*). Under this condition the R_f's are as follow: 2',3'-cAMP, 0.08; 2'-AMP, 0.23; 3'-AMP, 0.15.

Metal-Ion Dependency of the MptB Reaction. Assay for metal dependency of MptB was performed in presence of either 0.75 mM of $MnCl_2.4H_2O$, $ZnCl_2$, $MgCl_2 \cdot 6H_2O$, $CoCl_2 \cdot 6H_2O$, $NiCl_2 \cdot 6H_2O$, $Fe(NH_4)_2(SO_4)_2 \cdot 6H_2O$, $FeNH_4(SO_4)_2 \cdot 12H_2O$ or no metal under standard spectrophotometric assay conditions with bis-pNPP as substrate.

Temperature Stability of MptB. The temperature stability of MptB was determined by treatment of the enzyme under different conditions. These included incubation of 13 μg enzyme in standard spectrophotometric assay buffer in total volume of 34 μL containing 0.73 mM $MnCl_2$ at 70, 80, 90 and 100 °C for either 45 minutes or 2.5 h in sealed tubes. A sample that did not contain $MnCl_2$ was also heated for 45 min at these different temperatures. Following heating, the enzyme mixture was cooled on ice, centrifuged and bis-pNPP was added as substrate. The final composition, volumes of the reaction mixture and incubation condition were as described for the bis-pNPP standard assay above. The samples were incubated at 70 °C for 10 min and analyzed as described above for standard spectrophotometric assay.

pH Optimum of the Recombinant Enzyme. The activity of MptB was determined at 0.5 pH increments between pH 5-9 using a three component buffer system consisting of BisTris, HEPES, and CHES (*17*). The assay was performed by the incubation of 33 mM BisTris, 17 mM

HEPES and 17 mM CHES, 8.4 μg of MptB, 0.75 mM $MnCl_2$, 1.5 mM bis-pNPP at the indicated pH's in total volume of 134 μL at 70 °C for 10 min. After incubation 1 ml of 0.02 M NaOH was added to all samples followed by measuring the absorbance at 405 nm.

Titration of MptB with Metals. The enzymatic activity of MptB was assayed by incubation with different concentrations of Mn^{2+} and Fe^{2+} and using the bis-pNPP standard spectrophotometric assay. The ratio of Mn^{2+} and Fe^{2+} to MptB protomer ranged from 0 to 682 and from 0 to 3.4, respectively. The assays were performed in a total volume of 134 μL in presence of 2.2 μM of MptB at 70 ˚C for 10 min. Experiments using $Fe(NH_4)_2(SO_4)_2$ were done in presence of 4 mM DTT and under Ar gas.

Oxygen Sensitivity of MptB Activated with Fe^{2+}. The inactivation of Fe^{2+} activated MptB by air was measured by exposing a Fe^{2+} activated sample to air and following the loss of activity with time. Thus to a stirred 10 μM anaerobic solution of MptB in 40 mM TES buffer, pH 7.2 was added 20 μM $Fe(NH_4)_2(SO_4)_2$. At times 0, 2, 10, 30, 60 and 120 min, 37 μL of mixture was transferred to a sealed tube containing Ar gas and 100 μL of 2 mM of bis-pNPP was added. After 10 min at 70 ˚C the released pNP was measured as described above.

2.4 RESULTS

Identification of MptB

Based on the information that HD domain superfamily of enzyme has phosphohydrolase activity (*18*), we first considered that the MJ0778 derived protein, which is a member of this superfamily, to be our desired enzyme since it is clustered with the MptA coding gene in several methanogenic archaeal genomes. This protein could generate H_2neopterin by hydrolyzing the H_2N-cP to H_2N-3'P. We recombinantly expressed the MJ0778-derived enzyme and found that it did not catalyze the hydrolysis of H_2N-cP. Several other homologs to MJ0778, containing the HD motif, were also identified in the *M. jannaschii* genome by Aravind and Koonin (*18*). We then checked another proposed member of this superfamily, MJ0837. The protein product of the MJ0837 gene readily catalyzed the hydrolysis of H_2N-cP to H_2N-P as shown in Figure 2.1.

Purification and Characterization of MptB

The MJ0837 gene from *M. jannaschii* was cloned and overexpressed in *E. coli.* The resulting protein was purified first by heating the cell extract at 80 ^{o}C followed by anion-exchange chromatography of the soluble proteins. The SDS-PAGE analysis of the purified MptB with Coomassie staining showed a single band corresponding to the mass of about 29-30 kDa with a purity of >95%. This molecular weight is consistent with the predicted monomeric molecular mass of 28.5 kDa. Size exclusion chromatography showed a molecular mass of 280 kDa consistent with the MptB existing as a dodecamer.

TEM analysis posed some difficulties as MptB sample contained some impurities. However, rosettes with six petals of consistent size were visible (Fig. 2.2). The rosettes are quite small (~10 nm) so very high magnification was needed to try to capture them. I conclude from this data that MptB may be a dimer of hexamers.

The MonoQ-purified recombinant MptB showed no activity with the range of substrates discussed below presumably due to the oxidation of Fe^{2+} to Fe^{3+}. This activity could be restored by the addition of either Fe^{2+} or Mn^{2+} to the purified enzyme. After the addition of 1.4 mM Fe^{2+}, the enzyme showed a specific activity of 29 ± 3
nmol min^{-1} mg^{-1} and 360 ± 30 nmol min^{-1} mg^{-1} for the hydrolysis of H_2neopterin 2',3'-cyclic phosphate (H_2N-cP) and bis-pNPP, respectively (Table 2.1). Experiments with the Fe^{2+} reconstituted enzyme acting on H_2N-cP greatly complicated the enzymatic assay due to both the inactivation of the enzyme and destruction of this substrate by oxygen. Both of these problems were eliminated by the use of 0.75 mM Mn^{2+} to activate the enzyme and the use of bis-pNPP as substrate. With these changes the enzyme has a specific activity of 430 ± 20 nmol min^{-1} mg^{-1} with bis-pNPP as substrate (Table 2.1).

Efficiency of Oxidation of 7,8-Dihydroneopterin to Neopterin

7,8-Dihydropterins are not fluorescent whereas pterins are, so it is necessary to oxidize the products of the reaction to pterins so that they could be analyzed by fluorescence. It is well known that dihydropterins can be oxidized to pterins with I_2 in dilute HCl (*19*). However such acidic conditions cannot be used in our assay, because it will result in acid catalyzed opening the 5-member cyclic phosphate. Iodine oxidation in basic solution, which will prevent this hydrolysis of the cyclic phosphate, can also do the desired oxidation (*20*), however basic solution

can not be used in our assay because it is known to result in removal of the chain from the pterin ring during oxidation (*20*). In this work we used I_2 in methanol at neutral pH to oxidize the dihydroneopterins to pterins. To determine the efficiency of this oxidation, known concentrations of H_2pterin and H_2neopterin were oxidized with I_2 in methanol and the efficiency of the conversion to pterin and neopterin respectively was measured by HPLC. The efficiency of oxidation with I_2 in methanol for 30 min at room temperature was determined to be 80% for H_2pterin and 90% for H_2neopterin.

Use of a Coupled Assay

Since 6,7-dihydroneopterin 2',3'-cyclic phosphate (H_2N-cP) was not easily prepared synthetically we generated it enzymatically from GTP using MptA. During this assay about 0.4 mM H_2N-cP was made before the MptB enzymatic reaction was started.

Identification of MptB Reaction Product(s)

Hydrolysis of 6,7-dihydroneopterin 2',3'-cyclic phosphate with MptB at 70 °C for 30 min produced two products when assayed by HPLC using fluorescence detection at the pterin λ_{max} of excitation and λ_{max} of emission wavelengths (Fig. 2.3). These two peaks were identified based on their elution times as D-neopterin 2'-phosphate (about 40% of the total) and D-neopterin 3'-phosphate (about 60% of the total). Both showed fluorescent spectra consistent with the presence of pterins. Acid hydrolysis of neopterin 2',3'-cyclic phosphate produced the same two products with the ratio of 1:4 for H_2N-3'P and H_2N-2'P when analyzed by HPLC (*9*). Treatment of the MptB reaction mixture with alkaline phosphatase resulted in the removal of the phosphate from both isomers with the resulting formation of D-neopterin that was confirmed by HPLC.

Substrate Specificity of the MptB Reaction

MptB was able to utilize a variety of phosphodiesters as substrates: H_2N-cP produced H_2N-2'-P and H_2N-3'-P; bis-pNPP and pNPPC produced nitrophenyl phosphate; and 2',3'-cAMP produced 3'-AMP. Other phosphate ester containing compounds including ATP, 3',5'-cAMP, GTP, 3',5'-cGMP and 4',5'-cFMN did not serve as substrates for MptB. Bis-pNPP was used as substrate in all characterization experiments since the assay can be done under aerobic

condition. The specific activity of the Mn^{2+} activated enzyme was 430 ± 20 nmol min^{-1} mg^{-1} for bis-pNPP and 710 nmol min^{-1} mg^{-1} for 2', 3'-cAMP (Table 2.1).

Attempt to Determine the Kinetic Values

H_2N-cP is not commercially available, which makes it hard to determine the kinetic values of MptB with H_2N-cP as a substrate. Even by producing H_2N-cP by the MptA catalyzed transformation of GTP, high sensitivity of the H_2N-cP to oxygen makes working with this substrate almost impossible without anaerobic facilities. The activity of MptB measured with different concentrations of either bis-pNPP or pNPPC as substrate increased in a linear manner up to 15 mM. Even at high concentration of bis-pNPP or pNPPC, MptB's specific activity continued to increase up to the solubility limit of these compounds. As a result we were not able to determine the kinetic values of MptB with either bis-pNPP or pNPPC as substrates.

Metal-Ion Dependency of the MptB Reaction

As isolated, MptB is inactive in the absence of added metal ions. By adding different metal ions to the assay mixture it was revealed that MptB hydrolyzes the phosphodiester bond of bis-pNPP most efficiently in presence of added Mn^{2+} or Fe^{2+} but not Fe^{3+} (Table 2.2). Activity of MptB was restored by using Fe^{2+} at the physiologically relevant concentrations of about 4 μM although higher concentrations of Mn^{2+} (750 μM) were able to restore activity comparable to that seen with ferrous ion. Also Co^{2+} was found to restore some activity at 0.75 mM but the level was only 3.2% of that of Fe^{2+} (Table 2.2).

Since high concentrations of Mn^{2+} were able to restore most of the activity of MptB, and it is more convenient to work with Mn^{2+} than with Fe^{2+} under aerobic condition due to air oxidation of Fe^{2+} to Fe^{3+}, most of the experiments were done with Mn^{2+}.

Identification of Catalytically Important Residues

Alignment of MptB homologs from the HD superfamily allowed for the identification of two conserved histidine and two conserved aspartate residues, H61, H96, D97, and D167 (*18*). With this knowledge, three of those residues in MptB, H61, H96, and D167 were chosen to change to asparagines, the most conservative changes possible. ICPES was used to determine the identity and quantity of metal ions present in the purified recombinant enzymes. Isolated

pure recombinant MptB was found to contain 0.8 moles of iron and 1.0 mole of zinc per protomer using the Bradford protein assay to measure the protein concentrations. The metal content of the wild type and mutants and their specific activity with H_2N-cP, bis-pNPP and 2',3'-cAMP are summarized in Table 2.1. With one exception, all of the mutant enzymes showed reduced activities when assayed with each of the three substrates. The exception was the H96N mutant that showed about 1.9 fold higher specific activity with bis-pNPP than that of the wild type (Table 2.1).

Temperature Stability of Recombinant MptB

Heating of MptB at 70, 80, 90, and 100 °C, in either presence or absence of Mn^{2+} reveals interesting results. In the first case by heating MptB at 70, 80, 90, and 100 °C in absence of Mn^{2+} for 45 min, the activity of the enzyme drops about 30% from the 70 °C heated sample to the 100 °C heated sample. In presence of Mn^{2+}, however in the case of 45 min heating the activity of the enzyme increases about 53% from the 70 °C heated sample to the 100 °C heated sample. But in the case of 2.5 hr heating the activity of the enzyme drops about 26% from the 70 °C heated sample to the 100 °C sample. Adding Mn^{2+} to the enzyme was observed to increase the temperature stability of the protein.

pH Optimum of the Recombinant Enzyme

Using a three component buffer system consisting of BisTris, HEPPS and CHES allowed a pH range from 5 to 9 to be determined in one buffer system. The best activity of MptB with bis-pNPP in this buffer system was observed at pH 7.5 (Fig. 2.4).

Titration of MptB with Metals

The activity of MptB increased by increasing the ratio of either Fe^{2+} to MptB from 0 to 2.1 (Figure 2.5) or Mn^{2+} to MptB from 0 to 682 (Figure 2.6). When doing these experiments it was found that DTT is required in the activation experiments using Fe^{2+}. It is not clear why DTT was required for the Fe^{2+} activation of MptB but there are several examples of were thiol compounds are required to remove Fe^{3+} from a protein and so it can be replace with Fe^{2+} (*21*).

Since we are using the enzymatic rate to determine Fe^{2+} binding to the enzyme, KeleidaGraph 4.0 was used to fit the metal titration data (Fig. 2.5, 2.6) to a rectangular

hyperbolic equation to determine the dissociation constants (K_D) of about 1.6 ± 0.35 μM for iron and 739 ± 0.1 μM for manganese.

Oxygen Inactivation of MptB

The specific activity of Fe^{2+} activated MptB toward hydrolysis of bis-pNPP upon exposure to air assuming an exponential decay was determined to have a half-life of about 5 min.

2.5 DISCUSSION

MptB contains the HD motif and is annotated as a member of the metal-dependent phosphohydrolase superfamily (*18*). The members of this superfamily are very different in sequence but they all have conserved histidines and aspartates, which are involved in divalent metal binding and in forming the catalytic site (*18*). Some of the HD domain enzymes have been crystallized and, according to their structures, HD domain proteins can even have different folds. By using the DALI-structural similarity search program it is revealed that the local structure around the putative active sites in all HD-domain enzymes, however, are similar (*22*). Based on the secondary structure threading, the most similar known structure to MptB is a protein with HD domain that is predicted to be a hydrolase. This structurally analogous protein to MptB was produced from uncultured thermotogales bacterium, and was also found to contain two irons (PDB id: 2pq7).

Characterized HD domain enzymes catalyze many different reactions but the functions of many are presently unknown. There are 11 known families of phosphodiesterases (PDEs), which are members of the HD domain superfamily (*23*). All eleven families contain two histidine and two aspartate metal binding residues that are conserved (*24*). All of the known enzymes in PDEs family that use cyclic nucleotides 3',5'-cAMP, or 3',5'-cGMP as substrates produce 5'-AMP or 5'-GMP as products (Table 2.3) (*25-33*). All of these PDEs function in signaling pathways to regulate the concentration of intracellular secondary messengers 3',5'-cAMP or 3',5'-cGMP. Also there are some cyclic phosphodiesterases which hydrolyze 2',3'-cNMP to produce either 2'-NMP (CthPnkp) (*34*), 3'-NMP (DR1281) (*35*) or both (λ-phage and

Rv0805) (*34, 36*). It is proposed that the role of these 2',3'-cNMP phosphodiesterases are to repair RNA 2',3' cyclic ends (*34*), which are intermediates in RNA processing. MazF, an mRNA interferase in *E. coli*, is an example of these cyclic phosphodiesterases that is highly conserved among prokaryotes. MazF is a endonuclease that produces a 2',3'-cP at the 3' end of RNA and a hydroxyl group on the 5' end (*37*). tRNA splicing endonuclease in yeast is another characterized endonuclease, which converts pre-tRNA to mature tRNA, by producing 2',3'-cyclic nucleotides (*38*). An archaeal tRNA endonuclease which is homologous to yeast tRNA splicing gene, has also been identified (*39*). There are even members of HD-domain family that have both 2', 3'-cyclic phosphodiesterase and phosphomonoesterase activities (*40*).

Based on this information we first considered that the MJ0778, which is a HD domain enzyme that is also clustered with the MptA coding gene in several methanogenic archaeal genomes. We recombinantly expressed the MJ0778-derived enzyme and found that it did not catalyze the hydrolysis of H_2N-cP. Several other homologs to MJ0778, containing the HD motif, are also found in the *M. jannaschii* genome (*18*). Among these is MJ0837. The protein product of the MJ0837 gene readily catalyzed the hydrolysis of H_2N-cP to H_2N-P as shown in Figure 2.1. Unlike most enzymes that produce a single enzymatic product, this enzyme catalyzed the formation of both H_2N-2'P (about 40% of the total) and H_2N-3'P (about 60% of the total) positional isomers from H_2N-cP. The formation of both isomers is of no consequence since we have shown that both isomers are readily metabolized to H_2neopterin by *M. jannaschii* cell extracts (unpublished data). MptB is also able to hydrolyze the cyclic phosphate of 2',3'-cAMP but not that of 3',5'-cAMP, 3',5'-cGMP or 4',5'-cFMN. Interestingly only 3'-AMP was formed from 2',3'-cAMP. We propose that the production of the two isomers results from the binding of the H_2N-cP in two different conformations that allows for two different orientations of the cyclic phosphate as shown in Figure 2.7. As the adenine ring binds to its binding pocket in MptB, the 2',3'-cyclic phosphate of the cAMP is fixed in place because of the presence of the ribose ring, which causes strict orientation of the cyclic phosphate in the active site containing the nucleophilic Fe^{2+} bound water (Fig. 2.7A). In the case of the H_2N-cP, that does not contain the ribose ring, two different orientations of the cyclic phosphate can occur upon binding to MptB thus allowing for the hydroxide to attack the phosphate from either apical position, one producing H_2N-3'P (Fig. 2.7B) and the other producing H_2N-2'P (Fig. 2.7C). This can occur because H_2N-cP does not have the β-substituted ribose ring in its structure so the cyclic

phosphate may rotate freely around the C1'-C2' bond ("b" bond in Figure 2.7) and as a result H_2N-cP can have two different orientations. The nucleophilic attack of a hydroxide at the phosphorus by applying the "apical in-apical-out" rule, which is applied in all phosphoryl exchange reactions involving a pentavalent intermediate, forms only 3'-AMP in case of consuming 2',3'-cAMP as substrate.

Another possible explanation for the production of two different isomers is by the binding of the H_2N-cP in two different binding sites that results the orientation of the cyclic phosphate in the active site to be in the two different orientations as described above. The resolution of this issue must await the structural determination of the enzyme.

The metal dependency of phosphodiesterases varies widely. We have summarized in Table 2.3 the list of metals, which are either observed in the crystal structure of some of the phosphodiesterases (*25-28, 32, 33, 41*) or have been observed to be required for the activity of these enzymes (*30, 34-36, 42, 43*). ICPES analysis of purified inactive MptB indicated the presence of 0.8 mole iron and 1.0 mole zinc per protomer. Although ICPES analysis was able to detect the presence of iron, the exact location and ligands of both the iron and zinc are unknown. Since the enzyme is inactive when purified aerobically on MonoQ or when incubated with Fe^{3+} and the enzymatic activity was restored by the addition of Fe^{2+}, we can conclude that the iron needs to be in the reduced state. Also the time course assay of the O_2-dependent loss of activity of the MptB in presence of Fe^{2+} emphasized that this reaction is Fe^{2+}-dependent. An Fe^{2+} aquo complex has an acid dissociation constant that would allow for the production of the required nucleophilic hydroxide (*44*). Although the Fe^{3+} enzyme was expected to have an even lower pKa, the additional positive charge on the metal to which the hydroxide is bound will not allow the hydroxide to function as a nucleophile. The utilization of Fe^{2+} by the enzymes from anaerobic methanogens may relate to the higher availability of the soluble, reduced form of iron present in the habitats of the methanogens.

Adding either DTT or dithionite to the enzyme containing assay mixture was not able to restore the activity of the enzyme by reducing the Fe^{3+} bound to MptB back to Fe^{2+} (unpublished data). As shown here adding either Fe^{2+} or Mn^{2+} was able to restore the MptB activity. This regeneration of activity could either result from the replacement of the bound Fe^{3+} by either Fe^{2+} or Mn^{2+} or by reduction of the bound Fe^{+3} with the added Fe^{2+}. However since other reducing agents failed to restore the enzymatic activity and the non-reducing Mn^{2+} did restore activity, the

replacement of the Fe^{3+} by Fe^{2+} is the most likely scenario. This replacement is also expected considering that catalytically active Fe^{2+} is likely bound more tightly than catalytically inactive Fe^{3+}.

Having metal ions in the catalytic site of phosphodiesterase can also stabilize the transition state of hydrolysis by neutralization of negative charge on phosphate, and to interact with the oxygen of the leaving alcohol (*45*). Metal ions can accelerate the hydrolysis of phosphate diesters due to three factors: Lewis acid activation ($<10^2$-fold), intermolecular nucleophile activation (10^8-fold), and leaving group stablization (10^6-fold). In some cases these factors can combine to give the overall rate acceleration more than 10^{16} (*46*).

In the site directed mutant H61N, MptB loses almost all of the iron and its specific activity is about 13% of that of wild type for H_2neopterin-cP, 7.6% for 2'3'-cAMP and about 17% for bis-pNPP. In the case of H96N, MptB loses half of the iron and so its specific activity is about half of that of wild type for 2'3'-cAMP, 65% for H_2neopterin-cP but 186% for bis-pNPP. The reason for the higher activity of H96N in the case of using bis-pNPP as substrate is not clear but the same result was observed for a phosphodiesterase from *Mycobacterium tuberculosis* (*34*). In the case of the site directed mutant D167N, MptB has almost all of the iron but its specific activity is only about 3.5% of that of wild type for H_2neopterin-cP in presence of added Fe^{2+}, 3% for 2'3'-cAMP and about 17% for bis-pNPP in presence of added Mn^{2+}. We propose that the reason for this decrease in the specific activity without losing any iron is that D167 is the base (Fig. 2.6) that abstracts the proton of the Fe^{2+} or Mn^{2+} bound hydroxide ion that facilitates its nucleophilic attack on phosphate.

Because adding Zn^{2+} plus Fe^{2+} caused lower activity (26 nmol min^{-1} mg^{-1}) compared to adding Fe^{2+} alone in the assay (370 ± 30 nmol min^{-1} mg^{-1}), we can speculate that Zn^{2+} replaces Fe^{2+} resulting in decreased activity. This result is consistent with a proposed structural role for Zn^{2+} and a catalytic role for Fe^{2+} in MptB.

The only well studied example of the enzymatic hydrolysis of 5-member cyclic phosphodiesters is concerned with their involvement as proposed intermediates in the hydrolysis RNA by ribonuclease. Nucleoside 2',3'-cyclic phosphates can serve as substrates for RNase (*47*). The absolute stereochemistry of this hydrolysis has been studied and shown to proceed by an in-line mechanism (*48, 49*). The same stereochemistry has been found in ribonuclease-T_1 (*50*) and by a nonspecific phosphohydrolase (*51*) and is likely to be the same for MptB.

MptA is present in the genomes of almost all the archaea except in the Class Thermoprotei, while MptB is present in members of the Class Methanococcales as well as in only a few other archaea. Since the other methanogens contain methanopterin or one of its many derivatives, then there should be at least one other gene in the other methanogens that encodes for a protein to hydrolyze the cyclic phosphate intermediate in their methanopterin biosynthetic pathway. Since the halobacteria contain folate but no methanopterin, then it is likely their MptA is producing the folate pterin without the help of MptB.

2.6 ACKNOWLEDGMENT

We would like to thank Laura Grochowski and Walter Niehaus for assistance with editing this manuscript. Also we would like to thank staff in Life Science Microscopy Facility at Purdue University for the TEM data.

2.7 TABLES AND FIGURES

Table 2.1 The metal content and specific activities of MptB and its mutants with either H_2neopterin-cP, bis-pNPP or 2',3'-cAMP as a substrate.

Protein	Specific Activity [(a)] (nmol min^{-1} mg^{-1})			Metal/Protomer [(b)]			
	H_2neopterin-cP in presence of Fe^{2+}	bis-pNPP in presence of Mn^{2+}	2',3'-cAMP in presence of Mn^{2+}	Fe	Zn	Ni	Mn
MptB wild type	29 ± 3	430 ± 20	710	0.8	1.0	< 0.36	< 0.03
MptB H61N	3.8 ± 0.2	74	54	< 0.05	0.6	< 0.25	< 0.02
MptB H96N	19 ± 7	800	350	0.4	0.77	< 0.3	< 0.02
MptB D167N	1 ± 0.3	75	15	0.76	0.47	< 0.07	0.05

(a) The specific activity measurement with H_2neopterin-cP as the substrate was done at an Fe^{2+} concentration of 1.4 mM. The concentrations of Mn^{2+} in the bis-pNPP and 2',3'-cAMP experiments were 0.75 mM and 5.8 mM, respectively.

(b) The metals in the proteins were measured from MonoQ purified samples without the addition of any metals.

Table 2.2 Dependency of the activity of MptB on different divalent metal ions.

The assay was done in presence of either 0.75 mM $MnCl_2$, $ZnCl_2$, $CuCl_2$, $CoCl_2$, $NiCl_2$, $Fe(NH_4)_2(SO_4)_2$, $FeNH_4(SO_4)_2$ or no added metal with bis-pNPP as substrate.

	No metal	Mn^{2+}	Fe^{2+}	Co^{2+}	Ni^{2+}	Mg^{2+}	Zn^{2+}	Fe^{3+}
Specific Activity (nmol mg^{-1} min^{-1})	2.0	430 ± 20	370 ± 30	12.0	3.0	0.0	0.0	0.0

Table 2.3 List of the known phosphodiesterases and phosphomonoesterases where their metal dependency and substrates are known.

Enzyme	Metal	Substrate	Ref.
PDEs 2	Zn^{+2}, Mg^{+2}	cAMP, cGMP	(*32*)
PDEs 3	Fe^{+2}, Fe^{+3}	cAMP	(*30*)
PDEs 3B	Mg^{+2}, Mg^{+2}	cAMP, cGMP	(*29*)
PDEs 4	Zn^{+2}, Mn^{+2}	cAMP	(*31*)
PDEs 5	Zn^{+2}, Mg^{+2}	cGMP	(*27*)
PDEs 7	Zn^{+2}, Mg^{+2}	cAMP	(*26*)
PDEs 10	Zn^{+2}, Mg^{+2}	cAMP, cGMP	(*25*)
cNMP PDEs	Zn^{+2}	cGMP	(*33*)
cNMP PDE (Rv0805) from *M. tuberculosis*	Mn^{+2}, Fe^{+3}	cAMP, cGMP	(*28*)
Mammalian PAPs	Fe^{+2}, Fe^{+3}	Non-specific hosphomonoesterase	(*41*)
Plant PAPs	Zn^{+2}, Fe^{+3}	Non-specific hosphomonoesterase	(*41*)
YfcE	Zn^{+2}(PDB 1SU1), requires Mn^{+2}	No natural substrate is detected.	(*42*)
*Cth*Pnkp	Ni^{+2}, Mn^{+2}	2',3'-cAMP	(*36*)
Bacteriophage λ phosphatase (λ-Pase)	Mn^{+2}, Mn^{+2}	2',3'-cAMP	(*36*)
MJ0936	Mn^{+2}, Mn^{+2}	Phosphodiesters but not cyclic phosphodiesters	(*43*)
DR1281	Mn^{2+}, Fe^{2+} or Co^{2+}	2',3'-cAMP	(*35*)
Rv0805	Mn^{+2}, Mn^{+2}	2',3'-cAMP	(*34*)

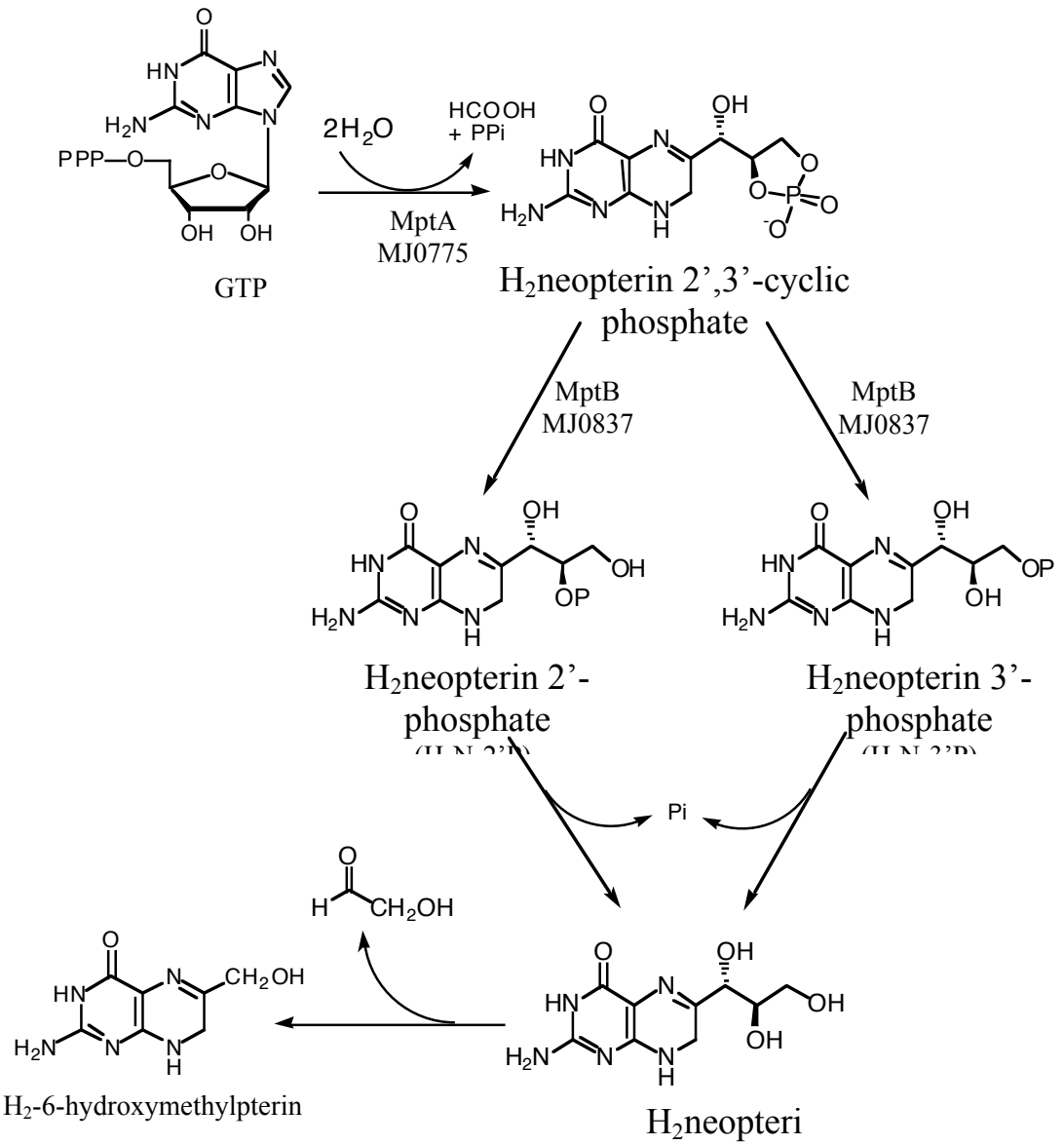

Figure 2.1 The early steps of the methanopterin biosynthetic pathway.

GTP is the precursor for the synthesis of the pterin portion of the methanopterin. MptA, which is a GTP cyclohydrolase, catalyzes conversion of GTP to H_2N-cP. MptB catalyzes the second step, hydrolysis of the cyclic phosphate into two products, H_2N-2'P and H_2N-3'P. One or two phosphatase(s) and an aldolase, that have yet to be identified, catalyze the next two steps to give H_2-6-hydroxymethylpterin.

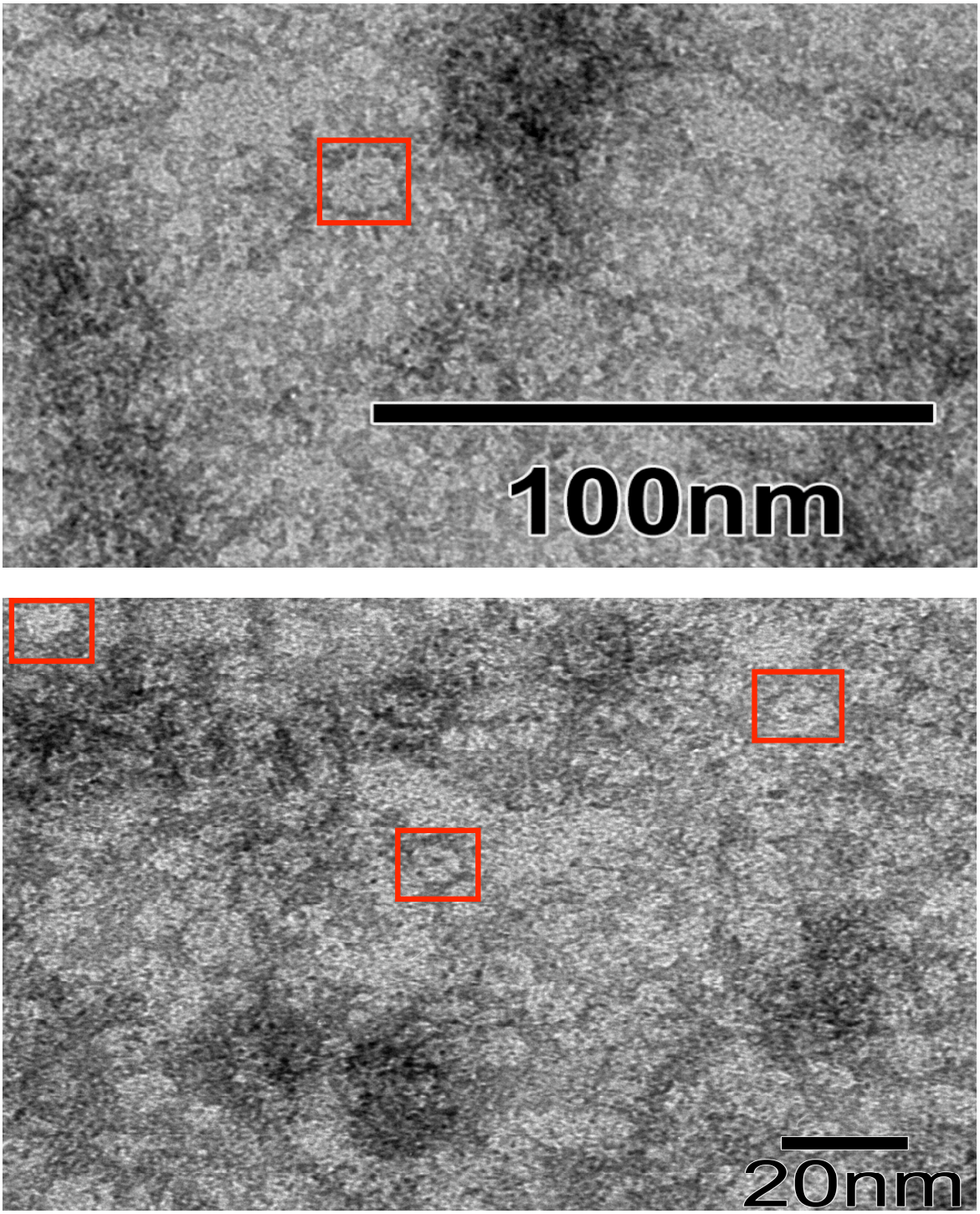

Figure 2.2 Transmission Electron Microscopy (TEM) of MptB.

Rosettles of consistent size are visible. The most clear one are boxed.

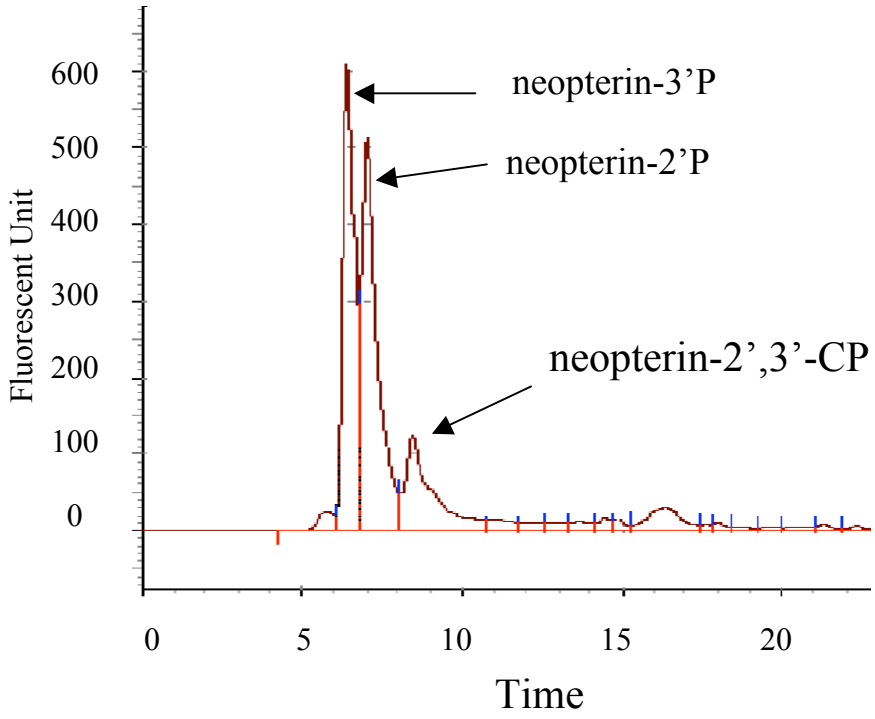

Figure 2.3 HPLC trace of the assay mixture that shows hydrolysis of H_2neopterin-cP to H_2N-2'P and H_2N-3'P by MptB.

The substrate and both products are oxidized to neopterin-cP, N-2'P and N-3'P, respectively, to be visualized by their fluorescence.

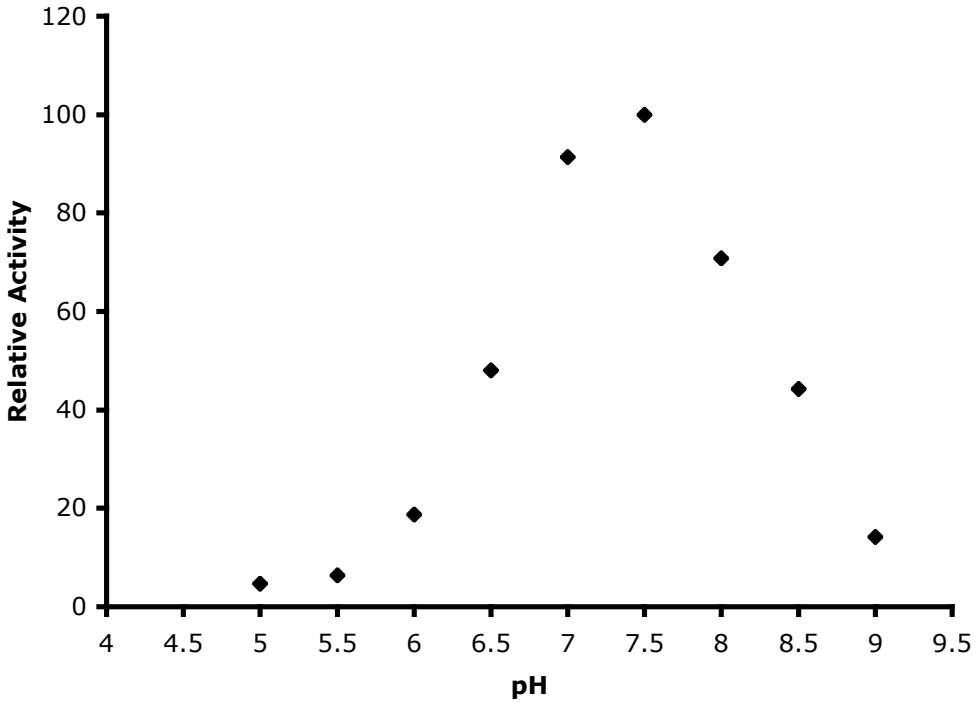

Figure 2.4 Effect of pH on hydrolysis of bis-pNPP by MptB.

The best activity for MptB was observed at pH 7.5.

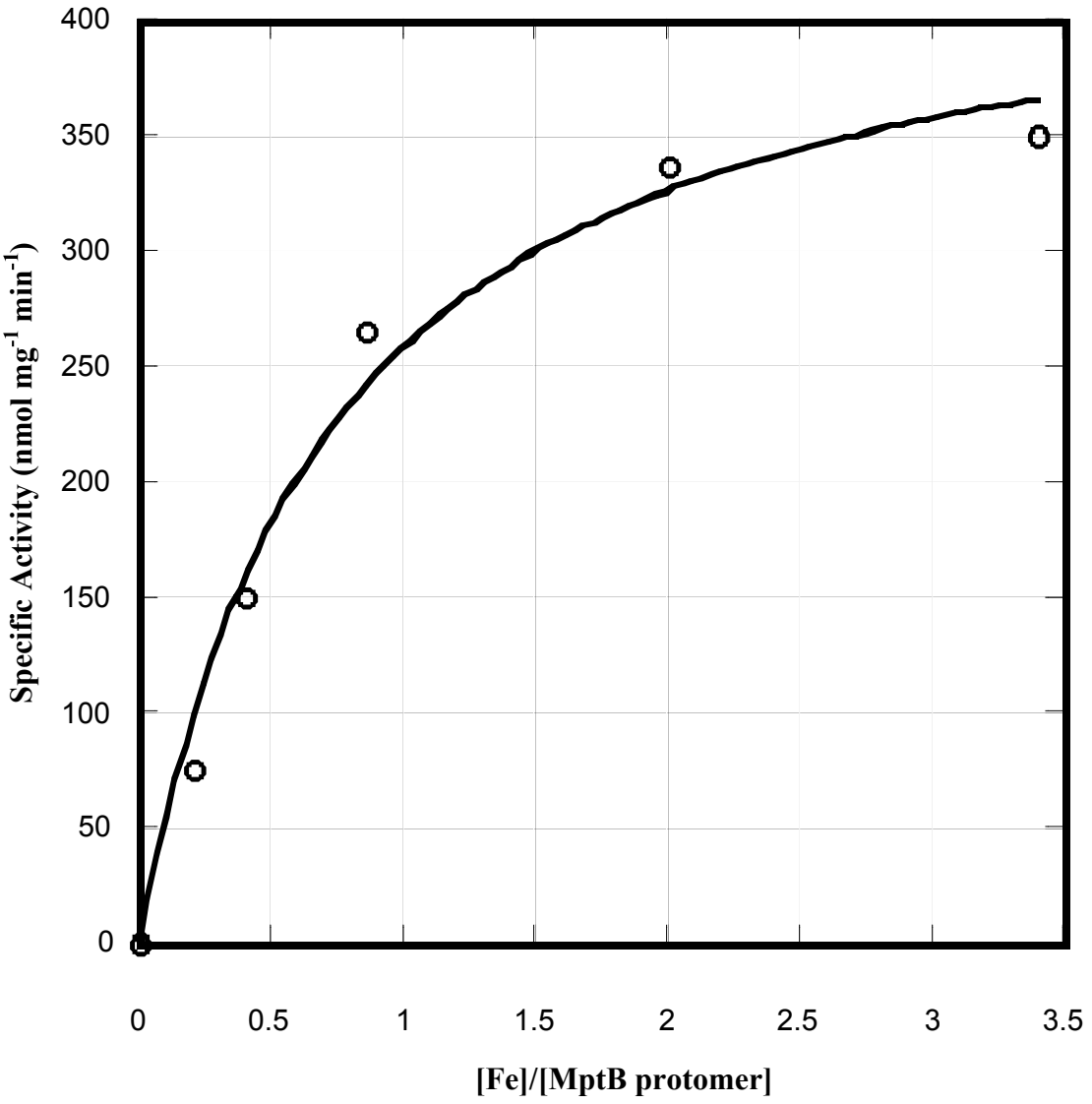

Figure 2.5 Titration of MptB with Fe^{2+}.

The activity of MptB toward bis-pNPP was measured while the ratio of $Fe(NH_4)_2(SO_4)_2$ to MptB was varied from 0 to 3.4 in presence of 2.2 μM of MptB.

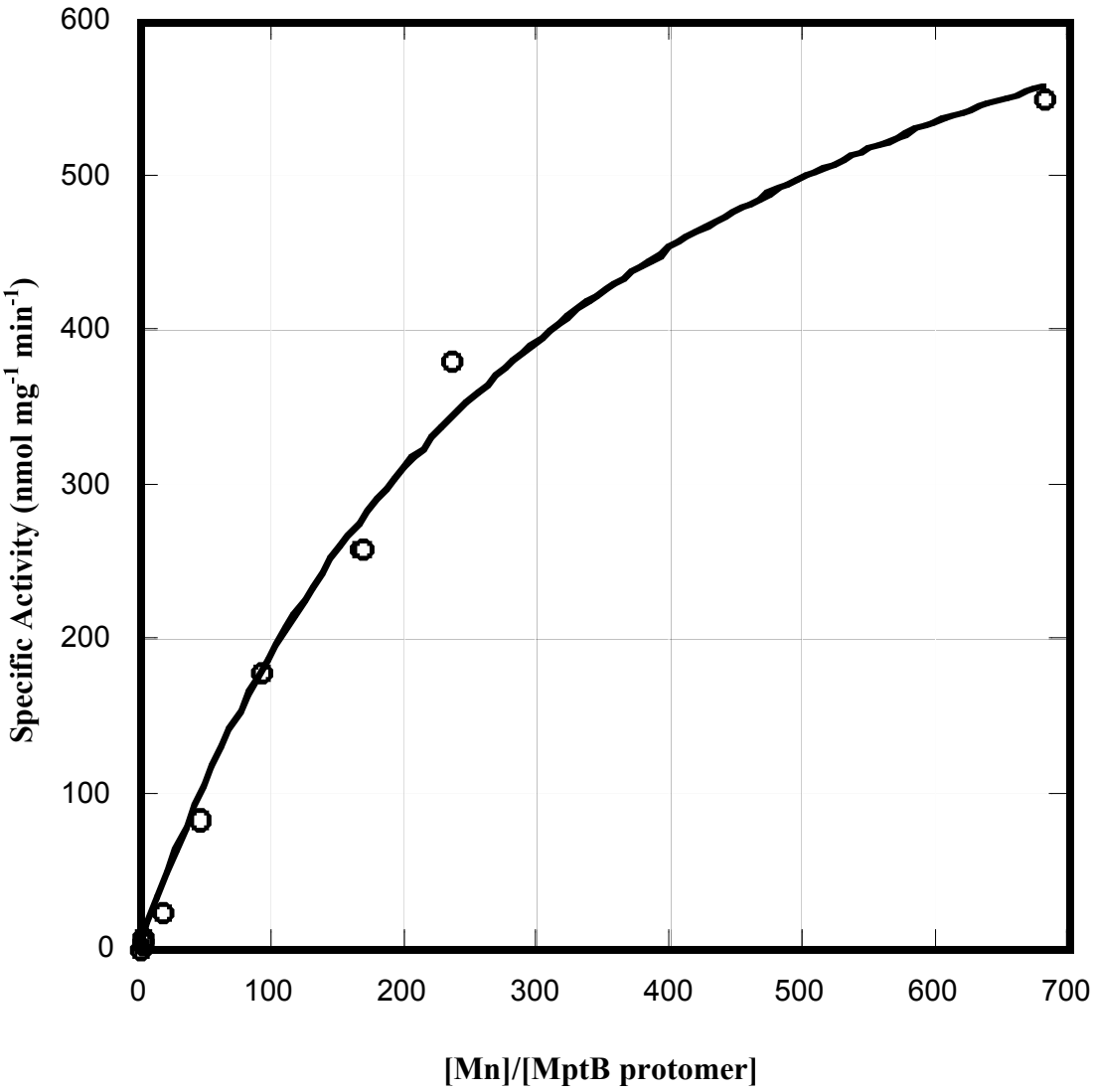

Figure 2.6 Titration of MptB with Mn^{2+}.

The activity of MptB bis-pNPP was measured while the ratio of $MnCl_2$ to MptB was varied from 0 to 682 in presence of 2.2 μM of MptB.

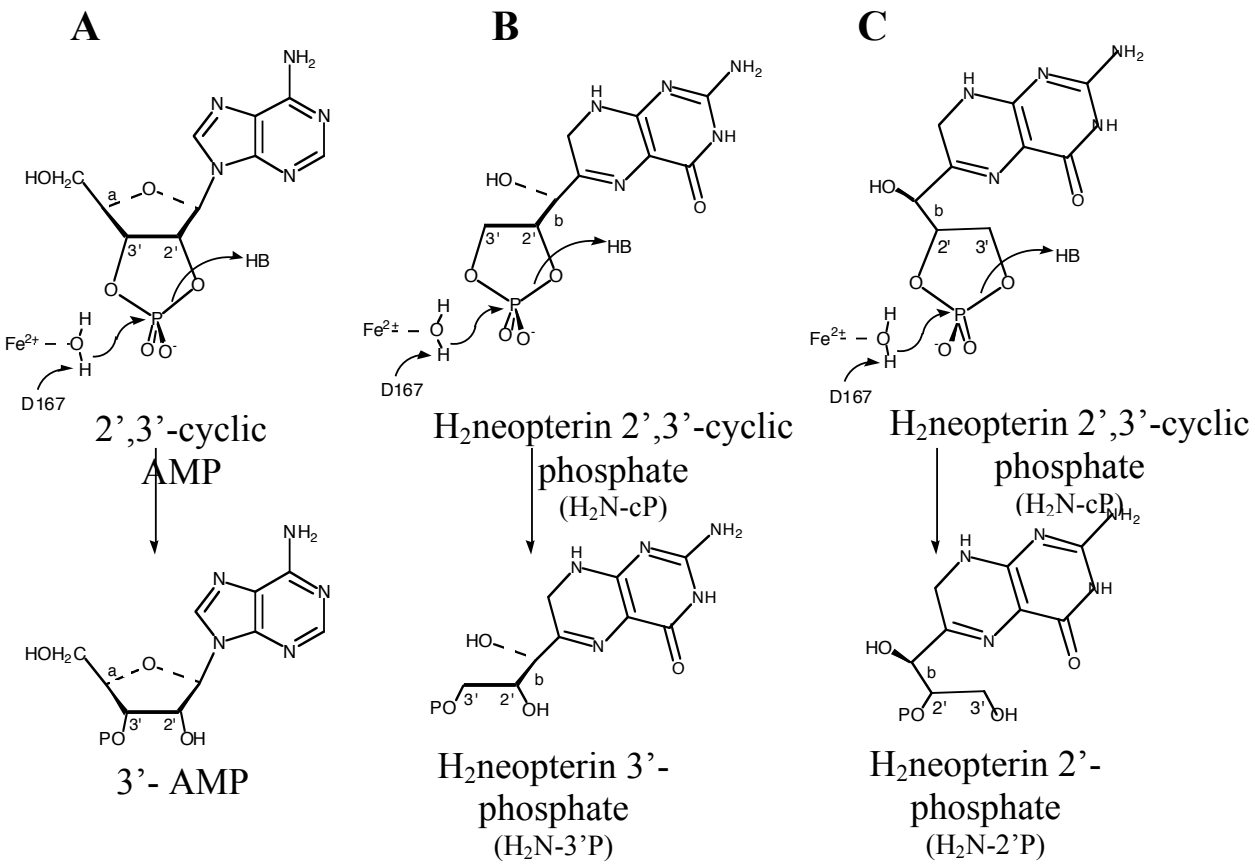

Figure 2.7 A proposed MptB cyclic phosphodiesterase mechanism.

When 2',3'-cAMP is used as substrate (A), the presence of the ribose ring, allows only one orientation of the cyclic phosphate when bound to the enzyme. Under these conditions the nucleophilic attack of a Fe^{2+} bound hydroxide at the phosphorus allows for the formation of only 3'-AMP. In case of H_2N-cP, because of the absence of the ribose ring, the cyclic phosphate ring can easily rotate around bond "b". H_2N-cP can have one orientation as shown in (B) and nucleophilic attack of a hydroxide at the phosphorus produces H_2neopterin-3'P. By rotating the cyclic phosphate around bond "b" H_2N-cP will produce another orientation as shown in (C) and nucleophilic attack of a hydroxide at the phosphorus produces H_2neopterin-2'P.

REFERENCES

(1) Escalante-Semerena, J. C., Rinehart, K. L., Jr., and Wolfe, R. S. (1984) Tetrahydromethanopterin, a carbon carrier in methanogenesis. *J. Biol. Chem. 259*, 9447-55.

(2) Worrell, V. E., and Nagle, D. P., Jr. (1988) Folic acid and pteroylpolyglutamate contents of archaebacteria. *J. Bacteriol. 170*, 4420-3.

(3) White, R. H. (1993) Structures of the modified folates in the thermophilic archaebacteria *Pyrococcus furiosus*. *Biochemistry 32*, 745-53.

(4) Delle Fratte, S., White, R. H., Maras, B., Bossa, F., and Schirch, V. (1997) Purification and properties of serine hydroxymethyltransferase from *Sulfolobus solfataricus*. *J. Bacteriol. 179*, 7456-7461.

(5) Buchenau, B., and Thauer, R. K. (2004) Tetrahydrofolate-specific enzymes in *Methanosarcina barker*i and growth dependence of this methanogenic archaeon on folic acid or *p*-aminobenzoic acid. *Arch. Microbiol. 182*, 313-25.

(6) Howell, D. M., and White, R. H. (1997) D-erythro-neopterin biosynthesis in the methanogenic archaea *Methanococcus thermophila* and *Methanobacterium thermoautotrophicum* ΔH. *J. Bacteriol. 179*, 5165-70.

(7) White, R. H. (1990) Biosynthesis of methanopterin. *Biochemistry 29*, 5397-404.

(8) El Yacoubi, B., Bonnett, S., Anderson, J. N., Swairjo, M. A., Iwata-Reuyl, D., and de Crecy-Lagard, V. (2006) Discovery of a new prokaryotic type I GTP cyclohydrolase family. *J. Biol. Chem. 281*, 37586-93.

(9) Grochowski, L. L., Xu, H., Leung, K., and White, R. H. (2007) Characterization of an Fe^{2+}-dependent archaeal-specific GTP cyclohydrolase, MptA, from *Methanocaldococcus jannaschii*. *Biochemistry 46*, 6658-67.

(10) Auerbach, G., Herrmann, A., Bracher, A., Bader, G., Gutlich, M., Fischer, M., Neukamm, M., Garrido-Franco, M., Richardson, J., Nar, H., Huber, R., and Bacher, A. (2000) Zinc plays a key role in human and bacterial GTP cyclohydrolase I. *Proc. Natl. Acad. Sci. U S A 97*, 13567-72.

(11) Pinto, R. M., Fraiz, F. J., Cabezas, A., Avalos, M., Canales, J., Costas, M. J., and Cameselle, J. C. (1999) Preparation of riboflavin 4',5'-cyclic phosphate by incubation of flavin-adenine dinucleotide with Mn^{2+} in the absence of riboflavin 5'-phosphate cyclase. *Anal. Biochem. 268*, 409-11.

(12) Bult, C. J., White, O., Olsen, G. J., Zhou, L., Fleischmann, R. D., Sutton, G. G., Blake, J. A., FitzGerald, L. M., Clayton, R. A., Gocayne, J. D., Kerlavage, A. R., Dougherty, B. A., Tomb, J. F., Adams, M. D., Reich, C. I., Overbeek, R., Kirkness, E. F., Weinstock, K. G., Merrick, J. M., Glodek, A., Scott, J. L., Geoghagen, N. S., and Venter, J. C. (1996) Complete genome sequence of the methanogenic archaeon, *Methanococcus jannaschii*. *Science 273*, 1058-73.

(13) Tabor, S., and Richardson, C. C. (1985) A bacteriophage T7 RNA polymerase/promoter system for controlled exclusive expression of specific genes. *Proc. Natl. Acad. Sci. U S A 82*, 1074-1078.

(14) Bradford, M. M. (1976) A rapid and sensitive method for the quantitation of microgram quantities of protein utilizing the principle of protein-dye binding. *Anal. Biochem. 72*, 248-54.

(15) Higashida, H., Hossain, K. Z., Takahagi, H., and Noda, M. (2002) Measurement of adenylyl cyclase by separating cyclic AMP on silica gel thin-layer chromatography. *Anal. Biochem. 308*, 106-11.
(16) Genschik, P., Billy, E., Swianiewicz, M., and Filipowicz, W. (1997) The human RNA 3'-terminal phosphate cyclase is a member of a new family of proteins conserved in Eucarya, Bacteria and Archaea. *Embo J. 16*, 2955-67.
(17) Pham, D. N., and Burgess, B. K. (1993) Nitrogenase reactivity: effects of pH on substrate reduction and CO inhibition. *Biochemistry 32*, 13725-31.
(18) Aravind, L., and Koonin, E. V. (1998) The HD domain defines a new superfamily of metal-dependent phosphohydrolases. *Trends Biochem. Sci. 23*, 469-72.
(19) Woo, H. J., Hwang, Y. K., Kim, Y. J., Kang, J. Y., Choi, Y. K., Kim, C. G., and Park, Y. S. (2002) *Escherichia coli* 6-pyruvoyltetrahydropterin synthase ortholog encoded by *ygcM* has a new catalytic activity for conversion of sepiapterin to 7,8-dihydropterin. *FEBS Lett. 523*, 234-8.
(20) Smith, G. K., Cichetti, J. A., Chandrasurin, P., and Nichol, C. A. (1985) The C-6 proton of tetrahydrobiopterin is acquired from water, not NADPH, during de novo biosynthesis. *J. Biol. Chem. 260*, 5221-4.
(21) Bonomi, F., Cerioli, A., and Pagani, S. (1989) Molecular aspects of the removal of ferritin-bound iron by DL-dihydrolipoate. *Biochim Biophys Acta 994*, 180-6.
(22) Kondo, N., Nakagawa, N., Ebihara, A., Chen, L., Liu, Z. J., Wang, B. C., Yokoyama, S., Kuramitsu, S., and Masui, R. (2007) Structure of dNTP-inducible dNTP triphosphohydrolase: insight into broad specificity for dNTPs and triphosphohydrolase-type hydrolysis. *Acta Crystallogr. D Biol. Crystallogr. 63*, 230-9.
(23) Bender, A. T., and Beavo, J. A. (2006) Cyclic nucleotide phosphodiesterases: molecular regulation to clinical use. *Pharmacol. Rev. 58*, 488-520.
(24) Huai, Q., Wang, H., Sun, Y., Kim, H. Y., Liu, Y., and Ke, H. (2003) Three-dimensional structures of PDE4D in complex with roliprams and implication on inhibitor selectivity. *Structure 11*, 865-73.
(25) Wang, H., Liu, Y., Hou, J., Zheng, M., Robinson, H., and Ke, H. (2007) Structural insight into substrate specificity of phosphodiesterase 10. *Proc. Natl. Acad. Sci. U S A 104*, 5782-7.
(26) Wang, H., Liu, Y., Chen, Y., Robinson, H., and Ke, H. (2005) Multiple elements jointly determine inhibitor selectivity of cyclic nucleotide phosphodiesterases 4 and 7. *J. Biol. Chem. 280*, 30949-55.
(27) Sung, B. J., Hwang, K. Y., Jeon, Y. H., Lee, J. I., Heo, Y. S., Kim, J. H., Moon, J., Yoon, J. M., Hyun, Y. L., Kim, E., Eum, S. J., Park, S. Y., Lee, J. O., Lee, T. G., Ro, S., and Cho, J. M. (2003) Structure of the catalytic domain of human phosphodiesterase 5 with bound drug molecules. *Nature 425*, 98-102.
(28) Shenoy, A. R., Capuder, M., Draskovic, P., Lamba, D., Visweswariah, S. S., and Podobnik, M. (2007) Structural and biochemical analysis of the Rv0805 cyclic nucleotide phosphodiesterase from *Mycobacterium tuberculosis*. *J. Mol. Biol. 365*, 211-25.
(29) Scapin, G., Patel, S. B., Chung, C., Varnerin, J. P., Edmondson, S. D., Mastracchio, A., Parmee, E. R., Singh, S. B., Becker, J. W., Van der Ploeg, L. H., and Tota, M. R. (2004) Crystal structure of human phosphodiesterase 3B: atomic basis for substrate and inhibitor specificity. *Biochemistry 43*, 6091-100.

(30) Richter, W. (2002) 3',5' Cyclic nucleotide phosphodiesterases class III: members, structure, and catalytic mechanism. *Proteins 46*, 278-86.
(31) Ke, H., and Wang, H. (2007) Crystal structures of phosphodiesterases and implications on substrate specificity and inhibitor selectivity. *Curr. Top. Med. Chem. 7*, 391-403.
(32) Iffland, A., Kohls, D., Low, S., Luan, J., Zhang, Y., Kothe, M., Cao, Q., Kamath, A. V., Ding, Y. H., and Ellenberger, T. (2005) Structural determinants for inhibitor specificity and selectivity in PDE2A using the wheat germ in vitro translation system. *Biochemistry 44*, 8312-25.
(33) Francis, S. H., Colbran, J. L., McAllister-Lucas, L. M., and Corbin, J. D. (1994) Zinc interactions and conserved motifs of the cGMP-binding cGMP-specific phosphodiesterase suggest that it is a zinc hydrolase. *J. Biol. Chem. 269*, 22477-80.
(34) Keppetipola, N., Shuman, S. (2008) A phosphate-binding histidine of binuclear metallo phosphodiesterase enzyme is a determinant of 2',3' cyclic nucleotide phosphodiesterase activity. *J. Biol. Chem. 283*, 30942-30949.
(35) Shin, D. H., Proudfoot, M., Lim, H. J., Choi, I. K., Yokota, H., Yakunin, A. F., Kim, R., and Kim, S. H. (2008) Structural and enzymatic characterization of DR1281: A calcineurin-like phosphoesterase from *Deinococcus radiodurans*. *Proteins 70*, 1000-9.
(36) Keppetipola, N., and Shuman, S. (2007) Characterization of the 2',3' cyclic phosphodiesterase activities of *Clostridium thermocellum* polynucleotide kinase-phosphatase and bacteriophage _ phosphatase. *Nucleic Acids Res. 35*, 7721-32.
(37) Zhang, Y., Zhang, J., Hara, H., Kato, I., and Inouye, M. (2005) Insights into the mRNA cleavage mechanism by MazF, an mRNA interferase. *J. Biol. Chem. 280*, 3143-50.
(38) Abelson, J., Trotta, C. R., and Li, H. (1998) tRNA splicing. *J. Biol. Chem. 273*, 12685-8.
(39) Kleman-Leyer, K., Armbruster, D. W., and Daniels, C. J. (1997) Properties of *H. volcanii* tRNA intron endonuclease reveal a relationship between the archaeal and eucaryal tRNA intron processing systems. *Cell 89*, 839-47.
(40) Yakunin, A. F., Proudfoot, M., Kuznetsova, E., Savchenko, A., Brown, G., Arrowsmith, C. H., and Edwards, A. M. (2004) The HD domain of the *Escherichia coli* tRNA nucleotidyltransferase has 2', 3'-cyclic phosphodiesterase, 2'-nucleotidase, and phosphatase activities. *J. Biol. Chem. 279*, 36819-36827.
(41) Klabunde, T., Strater, N., Frohlich, R., Witzel, H., and Krebs, B. (1996) Mechanism of Fe(III)-Zn(II) purple acid phosphatase based on crystal structures. *J. Mol. Biol. 259*, 737-48.
(42) Miller, D. J., Shuvalova, L., Evdokimova, E., Savchenko, A., Yakunin, A. F., and Anderson, W. F. (2007) Structural and biochemical characterization of a novel Mn^{2+}-dependent phosphodiesterase encoded by the *yfcE* gene. *Protein Sci. 16*, 1338-48.
(43) Chen, S., Yakunin, A. F., Kuznetsova, E., Busso, D., Pufan, R., Proudfoot, M., Kim, R., and Kim, S. H. (2004) Structural and functional characterization of a novel phosphodiesterase from *Methanococcus jannaschii*. *J. Biol. Chem. 279*, 31854-62.
(44) Huheey, J. E. (1972) Inorganic chemistry, principles of structure and reactivity. 214.
(45) Blaskó, A., and Bruice, T. C. (1999) Recent studies of nucleophilic, general-acid, and metal ion catalysis of phosphate diester hydrolysis. *Acc. Chem. Res. 32*, 475-484.
(46) williams, N. H., Takasaki, B., and Wall, M., Chin, J. (1999) Structure and Nuclease Activity of Simple Dinuclear Metal Complexes: Quantitative Dissection of the Role of Metal Ions. *Acc. Chem. Res. 32*, 485-493.
(47) Barnard, E. (1969) Ribonucleases. *Annu. Rev. Biochem. 38*, 677-732.

(48) Usher, D. A., Erenrich, E. S., and Eckstein, F. . (1972) Geometry of the first step in the action of ribonuclease-A (in-line geometry-uridine2',3'-cyclic thiophosphate- 31 P NMR). *Proc. Natl. Acad. Sci. U S A 69*, 115-8.

(49) Usher, D. A., Richardson, D. I., Jr., and Eckstein, F. . (1970) Absolute stereochemistry of the second step of ribonuclease action. *Nature 228*, 663-5.

(50) Eckstein, F., Schulz, H. H., Ruterjans, H., Haar, W., and Maurer, W. ((1972) Stereochemistry of the transesterification step of ribonuclease T 1. *Biochemistry 11*, 3507-12.

(51) Gerlt, J. A., and Wan, W. H. . (1979) Stereochemistry of the hydrolysis of the endo isomer of uridine 2',3'-cyclic phosphorothioate catalyzed by the nonspecific phosphohydrolase from *Enterobacter aerogenes*. *Biochemistry 18*, 4630-8.

CHAPTER 3

Identification and Characterization of an Archaeal Specific Riboflavin Kinase

The result of this work is published in: *Journal of Bacteriology.* 190(7): 2615 – 2618 (2008)

Zahra Mashhadi, Hong Zhang, Huimin Xu, Robert H. White

As first author I designed and performed experiments, prepared the figures and helped to write the manuscript. Dr. Hong Zhang was involved in manuscript preparation, and Huimin Xu did all cloning and protein expression.

Department of Biochemistry, Virginia Tech, Blacksburg, VA, 24061

3.1 ABSTRACT

The riboflavin kinase in *Methanocaldococcus jannaschii* has been identified as the product of the MJ0056 gene. Recombinant expression of the MJ0056 gene in *E. coli* led to a large increase in the amount of FMN in the *E. coli* cell extract. The unexpected features of the purified recombinant enzyme were its use of CTP as the phosphoryl donor and the absence of a requirement for added metal ions to catalyze the formation of FMN from CTP and riboflavin. Identification of this riboflavin kinase fills another gap in the Archaeal flavin biosynthetic pathway. Some divalent metals were found to be potent inhibitors of the reaction. The enzyme is a unique CTP-dependent kinase, which maybe represents the first member of a new kinase family.

3.2 INTRODUCTION

Work on the biosynthesis of riboflavin, FMN, and FAD in the archaea has revealed a number of surprises both in terms of the genes encoding the pathway enzymes as well as the pathway itself. Analysis of archaeal genomes has generally shown the absence of *ribA*, the gene encoding for GTP cyclohydrolase II, the first enzyme involved in the presently established pathways to riboflavin in bacteria. In the archaea this reaction was found to be catalyzed by two separate enzymes (Fig. 1.5). The first enzyme GTP cyclohydrolase III (ArfA), produces 2-amino-5-formylamino-6-ribofuranosylamino 4(*3H*)-pyrimidinone 5'-phosphate (compound 2 in Fig. 1.5) and two inorganic phosphates by hydrolysis of GTP (*1*). This intermediate is subsequently hydrolyzed to 2,5-diamino-6-ribofuranosylamino 4(*3H*)-pyrimidinone 5'-phosphate (compound 3), by ArfB, the MJ0116 gene product in *M. jannaschii (2)*. Compound 3 is then converted into 5-amino-6-ribitylamino-2,4(1*H*,3*H*)pyrimidinedione (ARP, compound 6 in Fig. 1.5) by a dehydrogenase designated as ArfC (MJ0671 gene product in *M. jannaschii*) (*3, 4*), a deaminase and a phosphatase following the eukaryotic pathway (*3*). The involvement of compound 2 in the pathway does not occur in either the bacterial or eukaryotic pathways. The dehydrogenase and deaminase steps are in the same order as the eukaryotic pathway and are

reverse from that found in the bacterial pathway (Fig. 1.5). The product of this series of reactions, ARP, is the precursor to F_{420} and riboflavin (*5*). In the conversion of ARP to riboflavin in the archaea, there is a fundamental difference in the stereochemistry of the pentacyclic intermediate involved in the dismutation of 6,7-dimethyl-8-ribityllumazine into riboflavin and 5-amino-6-ribitylamino2,4(1H,3H)-pyrimidinedione in the last step of riboflavin biosynthesis (*6*).

Two different sets of known enzymes involved in the conversion of riboflavin to a redox active form as FMN or FAD. One set includes bacterial bifunctional enzyme (RibF) which catalyzes first the phosphorylation of riboflavin to FMN follow by adenylation of FMN to FAD (*7, 8*). ATP is the other substrate in both steps. In the other set these two consecutive steps are catalyzed by two separate enzymes, riboflavin kinase (RibR, flavokinase, or FMN1) and FAD synthetase (FAD1 in yeast) (*9*). Enzymes homologs to the yeast flavokinase (FMN1) (*10*) are widely distributed (*11*).

Aside from the differences in the enzymes used to generate FAD, other differences in the pathways and/or enzymes have been noted. It has been reported that the *ribF* gene in *Bacillus subtilis* uses reduced riboflavin as the substrate (*12, 13*), the *Corynebacterium ammoniagenes* RibF can use meta-phosphate as the phosphoryl donor (*14*) and the macrolide resistance gene *mreA* of *Streptococcus agalactiae* has also been shown to function as a riboflavin kinase (*15*).

The absence of identifiable genes encoding for any of these enzymes in the archaea has prompted a search for the genes/reactions required to carry out these last two steps of FAD biosynthesis in the methanogens. Here we report that the MJ0056 derived protein is an archaeal specific riboflavin kinase that catalyzes phosphorylation of riboflavin to produce FMN by using CTP as a phosphoryl donor (Fig. 3.1). We designate it RibK to indicate the unique character of this archaeal riboflavin kinase. To date, orthologs of MJ0056 are found only in archaea. These findings indicated that this gene product is the archaeal kinase despite the fact that it has no detectable sequence similarity to any known kinase.

3.3 MATERIALS AND METHODS

Chemicals. All chemicals were obtained from Sigma/Aldrich.

Cloning, Recombinant Expression and Purification of RibK. The *M. jannaschii* gene at locus MJ0056 (Swiss-Prot accession number Q60365) (*16*) was amplified by PCR from *M. jannaschii* genomic DNA using oligonuculeotide primers synthesized by Invitrogen. The primer MJ0056Fwd 5'-GGTCATATGATTATTGAGGGAGAAG-3' introduced an *Nde*I restriction site at the 5'-end of amplified DNA and MJ0056Rev 5'-GATCGGATCCTTATTCATCTTTATCTCCC-3' introduced an *Bam*HI restriction site at the 5'-end. PCR mixtures consisted of 1× GeneAmp PCR buffer (Invitrogen), 1 μM each primer, 200 μM each dNTP, 1 μg of *M. jannaschii* chromosomal DNA, and 5 units of AmpliTaq LD DNA polymerase (Invitrogen) in a volume of 100 μL. The MJ0056 gene was amplified during 35 cycles, and each cycle include incubation at 95 °C for 1 min, 55 °C for 2 min, and 72 °C for 3 min. PCR product was purified using a QIA spin column (QIAGEN Inc.). Purified PCR product was digested with *Nde*I and *Bam*HI restriction enzymes (Invitrogen). DNA fragments were ligated into compatible sites in plasmid pT7-7 (*17*) using bacteriophage T4 DNA ligase. Recombinant plasmid, pMJ0056, was transformed into *Escherichia coli* strain BL21-Codon Plus (DE3)-RIL (Stratagene). Plasmid DNA sequence was verified by dye terminator cycle sequencing at University of Iowa, DNA Facility.

Transformed *E. coli* cells were grown in Luria-Bertani/Miller broth (200 mL) supplemented with 1 mg/mL ampicillin. Cultures were shaken at 37 °C and 250 rpm until they reached an absorbance of 1.0 at 600 nm. Expression of the MJ0056 gene was then induced by adding 2% (w/v) of D-(+)-lactose. After an additional 4 h incubation with shaking at 37 °C, the cells were harvested by centrifugation (6000 × *g,* 10 min). The harvested cells were stored at –20 °C. Production of recombinant RibK was confirmed by SDS-PAGE analysis of the cellular proteins.

The frozen *E. coli* cell pellet (~0.5 g wet weight) was suspended in 3 mL of extraction buffer (50 mM *N*-tris(hydroxymethyl)methyl-2-aminoethanesulfonic acid (TES), pH 7.0, 10 mM $MgCl_2$, 20 mM DTT) and lysed by sonication using Heat Systems Ultrasonics/W-385 sonicator (3 min, 5 sec pulse with a 5 sec pause between pulses). RibK was found to remain soluble after heating the cell extracts for 10 min at 70 °C. This process allowed for its purification from the majority of *E. coli* proteins, which denature and precipitate under these conditions. In the second step of purification, RibK was purified by anion-exchange chromatography of the 70 ^{o}C soluble fraction on a MonoQ HR column (1 × 8 cm; Amersham Bioscience) using a linear gradient of

NaCl from 0 to 1 M in 25 mM TES buffer, pH 7.5 over 55 mL at one mL/min flow rate. Elution of the protein was monitored by UV absorbance at 280 nm. RibK elutes at about 0.2 M NaCl. All protein concentrations were determined by Bradford analysis (*18*).

Measurement of Native Molecular Weight of RibK. The native molecular weight of RibK was determined by size exclusion chromatography on a Superose 12HR column (1 × 30 cm; Amersham Biosciences) separated with aerobic buffer containing 50 mM HEPES pH 7.2, and 50 mM NaCl at 0.5 mL/min with detection at 280 nm. Protein standards used to calibrate the column included alcohol dehydrogenase (150 kDa), bovine serum albumin (66 kDa), carbonic anhydrase (29 kDa), and cytochrome c (12.4 kDa).

Metal Ion Analysis of RibK. The MonoQ purified protein was analyzed for iron, manganese, magnesium, and zinc at the Virginia Tech Soil Testing Laboratory using inductively coupled plasma emission spectrophotometry (ICPES). The ICPES was a Spectro CirOS VISION (Spectro Analytical Instruments) equipped with a Crossflow nebulizer with a Modified Scott spray chamber. A 50 mg/L yttrium internal standard was introduced by peristaltic pump. The protein fraction was diluted in elution buffer to give a final metal concentration of 0.5 ppm prior to analysis, assuming one equivalent of metal per protomer.

Analysis of Enzymatic Activity of RibK. The standard assay for RibK was performed by incubation of 47 mM TES buffer, pH 7.2, containing 1.2 μg of RibK, 1.7 mM CTP and 0.37 mM riboflavin in a final volume of 61 μL at 70 °C for 10 min. Following incubation 100 μL of methanol was added to stop the reaction. After centrifugation (14000*g*, 10 min) and evaporation of the methanol, H_2O was added to the supernatant to adjust the volume to 660 μL for HPLC analysis. Analysis of the enzyme-catalyzed reaction was conducted using HPLC with detection of riboflavin and FMN using a Shimadzu HPLC System with a C18 reverse-phase column (Varian PursuitXRs, 250 × 4.6 mm, 5 μm particle size) and detected by fluorescence using λ_{max} excitation of 450 nm and λ_{max} emission of 520 nm. The elution profile consisted of 5 min at 95% sodium acetate buffer (25 mM, pH 6.0, 0.2% NaN_3) and 5% methanol followed by a linear gradient to 20% sodium acetate buffer/80% MeOH over 40 min at 0.5 mL/min.

Characterization of the Enzymatically Prepared FMN. After incubation of RibK under standard assay as described above, the identification of FMN as a product was established by its absorbance spectra by SPD-M10AVP Diode Array detector after HPLC separation. Also,

electrospray mass spectroscopy (ES-MS) analysis by direct infusion. Known FMN also was used as control.

Testing Alternative Substrates. RibK was tested for its ability to use other nucleotides such as CTP and GTP as a phosphoryl donor to riboflavin to produce FMN. The standard assay conditions were used in the incubation in presence of either 1.7 mM ATP or GTP instead of CTP.

Metal-ion dependency of RibK reaction. The assay for metal dependency of RibK was performed by incubation of 1.2 μg RibK with 1.7 mM CTP, 0.37 mM riboflavin and 1.6 mM Mg^{2+}, Mn^{2+}, Zn^{2+}, Ni^{2+}, Cu^{2+} or Co^{2+}, no metal, or EDTA under standard assay conditions.

Determination of the Kinetic Constants for RibK. Assays to determine the kinetic constants for CTP were performed under standard assay conditions with the following modifications. In this assay 1.2 μg of RibK was incubated in 47 mM TES (K^+) buffer, pH 7.2, and 26 μM riboflavin in presence of either 0, 2, 4, 20, 61, 182, or 546 μM CTP in a total volume of 61 μL at 70 ˚C for 10 min. To determine the kinetic constants for riboflavin, the assay was performed as above in presence of 1.6 mM CTP and the concentration of riboflavin was varied from 0, 1.3, 2.6, 6.6, 13, or 26 μM riboflavin.

3.4 RESULTS

Recombinant Expression and Purification of RibK

The MJ0056 gene from *M. jannaschii* was cloned and RibK overexpressed in *E. coli.* The resulting protein was purified by first heating the cell extract at 70 °C followed by anion-exchange chromatography of the soluble proteins. The SDS-PAGE analysis of fractions of the purified RibK with Coomassie staining showed a single band corresponding to the mass of about 15 kDa with a purity of >95%. This molecular weight is consistent with the predicted monomeric molecular mass of 15.7 kDa. ES-MS measured a mass of 15218.1 ± 10 that agrees with the calculated mass of 15213.8 from the gene sequence for a protein of 132 amino acids. The data from size exclusion chromatography indicated that the enzyme was a monomer (19.7 kDa).

Identification of Reaction Catalyzed by RibK

Incubation of RibK with riboflavin and CTP at 70 °C for 10 min produced a new fluorescent compound when the reaction mixture was assayed by HPLC with detection at the flavin excitation/emission wavelength. Under these conditions riboflavin eluted at 31.1 min, FMN at 29 min and FAD at 26.5 min. The peak was identified as FMN based on its HPLC elution time (29 min) as compared to the known. The new peak had the FMN absorbance spectrum, which shows λ_{max} at 267, 370, and 446 nm. ES-MS analysis of direct infusion of the product, gave the same ES-MS spectrum as authentic FMN with a $[MH]^+$ ion at 457.0 *m/z* and $[MNa]^+$ ion at 479.0 *m/z* in the positive mode (Fig. 3.2 A) and a $[M-H]^-$ ion at 454.9 *m/z* in the negative mode (Fig. 3.2 B). The MS-MS of the 457.0 *m/z* ion for both the known and enzymatically generated FMN gave the same ions at 439.0 *m/z* for $[M-H_2O]^+$, 377.1 *m/z* for $[riboflavin]^+$, 359.1 *m/z* for $[riboflavin-H_2O]^+$ and 243.1 *m/z* for [flavin ring system]$^+$ (Fig. 3.2 C). The MS-MS of 454.9 *m/z* ion for both the known and enzymatically generated FMN gave the same ions at 241.0 *m/z* for [flavin ring system]$^-$, 212.9 *m/z* for [M-flavin ring system]$^-$ and 96.9 *m/z* for $[phosphate]^-$ (Fig. 3.2 D).

Testing Alternative Substrates

RibK was able to utilize other nucleotides such as ATP and GTP as phosphoryl donor, to convert riboflavin to FMN. The enzyme was most active with CTP as substrate. RibK activity with 1.7 mM ATP or GTP was 30% and 11% of that seen with CTP, respectively.

Metal Content and Metal-Ion Dependency of RibK Reaction

ICPES was used to determine the identity and quantity of metal ions present in the purified recombinant enzyme. The result showed four to five moles of Mg and 0.0013 moles of Zn per mole of protein. Using the standard assay method supplemented with ether no metal ions or with 1.6 mM Mg^{2+}, Mn^{2+}, Zn^{2+}, Ni^{2+}, Cu^{2+} or Co^{2+} or in present of EDTA the following specific activities were observed: 60.5, 57.1, 32.8, 10, 36, 2.2, 25, and 0.28 nmol min^{-1} mg^{-1}, respectively (Fig. 3.3).

Determination of the Kinetic Parameters of RibK

The RibK kinetics were determined under steady state conditions in the presence of saturating concentrations of either CTP or riboflavin. KeleidaGraph 4.0 was used to calculate the kinetic parameters from the Michaelis-Menten plot. The measured kinetic parameters for RibK with CTP as the phosphate donor are as follow: for riboflavin, K_M^{app} = 18.3 ± 0.8 μM, V_{max}= 109 ± 3 nmol min^{-1} mg^{-1}, and $K_{cat}/K_M = 1.5 \times 10^3$ $M^{-1}sec^{-1}$ and for CTP: K_M^{app} = 0.3 ± 0.05 mM, V_{max}= 72 ± 4 nmol min^{-1} mg^{-1}, and K_{cat}/K_M = 60 $M^{-1}sec^{-1}$.

Analysis of FMN in E. coli Overexpressing ribK

After overexpressing *ribK* in *E. coli* the cell extract was yellow indicating the presence of a flavin. Since these flavins eluted from MonoQ-separated cell extracts, the MonoQ fractions containing flavins were used to measure the amount of riboflavin, FMN, and FAD in the extracts. The flavins of the most intense fraction was separated by HPLC and then identified by their fluorescence. The fraction from the *ribK* expression contains about 8.7 μM FMN and it contains no FAD. This value was six fold higher than was observed in cell extracts from cells expressing other enzymes not related to FMN production.

3.5 DISCUSSION

Riboflavin serves as an redox active coenzyme either after phosphorylation, to form FMN, or after phosphorylation and then adenylation, to form FAD. Bacteria possess a bifunctional enzyme (RibF) that first acts as a kinase converting riboflavin to FMN in the presence of ATP and then acts as a nucleotidyl transferase using a second ATP to convert the FMN to FAD and PPi (*7, 8*). Conversion of riboflavin to FAD in Eukaryotes requires involvement of two separate monofunctional enzymes, riboflavin kinase (RibR, flavokinase, or FMN1) and FAD synthetase (FAD1 in yeast) (*9*). The absence of identifiable genes encoding for

any of these enzymes in archaea has prompted a search for the genes/reactions required to carry out these last two steps of FAD biosynthesis in the methanogens.

It was noticed that the crystal structure of MJ0056 gene product recently deposited in the PDB (code 2oyn) had a similar structural fold to that found in the human and yeast riboflavin kinases (*19, 20*), as well as the riboflavin kinase domain of the flavin-binding protein from *Thermotoga maritima*, annotated as an FAD synthetase (*21*). This crystal structure also contained a bound CDP in the same position as the ATP bound in the human enzyme. In addition, in the archaeal genomes of *Archaeoglobus fulgidus* DSM 4304, *Haloarcula marismortui* ATCC 43049, *Halobacterium* sp. NRC-1, *Methanothermobacter thermautotrophicus* str. ΔH, *Methanococcus maripaludis* S2, *Methanococcoides burtonii* DSM 6242, *Methanosarcina acetivorans* C2A, *Methanosarcina mazei* Go1, and *Methanopyrus kandleri* AV19, the MJ0056 gene (*ribK*) is next to the MJ0055 gene (*ribB*), which encodes 3,4-dihydroxy-2-butanone-4-phosphate synthase that is involved in the biosynthesis of riboflavin (Fig. 1.5). The MJ0056 derived protein is an archaeal specific riboflavin kinase that catalyzes the reaction shown in Figure 3.1. We designate it RibK to indicate the unique character of this archaeal riboflavin kinase. To date, orthologs of MJ0056 are found only in archaea.

The *E. coli* cells that overexpressed *ribK*, have more FMN compared to other *E. coli* cells overexpressing a gene not related to riboflavin biosynthesis. Our data shows that cell extracts derived from cells expressing *ribK* was found to have six fold more FMN than was observed in cell extracts from cells expressing other enzymes not related to FMN production.

RibK is unique in using CTP as a phosphoryl donor. RibK is also able to use other nucleotides, ATP and GTP, as a substrate. The activities with ATP and GTP at the same concentrations were 30% and 11% of that seen with CTP, respectively. All of the previously reported riboflavin kinases are metal dependent and they are mostly Zn^{2+} or Mg^{2+} dependent (*13, 22, 23*). Using the standard assay method supplemented with ether no metal ion or with 1.6 mM Mg^{2+}, Mn^{2+}, Zn^{2+}, Ni^{2+}, Cu^{2+} or Co^{2+} the following specific activities were observed: 0.7, 0.6, 0.35, 0.12, 0.4, 0.02, 0.27 $\mu mol\ min^{-1}\ mg^{-1}$.

As shown in Figure 3.3, RibK has the best activity without any added metal and EDTA causes total inactivation of the enzyme. Metal analysis of purified RibK revealed that it contains five moles of Mg per mole of protomer and so RibK does not need additional metal to be active.

Adding any metal except Mg^{2+} inhibits the activity of the RibK and Zn^{2+} and Cu^{2+} are the most powerful inhibitors for this enzyme (Fig. 3.3).

There is a wide range of kinetic values reported for riboflavin kinases from different organisms. The lowest K_M values reported for riboflavin and ATP are 120 nM and 210 nM, respectively, for flavokinase from *Neurospora crassa (22)* and the highest K_M values for riboflavin and ATP are reported as 420 μM and 4.55 mM, respectively, for the rat liver enzyme (*24*). Also the range of specific activities for flavokinases varies enormously, ranging from 0.00023 μmol min^{-1} mg^{-1} for flavokinase in rat liver (*24*) to 2.95 μmol min^{-1} mg^{-1} for flavokinase from *Neurospora crassa* (*22*). The RibK kinetic values (K_M^{app} = 18.3 ± 0.8 μM, V_{max}= 109 ± 3 nmol min^{-1} mg^{-1}, and $k_{cat}/K_M = 1.5 \times 10^3\ M^{-1}sec^{-1}$ and for riboflavin and K_M^{app} = 0.3 ± 0.05 mM, V_{max}= 72 ± 4 nmol min^{-1} mg^{-1}, and $k_{cat}/K_M = 60\ M^{-1}sec^{-1}$ for CTP) fall in the middle of this broad range. The reasons why this enzyme preferentially uses CTP as the phosphate donor instead of ATP, as is found in all most all known kinases, is not clear. ^{1}H-NMR analysis of *M. jannaschii* cell extracts indicates that the concentration of CTP is comparable to that of ATP (R. H. White, unpublished). Thus the enzyme could simply be taking advantage of the high CTP concentration. The only known example of a CTP dependent kinase is dolichol kinase (*25*). There are a few GTP-dependent kinases e.g. phosphoglycerate kinase (*26*), polyribonucleotide 5'-hydroxyl-kinase (*27*) and some kinases are probably promiscuous and can use either GTP or CTP. There are also some other non ATP-dependent kinases such as a few ADP-dependent and pyrophosphate kinases (*28, 29*).

The evolutionary lineage of this archaeal riboflavin kinase is not clear, as it is so different from all other kinases. This alternation in kinases is common in the archaeal biosynthetic pathways where we find a new shikimate kinase in the shikimate pathway (*30*), a new isopentenyl phosphate kinase in a new pathway to isoprenoids (*31*) and a new predicted panthothenate kinase in coenzyme A biosynthesis (*32*).

An important biological implication of the presence of RibK homologs in those archaeal genomes that have no genes for *de novo* riboflavin synthesis, such as: *Pyrococcus abyssi* GE5, *Pyrococcus horikoshii* OT3, and *Thermoplasma acidophilum* DSM 1728 is that RibK provides a route for FMN and FAD biogenesis via salvage pathway from exogenous riboflavin.

While this work was under review, Ammelburg, et. al., published data showing that the MJ0056 gene product was a riboflavin kinase and proposed a evolutionary lineage of MJ0056 to other riboflavin kinases (*33*).

3.6 ACKNOWLEDGMENT

The author wishes to thank Kim Harich for assistance with obtaining the mass spectral data, Keith Ray for ES-MS data and Walter Niehaus and Laura Grochowski for assistance in editing the manuscript.

3.7 FIGURES

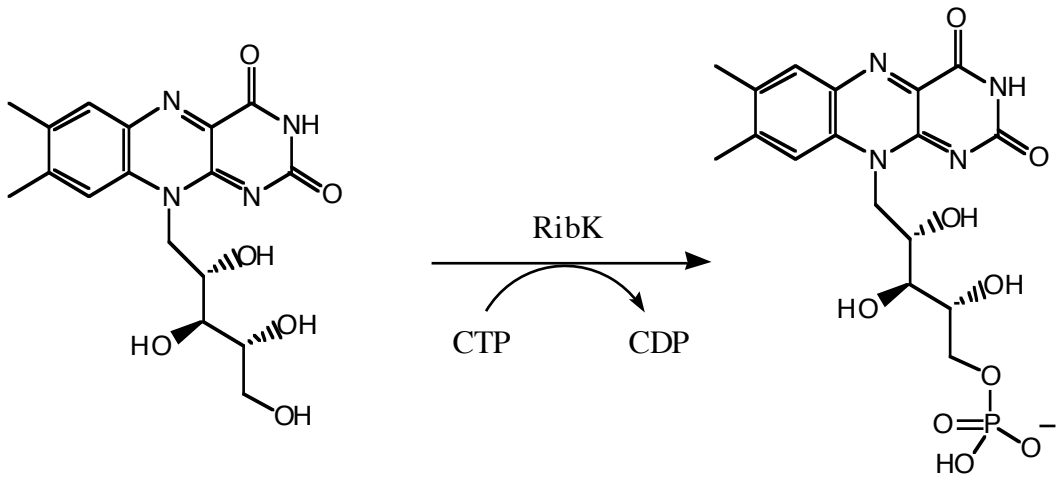

Riboflavin FMN

Figure 3.1 The reaction catalyzed by RibK.

RibK is unique in using CTP as phosphoryl donor for phosphorylation of riboflavin to form FMN.

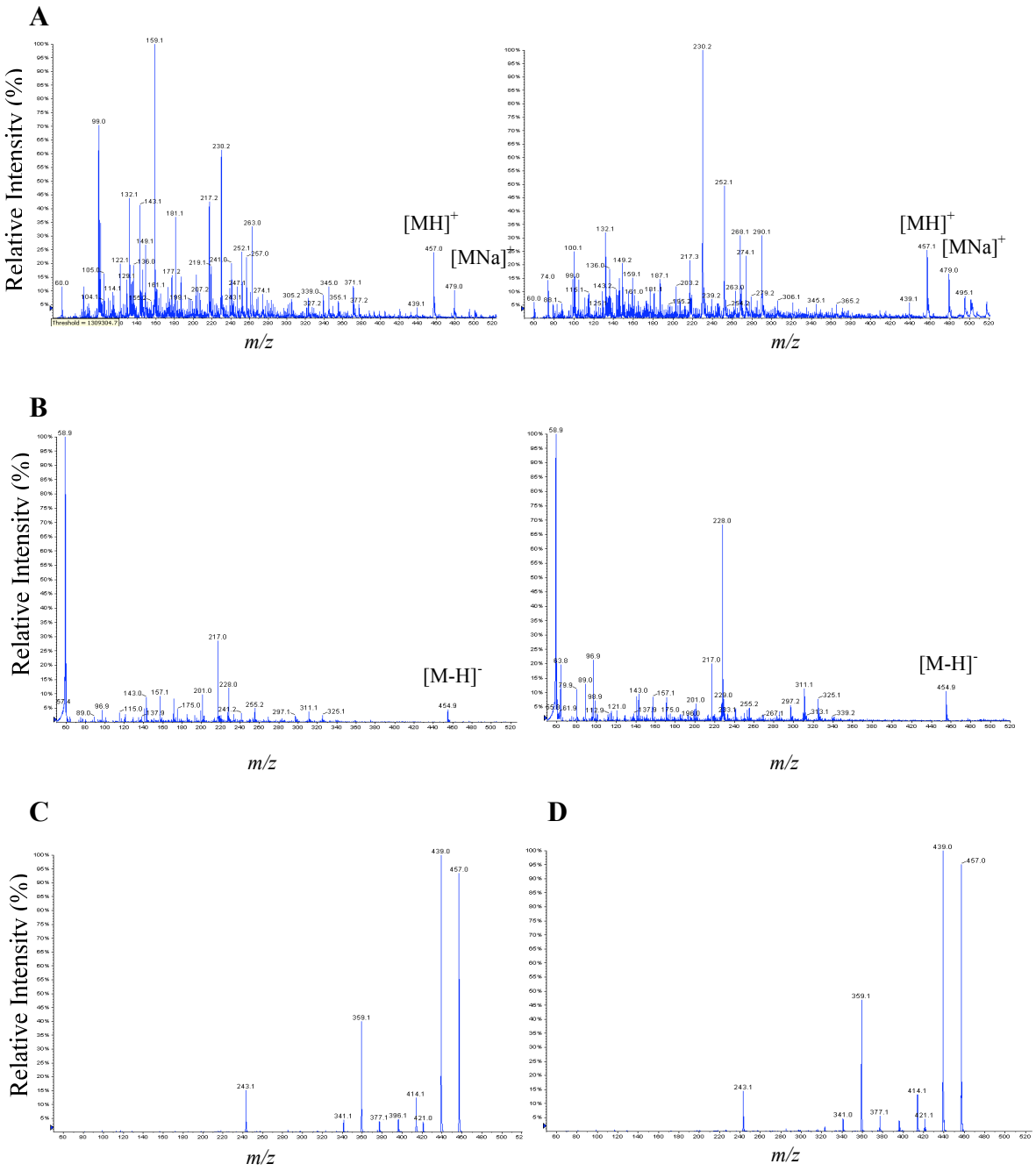

Figure 3.2 ES-MS and MS-MS spectrum of Known FMN and RibK-produced FMN.

ES-MS spectrum of authentic FMN (left) and enzymatically generated FMN (right) in the positive mode (A) and in the negative mode (B). The MS-MS of the 457.0 *m/z* ion for both the known and enzymatically generated FMN gave the same ions
(C). The MS-MS of 454.9 *m/z* ion for both the known and enzymatically generated FMN gave the same ions (D).

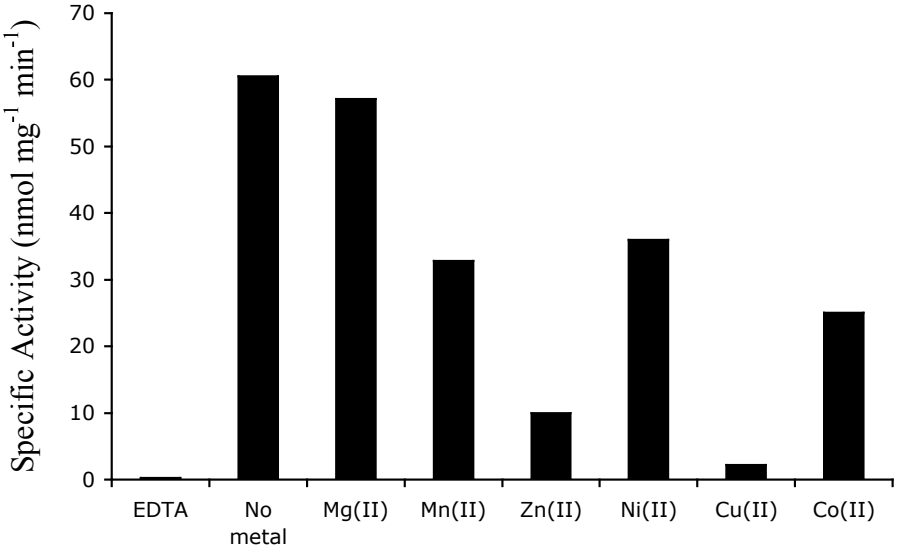

Figure 3.3 Specific activity of RibK assayed with different metals.

MonoQ purified RibL (1.2 μg) was incubated with 1.7 mM CTP, 0.37 mM riboflavin and either EDTA, no added metal, or the indicated metals at concentration of 1.6 mM in a total volume of 61 μL of TES buffer.

REFERENCES

(1) Graham, D. E., Xu, H., and White, R. H. (2002) A member of a new class of GTP cyclohydrolases produces formylaminopyrimidine nucleotide monophosphates. *Biochemistry 41*, 15074-84.

(2) Grochowski, L. L., Xu, H., and White, R. H. (2009) An iron(II) dependent formamide hydrolase catalyzes the second step in the archaeal biosynthetic pathway to riboflavin and 7,8-didemethyl-8-hydroxy-5-deazariboflavin. *Biochemistry 48*, 4181-8.

(3) Graupner, M., Xu, H., and White, R. H. (2002) The pyrimidine nucleotide reductase step in riboflavin and F_{420} biosynthesis in archaea proceeds by the eukaryotic route to riboflavin. *J. Bacteriol. 184*, 1952-7.

(4) Chatwell, L., Krojer, T., Fidler, A., Romisch, W., Eisenreich, W., Bacher, A., Huber, R., and Fischer, M. (2006) Biosynthesis of riboflavin: structure and properties of 2,5-diamino-6-ribosylamino-4(3*H*)-pyrimidinone 5'-phosphate reductase of *Methanocaldococcus jannaschii*. *J. Mol. Biol. 359*, 1334-1351.

(5) Graham, D. E., and White, R. H. (2002) Elucidation of methanogenic coenzyme biosynthesis: from spectroscopy to genomics. *Nat. Prod. Rep. 19*, 133-147.

(6) Illarionov, B., Eisenreich, W., Schramek, N., Bacher, A., and Fischer, M. (2005) Biosynthesis of vitamin B_2: diastereomeric reaction intermediates of archaeal and non-archaeal riboflavin synthases. *J. Biol. Chem. 280*, 28541-28546.

(7) Efimov, I., Kuusk, V., Zhang, X., and McIntire, W. S. (1998) Proposed steady-state kinetic mechanism for *Corynebacterium ammoniagenes* FAD synthetase produced by *Escherichia coli*. *Biochemistry 37*, 9716-9723.

(8) Manstein, D. J., and Pai, E. F. (1986) Purification and characterization of FAD synthetase from *Brevibacterium ammoniagenes*. *J. Biol. Chem. 261*, 16169-16173.

(9) Wu, M., Repetto, B., Glerum, D. M., and Tzagoloff, A. (1995) Cloning and characterization of FAD1, the structural gene for flavin adenine dinucleotide synthetase of *Saccharomyces cerevisiae*. *Mol. Cell. Biol. 15*, 264-271.

(10) Santos, M. A., Jimenez, A., and Revuelta, J. L. (2000) Molecular characterization of FMN1, the structural gene for the monofunctional flavokinase of *Saccharomyces cerevisiae*. *J. Biol. Chem. 275*, 28618-28624.

(11) von Mering, C., Jensen, L. J., Kuhn, M., Chaffron, S., Doerks, T., Kruger, B., Snel, B., and Bork, P. (2007) STRING 7--recent developments in the integration and prediction of protein interactions. *Nucleic Acids Res. 35*, D358-362.

(12) Solovieva, I. M., Kreneva, R. A., Leak, D. J., and Perumov, D. A. (1999) The *ribR* gene encodes a monofunctional riboflavin kinase which is involved in regulation of the *Bacillus subtilis* riboflavin operon. *Microbiology 145 (Pt 1)*, 67-73.

(13) Kearney, E. B., Goldenberg, J., Lipsick, J., and Perl, M. (1979) Flavokinase and FAD synthetase from *Bacillus subtilis* specific for reduced flavins. *J. Biol. Chem. 254*, 9551-7.

(14) Nakagawa, S., and al., e. (1995) Metaphosphate-dependent phosphorylation of riboflavin to FMN by *Corynebacterium ammoniagenes*. *Appl. Microbiol. Biotechnol. 43*, 325-329.

(15) Clarebout, G., Villers, C., and Leclercq, R. (2001) Macrolide resistance gene mreA of *Streptococcus agalactiae* encodes a flavokinase. *Antimicrob. Agents Chemother. 45*, 2280-2286.

(16) Bult, C. J., White, O., Olsen, G. J., Zhou, L., Fleischmann, R. D., Sutton, G. G., Blake, J. A., FitzGerald, L. M., Clayton, R. A., Gocayne, J. D., Kerlavage, A. R., Dougherty, B. A., Tomb, J. F., Adams, M. D., Reich, C. I., Overbeek, R., Kirkness, E. F., Weinstock, K. G., Merrick, J. M., Glodek, A., Scott, J. L., Geoghagen, N. S., and Venter, J. C. (1996) Complete genome sequence of the methanogenic archaeon, *Methanococcus jannaschii*. *Science 273*, 1058-73.

(17) Tabor, S., and Richardson, C. C. (1985) A bacteriophage T7 RNA polymerase/promoter system for controlled exclusive expression of specific genes. *Proc. Natl. Acad. Sci. U S A 82*, 1074-1078.

(18) Bradford, M. M. (1976) A rapid and sensitive method for the quantitation of microgram quantities of protein utilizing the principle of protein-dye binding. *Anal. Biochem. 72*, 248-54.

(19) Bauer, S., Kemter, K., Bacher, A., Huber, R., Fischer, M., and Steinbacher, S. (2003) Crystal structure of *Schizosaccharomyces pombe* riboflavin kinase reveals a novel ATP and riboflavin-binding fold. *J. Mol. Biol. 326*, 1463-1473.

(20) Karthikeyan, S., Zhou, Q., Mseeh, F., Grishin, N. V., Osterman, A. L., and Zhang, H. (2003) Crystal structure of human riboflavin kinase reveals a beta barrel fold and a novel active site arch. *Structure 11*, 265-73.

(21) Wang, W., Kim, R., Yokota, H., and Kim, S. H. (2005) Crystal structure of flavin binding to FAD synthetase of *Thermotoga maritima*. *Proteins 58*, 246-248.

(22) Rajeswari, S. R., Jonnalagadda, V. S., and Jonnalagadda, S. . (1999) Purification and characterization of flavokinase from *Neurospora crassa*. *Indian J. Biochem. Biophys. 36*, 137-142.

(23) Merrill, A. H., Jr., and McCormick, D. B. (1980) Affinity chromatographic purification and properties of flavokinase (ATP:riboflavin 5'-phosphotransferase) from rat liver. *J. Biol. Chem. 255*, 1335-8.

(24) Bandyopadhyay, D., Chatterjee, A. K., and Datta, A. G. (1997) Effect of cadmium on purified hepatic flavokinase: involvement of reactive -SH group(s) in the inactivation of flavokinase by cadmium. *Life Sci. 60*, 1891-903.

(25) Allen, C., M. Jr.,, Jack R. Kalin, Jonathan Sack, and Verizzo, D. CTP-Dependent Dolichol Phosphorylation by Mammalian Cell Homogenates. *Biochemistry 17*, 5020-5026.

(26) Reeves, R. E., and South, D. J. (1974) Phosphoglycerate kinase (GTP). An enzyme from *Entamoeba histolytica* selective for guanine nucleotides. *Biochem. Biophys. Res. Commun. 58*, 1053-7.

(27) Westaway, S. K., Belford, H. G., Apostol, B. L., Abelson, J., and Greer, C. L. (1993) Novel activity of a yeast ligase deletion polypeptide. Evidence for GTP-dependent tRNA splicing. *J. Biol. Chem. 268*, 2435-2443.

(28) Hansen, T., and Schonheit, P. (2004) ADP-dependent 6-phosphofructokinase, an extremely thermophilic, non-allosteric enzyme from the hyperthermophilic, sulfate-reducing archaeon *Archaeoglobus fulgidus* strain 7324. *Extremophiles 8*, 29-35.

(29) Ronimus, R. S., and Morgan, H. W. (2001) The biochemical properties and phylogenies of phosphofructokinases from extremophiles. *Extremophiles 5*, 357-73.

(30) Daugherty, M., Vonstein, V., Overbeek, R., and Osterman, A. (2001) Archaeal shikimate kinase, a new member of the GHMP-kinase family. *J. Bacteriol. 183*, 292-300.

(31) Grochowski, L. L., Xu, H., and White, R. (2006) *Methanocaldococcus jannaschii* uses a modified mevalonate pathway for the biosynthesis of isopentenyl diphosphate. *J. Bacteriol. 188*, 3192-3198.
(32) Genschel, U. (2004) Coenzyme A biosynthesis: reconstruction of the pathway in archaea and an evolutionary scenario based on comparative genomics. *Mol. Biol. Evol. 21*, 1242-1251.
(33) Ammelburg, M., Hartmann, M. D., Djuranovic, S., Alva, V., Koretke, K. K., Martin, J., Sauer, G., Truffault, V., Zeth, K., Lupas, A. N., and Coles, M. (2007) A CTP-Dependent Archaeal Riboflavin Kinase Forms a Bridge in the Evolution of Cradle-Loop Barrels. *Structure 15*, 1577-1590.

CHAPTER 4

Archaeal RibL: The First Example of an Air Sensitive FAD Synthetase

Zahra Mashhadi, Huimin Xu, Robert H. White

As first author I designed and performed experiments and prepared the figures and the manuscript. Huimin Xu did all cloning and protein expression.

Department of Biochemistry, Virginia Tech, Blacksburg, VA, 24061

4.1 ABSTRACT

FAD synthetases are monofunctional enzymes that catalyze the transfer of the AMP portion of ATP to FMN to produce FAD and pyrophosphate (PPi). Monofunctional FAD synthetases exist in eukaryotes while bacteria have bifunctional enzymes that catalyze both the phosphorylation of riboflavin and adenylation of FMN to produce FAD. Analyses of archaeal genomes did not reveal the presence of genes encoding for either group, yet the archaea contain FAD. Our recent identification of a CTP dependent archaeal riboflavin kinase strongly indicated the presence of a monofunctional FAD synthetase. Here we report the identification and characterization of archaeal FAD synthetase. The *Methanocaldococcus jannaschii* gene, MJ1179, encodes a protein which is classified in the nucleotidyl transferase protein family and was previously annotated as glycerol-3-phosphate cytidylyltransferase (GCT). GCTs are involved in teichoic acid biosynthesis, a key component of some bacterial cell walls but absent in archaea. The MJ1179 gene was cloned and its protein product heterologously expressed in *E. coli*. The resulting enzyme catalyzes adenylation of FMN with ATP to produce FAD and PPi. The MJ1179-derived protein has been designated as RibL, to indicate that it follows the riboflavin kinase (RibK) step in the FAD biosynthetic pathway. RibL is active only under reducing conditions. RibL was found to require divalent metals for activity with the best activity being observed with Co^{2+}, where the activity was four times greater than that with Mg^{2+}. RibL was also found to catalyze cytidylation of FMN with CTP, making the modified FAD, flavin cytidine dinucleotide (FCD). Unlike other FAD synthetases, RibL does not catalyze the reverse reaction to produce FMN and ATP from FAD and PPi. Also in contrast to other FAD synthetases, PPi inhibits the activity of RibL.

4.2 INTRODUCTION

Riboflavin (vitamin B_2) is the redox-active component of FMN and FAD, which are essential coenzymes in all free-living organisms. Phosphorylation of riboflavin to FMN and subsequent adenylation of FMN to FAD are catalyzed by the enzymes riboflavin kinase and FAD synthetase, respectively. It is known that bacteria have a bifunctional enzyme that catalyzes both phosphorylation and adenylation reactions to convert riboflavin to FMN and then FAD (*1, 2*). The kinase active site is located in the C-terminus and adenylyltransferase is located in the N-terminus of the bifunctional *E. coli* enzyme, RibF (3). Work on the *Corynebacterium ammoniagenes* bifunctional FAD synthetase revealed that there are two ATP binding sites, one in the N- terminus and one in the C-terminus (2), and two independent flavin-binding sites, one for the riboflavin kinase activity and one for the FAD synthetase activity (*4*). Eukaryotes have two separate monofunctional-enzymes each catalyzing one of the reactions (5).

The Archaeal riboflavin biosynthetic pathway has revealed a number of differences from the canonical pathway both in terms of the genes encoding the pathway enzymes and the pathway itself (*6-8*). One of the differences is that archaeal genomes do not contain homologs of canonical riboflavin kinase and FAD synthetase. Like eukaryotes, archaea have two separate monofunctional enzymes for FMN and FAD production. Although all known riboflavin kinases use ATP as a phosphoryl donor, archaea contain a monofunctional enzyme, RibK, that phosphorylates riboflavin with CTP (6). Here we report the identification and characterization of the archaeal monofunctional FAD synthetase, from *Methanocaldococcus jannaschii,* which is encoded by MJ1179. The MJ1179 encoded protein is classified as a nucleotidyl transferase and was previously annotated as glycerol-3-phosphate cytidylyltransferase (GCT) (www.ncbi.nlm.nih.gov). The product of the reaction catalyzed by GCTs, CDP-glycerol, is a key intermediate in teichoic acid biosynthesis, a component of the bacterial cell walls. Based on the fact that archaea do not have teichoic acid, this suggested the MJ1179 gene product might have a different function. MJ1179 encoded protein was tested for FAD synthetase activity. Here we report that MJ1179 gene product is the archaeal FAD synthetase that we designated as RibL. Aligning the RibL sequence with its homologs shows existence of two conserved cysteines at the C-terminal part of these proteins. The involvement of these cysteines in catalytic activity of RibL was also investigated.

4.3 MATERIALS AND METHODS

Chemical*s*. All chemicals were obtained from Sigma/Aldrich.

Identification of FAD in *M. jannaschii* by LC-ES-MS. Frozen *M. jannaschii* cells (9) (~50 mg wet weight) were suspended in 200 μL of extraction buffer (50 mM *N*-[tris(hydroxymethyl)methyl]-2-aminoethanesulfonic acid (TES), pH 7.0, 10 mM $MgCl_2$, 20 mM DTT) and lysed by sonication. All *M. jannaschii* proteins in the extracted sample (40 mg/mL) were denatured and precipitated by adding 20 μL of 2 M trichloroacetic acid (TCA). After the centrifugation (16,000*g* for 10 min) the pellet was washed with 50 μL water and combined with soluble fraction. The soluble fraction was washed three times with 100 μL of diethyl ether to remove all of the TCA and the resulting sample had a pH of ~6.5.

LC-ES-MS was used to separate and identify FAD in the prepared sample. An Agilent HPLC equipped with a ZORBAX Eclipse XDB-C18 column (4.6 mm i.d. × 50 mm length, 1.8 μm particle size) was used for separation of *M. jannaschii* cell extract components. This HPLC system was interfaced with a 3200 Q TRAP mass spectrometer to identify FAD from cell extract. The elution profile consisted of a linear gradient from 95% 25 mM ammonium acetate solution and 5% methanol to 35% 25 mM ammonium acetate solution and 65% methanol over 10 min at 0.5 mL/min. Known FAD eluted at 26.5 min.

Cloning and Recombinant Expression of RibL and its mutants. The MJ1179 gene which encodes the protein identified by Swiss-Prot accession number Q58579 (*10*) was amplified by PCR from genomic DNA using oligonuculeotide primers MJ1179Fwd: 5'-GGTCATATGAAAAAGAGGGTAG-3' and MJ1179Rev: 5'-GCTGGATCCTTAGATTTTA ATCTC-3'. Purified PCR product was digested with *Nde*I and *Bam*HI restriction enzymes. DNA fragments were ligated into compatible sites in plasmid pT7-7 to generate pMJ1179. Two mutations of MJ1179, C126S and C143S, were generated using the QuikChange site-directed mutagenesis kit using pMJ1179 as a template. The C126S primers were 5'-GGTTATAAAAAAGTCCATTTCACAG-3' (forward) and 5'-CTGTGAAATGGACTTTTTTTATAAC-3' (reverse). The C143S primers were 5'-GGAGATTCAGCAATAAAGAG-3' (forward) and 5'-CTCTTTATTGCTGAATCTC-3' (reverse). The mutations were confirmed by sequencing of their plasmid inserts (pMJ1179 C126S and pMJ179 C143S). Recombinant plasmids, either pMJ1179 or one of the mutated

plasmids, were transformed into *E. coli* strain BL21-Codon Plus (DE3)-RIL. Expression of RibL was done as described previously in Chapter 2. Expression of mutants was under the same condition as that of the wild type. Induction of RibL and its mutants were confirmed by SDS-PAGE.

Purification of recombinant RibL and its mutants. Frozen *E. coli* cell pellet (~0.4 g wet weight from 200 mL of medium) was suspended in 3 mL of extraction buffer and lysed by sonication. RibL and its mutants were found to remain soluble after heating the resulting cell extracts for 10 min at 70 °C followed by centrifugation (16,000*g* for 10 min). This process allowed for the purification of RibL and its mutants from the majority of *E. coli* proteins, which denature and precipitate under these conditions. The next step of purification was performed by anion-exchange chromatography of the 70 °C soluble fractions on a MonoQ HR column (1 × 8 cm; Amersham Bioscience) using a linear gradient from 0 to 1 M NaCl in 25 mM pH 7.5 TES buffer, over 55 min at a flow rate of one mL/min and 1 mL fractions were collected. Protein concentrations were determined by Bradford analysis (*11*).

Metal Ion Analysis of RibL and its Mutants. Metal analysis of purified RibL was performed at the Virginia Tech Soil Testing Laboratory using inductively coupled plasma emission spectrophotometry (ICPES). The MonoQ purified proteins were diluted in 25 mM Tris buffer, pH 7.5 to give a final calculated metal concentration of 0.05 ppm prior to analysis, assuming one equivalent of metal per protomer. Samples were analyzed for iron, manganese, magnesium, zinc and cobalt.

Measurement of the Native Molecular Weight of RibL. The native molecular weight of RibL was determined by size exclusion chromatography on a Superose 12HR column (10 mm x 300 mm) separated with buffer containing 50 mM HEPES pH 7.2, and 150 mM NaCl at 0.5 mL/min with detection at 280 nm. Protein standards used to calibrate the column included apoferritin (443 kDa) alcohol dehydrogenase (150 kDa), conalbumin (77 kDa), and vitamin B_{12} (1.4 kDa).

Analysis of Enzymatic Activity of RibL and its Mutants. The standard assay for RibL was performed by incubation of 2 μg of RibL in 35 mM TES (K^+) buffer, pH 7.2, 14 mM DTT, 7 mM $MgCl_2$, 5.7 mM ATP and 0.17 mM FMN in total volume of 35 μL at 70 ˚C for 15 min. The activity of the mutants was tested with 3.5 μg of the RibLC126S or 5.5 μg of the RibLC143S under the standard assay conditions. Following incubation, 70 μL of methanol was added to stop the reactions. After centrifugation (16,000*g*, 10 min) samples were separated from the pellet and

the methanol was removed by evaporation. Water was added to the supernatants to adjust the volumes to 100 μL for HPLC analysis. A Shimadzu HPLC System equipped with a RF-10AXL fluorescence detector and a C18 reverse-phase column (Varian PursuitXRs, 250 × 4.6 mm, 5 μm particle size) was used. The elution profile consisted of 95% sodium acetate buffer (25 mM, pH 6.0, 0.02% NaN_3) and 5% methanol for 5 min followed by a linear gradient to 20% sodium acetate buffer and 80% methanol over 40 min at 0.5 mL/min. Under these conditions flavins were eluted in the following order: FAD 26.5 min, FMN 29 min, and riboflavin 31 min. Flavins were detected by fluorescence using λ_{max} excitation of 450 nm and λ_{max} emission of 520 nm (6). A known concentration of FAD was used to calculate the conversion factor of fluorescent units to nmoles of FAD. This conversion factor was used to determine amount of FAD produced in our experiments.

Testing Alternative Substrates. RibL was tested for its ability to use other nucleotides such as CTP and GTP to transfer CMP and GMP to FMN to produce the modified FADs, flavin cytosine dinucleotide (FCD) and flavin guanine dinucleotide (FGD), respectively. The standard assay condition was used in the incubation in presence of either 5.7 mM CTP or GTP instead of ATP.

Metal-Ion Dependency of the RibL Reaction. Assay for metal dependency of RibL was performed by incubation of 2 μg RibL with 5.7 mM ATP, 0.084 mM FMN and 2.8 mM of $MgCl_2$, $MnCl_2$, $ZnCl_2$, $CoCl_2$, $NiCl_2$, $Fe(NH_4)_2(SO_4)_2$, or no metal under standard assay conditions. In the case of $Fe(NH_4)_2(SO_4)_2$, argon gas was used to remove oxygen and prevent oxidation.

Synthesis of Flavin Cytidine Dinucleotide (FCD). Synthesis of FCD was performed by dissolving of 0.1 g FMN and 35 mg CMP in 1 mL of trifluoroacetic anhydride (TFAA). The procedure was based on the previously described preparation of FAD from FMN and AMP (*12*) but with the following modifications: We did not grind the ingredients in mortar and a N_2 gas stream was used for evaporate the solvents from the reaction mixture at the completion of the reaction. The recovered dried yellow reaction powder was dissolved in water for purification by preparative thin layer chromatography (TLC) using a solvent system consisting of 0.2 M ammonium bicarbonate in acetonitrile, water and formic acid (80:20:10 v/v/v). The flavin containing compounds were visualized as yellow spots that were fluorescent when exposing the TLC plates to UV light. The identification of recovered FCD was established by its absorbance spectra and ES-MS analysis by direct infusion in ammonium acetate (1 g/L) buffer.

Characterization of the Enzymatically Prepared FCD and FAD. RibL (4 μg) was incubated in 28 mM TES (K^+) buffer, pH 7.2, containing 5.7 mM $MgCl_2$, 0.9 mM FMN and either 14 mM CTP or ATP in total volume of 30 μL at 70 ˚C for 45 min. Separation of product and substrates were performed by preparative TLC as described above. Under these conditions the retention factor (R_f) for FMN, FAD and FCD was 0.3, 0.15 and 0.18 respectively. The yellow FAD and FCD bands were eluted from silica plate with water and dissolved in 100 μL ammonium acetate (1 g/L) buffer for ES-MS by direct infusion.

Determination of the Enzymatic Reaction Product as Pyrophosphate. The PPi produced by the enzymatic reaction was assayed by enzymatic coupling to the oxidation of NADH utilizing pyrophosphate dependent fructose-6-phosphate kinase, fructose-1,6-diphosphate aldolase, triose phosphate isomerase, and glycerophosphate dehydrogenase. The enzymes and substrates necessary for the coupling were provided from pyrophosphate reagent kit for the enzymatic determination of pyrophosphate (Sigma P7275). The sample mixtures consisted of 29 mM TES pH 7.5, 1.8 mM $CoCl_2$, 0.4 mM FMN, 4.5 mM ATP, 12 μg RibL in total volume of 110 μL. The control mixture was the same as the sample mixture but FMN was omitted. Following incubation at 70 °C for 30 min, sample mixtures were cooled on ice, centrifuged and combined with 100 μL pyrophosphate reagent at 30 °C in a 100 μL cuvette. The oxidation of NADH was monitored at 340 nm.

Determination of the Kinetic Constants. Assays to determine the kinetic constants for ATP were performed under standard assay conditions with the following modifications. In this assay 2 μg of RibL was incubated in 35 mM TES (K^+) buffer, pH 7.2, 7 mM $MgCl_2$, 0.17 mM FMN in presence of either 0, 0.014, 0.03, 0.06, 0.2, 0.3, 0.6, 1.4, 2.8 or 5.7 mM ATP in total volume of 35 μL at 70 ˚C for 15 min. When CTP was used as substrate everything was as same as the standard assay and the concentration of CTP was varied from 0 to 5.7 mM. To determine the kinetic constants for FMN, the assay was performed as above in presence of 5.7 mM ATP and concentration of FMN was varied from 0, 5, 10.5, 21, 42, to 84 μM FMN.

Effect of Pyrophosphate on the Reaction. The assay was performed under standard assay conditions with different concentrations of PPi (0.28, 1.4, 7.1 mM) being added to the reaction mixture. HPLC was used to analyze the product as explained above.

Testing the Effects of the Redox State of RibL on Its Activity. Two sets of experiments were conducted to examine the role of the two conserved cysteines at the C-terminal end of the RibL.

In the first experiment 2 μg of RibL was incubated in 37.5 mM TES (K^+) buffer, pH 7.2, 5.6 mM DTT, and 0.1 mM FMN in the total volume of 32 μL at room temperature for 15 min under argon gas. ATP (5 mM) and either $MnCl_2$ or $Fe(NH_4)_2(SO_4)_2$ at total concentration of 2.5 mM were added. Samples were incubated at 70 ˚C for 15 min and then assayed for FAD. A control mixture contained the same as components but in the absence of DTT and in presence of $MnCl_2$. In the second experiment cysteines were alkylated to see if this affected the activity of RibL. The samples which contained 2 μg of RibL in 37.5 mM TES (K^+) buffer, pH 7.2, 4 mM DTT, in the total volume of 11 μL were incubated at room temperature for 15 min. Argon gas was used to remove the oxygen from incubating mixture. Iodoacetamide (IAA) at the final concentration of 11.8 mM was added to the sample followed by 25 min incubation at room temperature followed by adding β-mercaptoethanol at final concentration of 48 mM to remove excess IAA. ATP (5.7 mM), 0.1 mM FMN and $MnCl_2$ in total concentration of 2.9 mM were added. Sample in the total volume of 35 μL were incubated at 70 ˚C for 15 min and then assayed for FAD by HPLC.

4.4 RESULTS

Identification of FAD in M. jannaschii

Existence of FAD in *M. jannaschii* was investigated and its presence was confirmed by both LC-MS/MS and by its fluorescence by HPLC analysis with fluorescence detection.

Expression and Purification of RibL and its Mutants

The MJ1179 gene from *M. jannaschii* and both its C126S and C143S mutants, were cloned and overexpressed in *E. coli*. The recombinantly expressed proteins were extracted from the cells by sonication and purified first by heating the extract at 70 °C for 10 min followed by anion-exchange chromatography of the soluble proteins. The SDS-PAGE analysis of the purified RibL and the mutants with Coomassie staining showed a single band corresponding to the molecular mass of about 17 kDa with a purity of >95% (Fig. 4.1). This molecular mass is consistent with the predicted monomeric molecular mass of 17,288 Da for RibL. About the same amount of each protein was isolated indicating that the mutations did not reduce the protein

stability. Based on the size of the ORF, MALDI-MS was used to analyze the protein sample for its precise molecular mass. Size exclusion chromatography showed a molecular weight of 29 kDa consistent with the RibL existing as a dimer.

Identification of Reaction Catalyzed by RibL

Incubation of RibL with FMN and ATP at 70 °C for 15 min produced a new fluorescent compound when the reaction mixture was assayed either by HPLC using fluorescence detection at the flavin excitation and emission wavelength or by TLC. The peak was identified as FAD based on its HPLC elution time (26.5 min) and its TLC R_f (0.15) as compared to the known. The new peak had the FAD absorbance spectrum, which shows λ_{max} at 266, 371 and 450 nm. LC-MS of the TLC-purified product, gave the same ES-MS spectrum as an authentic sample of FAD showing a $[M-H]^-$ ion at 784.4 *m/z*. The Ar-collisionally induced fragmentation of the 784.4 *m/z* ion for both known and enzymatically generated FAD, gave the same set of fragment ions at 517.1, 455.3, 437.3, 408.3, and 346.3 *m/z*.

To determine if the other product(s) of this reaction was one pyrophosphate or two inorganic phosphates, the PPi generated in the reaction mixture was enzymatically assayed. The enzymatic coupling assay revealed that PPi is the other product of adenylation of FMN by RibL. The data shows that 0.1 mM PPi was produced which was equal to the amount of FAD produced indicating that no phosphate was generated in the incubation.

Substrate Specificity of the RibL Reaction

RibL was able to utilize other nucleotides such as CTP and GTP as substrates, producing the modified coenzymes, FCD and FGD, respectively. The FCD product was confirmed by comparison to a known, synthetically prepared sample. The specific activity of RibL with ATP, CTP, or GTP as the nucleotidyl donor was measured under standard assay conditions with incubation of 2 μg RibL and 0.084 mM FMN and either 5.7 mM ATP, CTP or GTP. The specific activity of RibL is 10, 4, and 1 nmol mg^{-1} min^{-1} with ATP, CTP, and GTP, respectively. LC-MS of the TLC-purified FCD produced by RibL gave the same ES-MS spectrum as authentic sample showing a $[M-H]^-$ ion at 760.2 *m/z*. The Ar-collisionally induced fragmentation of the 760.2 *m/z* ion for both the synthesized and enzymatically generated FCD gave ions at 517.1, 437.2, 384.1, and 322.1 *m/z*.

Metal content and Metal-Ion Dependency of RibL Reaction

ICPES was used to determine the identity and quantity of metal ions present in the purified recombinant enzyme. MonoQ purified RibL was found to contain 0.2 mole of iron and 8.4 mole of magnesium per protomer. The Bradford protein assay was used to measure the protein concentration. Both the RibLC126S and RibLC143S were found to contain no detectable metals. A metal dependency assay revealed that RibL has its best activity in presence of Co^{2+} (Fig. 4.2) where the activity was four times greater than with Mg^{2+}.

Determination of the Kinetic Parameters

The specific activity of RibL versus different concentrations of ATP up to 1.4 mM was fit into a hyperbolic curve (Fig. 4.3A) and shows that RibL reaches its maximum activity at an ATP concentration of about 1.4 mM. The RibL activity decreases about 20% when the concentration of ATP is higher than physiologically relevant concentration (~5 mM). When using CTP as the nucleotidyl donor the activity of RibL reaches the maximum activity at a CTP concentration of also about 1.4 mM (Fig. 4.3B). In this case, the RibL activity decreases about 68% and 95% when the concentration of CTP was 5.7 and 11.4 mM, respectively (data not shown for the later one). The RibL kinetics was determined under steady state conditions in the presence of either 5.7 mM ATP or 0.17 mM FMN as fixed substrate concentration. The KeleidaGraph 4.0 was used to fit the data (Fig. 4.3, A and B) to Michaelis-Menten plot with substrate inhibition using the equation Y= Vmax * X / (Km + X * (1+X/Ki)). In the case of FMN as variable substrate, the data was fitted to a Michaelis-Menten plot. The measured kinetic parameters for RibL with ATP as the nucleotidyl donor are as follow: for FMN, K_M^{app} = 63 ± 21 μM, V_{max}= 14 ± 2.6 nmol min^{-1} mg^{-1}, k_{cat}/K_M^{app} = 64 $M^{-1}sec^{-1}$; for ATP: K_M^{app} = 25 ± 7.7 μM, V_{max}= 14 ± 0.97 nmol min^{-1} mg^{-1}, k_{cat}/K_M^{app} = 160 $M^{-1}sec^{-1}$, and K_i = 31 ± 28 mM. The high error is due to the one data point in the graph (Fig. 4.3A) that shows inhibition with ATP. When CTP is used as substrate, the K_M^{app}, V_{max} and k_{cat}/K_M^{app} for CTP was 480 ± 170 μM, 10 ± 1.1 nmol min^{-1} mg^{-1}, and 6 $M^{-1}sec^{-1}$ respectively. Kinetic parameters for CTP were determined by fitting the first half of the data points from Figure 4.3B (eliminate the inhibited part) to Michaelis-Menten plot because the inhibition in this case is dramatic.

Inhibition of RibL reaction by Pyrophosphate

Adenylation of FMN by ATP catalyzed by RibL is inhibited by PPi. The activity of the RibL decreased by 30%, 85%, and 95% when the incubation of RibL with FMN and ATP assay was done under standard condition in the presence of 0.28, 1.4 and 7.1 mM PPi, respectively.

Testing the Effects of the Redox State of RibL on the Activity

Sequence alignment of the homologs of RibL shared a motif contains two conserved cysteines that could either be involved as a redox sensor by forming a disulfide or in metal binding. To test these ideas two different sets of experiments were conducted. In the first set of experiments the specific activity of the enzyme was measured under standard assay condition with $MnCl_2$, when the enzyme was assayed either in presence of DTT under argon or with DTT under air (Table 4.1). Specific activity of RibL was the highest, 39.7 nmol mg^{-1} min^{-1}, in the presence of DTT under argon and decreased to 22 nmol mg^{-1} min^{-1} when the incubation was conducted with DTT in the presence of air which is the standard assay conditions. In absence of DTT, RibL showed a specific activity of only 3.3 nmol mg^{-1} min^{-1}.

In another experiment the two cysteines were first reduced by DTT and alkylated with iodoacetamide. Alkylation of both cysteines was confirmed with electrospray mass spectroscopy (ES-MS) by detection of the expected alkylated tryptic peptides (data not shown). After treating the RibL with IAA, RibL lost almost all of its activity as shown in Table 4.1.

Activity of RibL's Mutants

The activity of the RibL mutants and also RibL as a control were tested under standard assay conditions. The activity of the mutants was tested in presence of Mg^{2+} and Co^{2+} (Table 4.2). This experiment revealed that in presence of $MgCl_2$, RibLC126S had about two times higher activity than wildtype, 12 nmol mg^{-1} min^{-1} and 5.1 nmol mg^{-1} min^{-1}, respectively. The activity of the RibLC143S is about that of the wildtype, 4.03 nmol mg^{-1} min^{-1}. The specific activity of RibLC126S and RibLC143S in presence of $CoCl_2$ is 0.64 nmol min^{-1} mg^{-1} and 0.24 nmol min^{-1} mg^{-1}, respectively, which is very low compared to the wildtype activity 59.7 nmol min^{-1} mg^{-1}.

Analysis of Flavins in* E. coli *Overexpressing ribL and its Mutants

After overexpressing wildtype *ribL* in *E. coli* the cell extract was slightly yellow however the *E. coli* cell extracts after overexpressing of the mutated *ribL* constructs had a much more intense visible yellow color. Flavins eluted from MonoQ-separated cell extracts were used to measure the amount of riboflavin, FMN, and FAD in the extracts. The flavins of the most intense fraction of either RibL or its mutants were separated by HPLC and then identified by fluorescence. The fraction from the *ribL* expression contains about 4.8 μM riboflavin and 3.3 μM FMN and it contains no FAD. The FMN and FAD concentration in the fractions from C126S and C143S mutants were 4.8 μM FMN, 19.1 μM FAD, and 6.4 μM FMN, 21.3 μM FAD, respectively. No riboflavin was detected in MonoQ-purified fractions from either of mutants.

4.5 DISCUSSION

Currently two pathways are known for the conversion of riboflavin to FAD, one using a single bacterial bifunctional protein, RibF, and the other using two separate eukaryotic proteins, a riboflavin kinase followed by a FAD synthetase (*1, 2, 5*). Recently two homologous genes were identified in plants, which both contain FAD synthetase activities but not riboflavin kinase activities (*13*).

Until recently no evidence for either of these pathways were apparent in the archaea despite the fact that *M. jannaschii* does contain FAD as indicated by direct analysis of the cells as shown here. Additionally, gene products that have been studied in other organisms and are known to function with FAD are also encoded in *M. jannaschii* genome. Recently a new riboflavin kinase was discovered in *M. jannaschii* (RibK) that used CTP as the phosphate donor (6). Here we have shown that the MJ1179 gene product is an archaeal FAD synthetase. The MJ1179 gene product is designated as RibL to indicate that it catalyzes the last step of the biosynthesis of FAD.

RibL is in the nucleotidyltransferase family of proteins and was annotated as a glycerol-3-phosphate cytidylyltransferase (GCT). The chemistry of the reactions catalyzed by GCTs and FAD synthetases are the same (Fig. 4.4). In both cases a nucleophilic phosphate attacks the α-phosphate of a nucleotide triphosphate, ATP in FAD synthetases and CTP in GCTs.

Pyrophosphate is released as the other product in both reactions. GCTs have three conserved sequence motifs: HXGH, which is conserved in almost all nucleotidyltransferases, RYVDEVI, which is conserved in all GCT proteins and RTXGISTT, which is a signature motif found only in the GCT family (Bold in Fig. 4.5) (*14*). HXGH and RTXGISTT motifs form the binding site for CTP in GCTs (*14*). The residues in the HXGH motif interact with phosphate groups of nucleotides and stabilize the transition state (*15*) while RTXGISTT motif residues form that primarily interact with cytidine. The RYVDEVI motif is the site for homodimer interaction (*14*). Among these three motifs only the HXGH motif is conserved both in the archaeal RibL and the bacterial RibF enzymes (*16*). The archaeal RibLs also have a conserved $CX_2HSX_5KEX_5C$ motif in the C-terminal starting in about the same location as the conserved RTEGISTT motif found in the GCT enzymes. Having a pair of conserved cysteines (Fig. 4.5, highlighted in black) made us consider their possible function in this enzyme. One possibility considered is that they could be as a redox sensor (*17*) undergoing oxidation to the disulfide during oxidative stress reducing enzymatic activity and thereby reducing FAD production in the cell. Although one could easily understand how cysteine residues located only a few residues from each other could readily form a disufide in a protein in our case the cysteines are separated by 16 amino acids. It has however been shown that cysteines located far from each other in primary and secondary structure can make disulfide bond by causing protein rearrangement (*18*). Also we found that the *M. jannaschii* cell extract converts the added FAD to riboflavin-4',5'-cyclic phosphate (cFMN). This indicates that FAD biosynthesis would be blocked and FAD levels in the cells would be reduced. By knowing that FAD is required by several enzymes involved in methanogenesis which is the energy producing pathway in methanogens including *M. jannaschii*, it can be concluded that in oxidative stress the FAD synthetase (RibL) will stop making FAD and also the already exist FAD in the cell eventually will be converted to cFMN then the whole methanogenic pathway will shut down. Alternatively the conserved cysteines could serves as ligands for metal binding that could be involved in the enzyme reaction mechanism (*19*). Since the air-oxidized enzyme has no activity and the DTT-reduced enzyme had full activity this suggests that formation of the disulfide bond completely blocks the activity. That disulfide was mostly likely between these two conserved cysteines is supported by the observation that these two cysteines are the only cysteines in the whole protein. However alkylation of these two

cysteines with IAA that would have also blocked disulfide bond formation results in almost inactivation of the protein.

Generating of two mutants of RibL in which each of the cysteines was mutated to serine, C126S and C143S, resulted in higher activity than wild type RibL. Unlike wildtype RibL that has best activity in presence of Co^{2+}, none of these mutants showed activity with Co^{2+}. Our data also shows that overexpression of either mutant in *E. coli* results in the producion of more FMN and much more FAD and a consumption of riboflavin.

We thus see a complex pattern of activation/inactivation of the RibL. The enzyme with reduced cysteines or when one of the two cysteines is replaced with serine is active. Only when the protein has two reduced cysteines can Co^{2+}, Mn^{2+}, or Mg^{2+} further activate the enzyme. This could occur by the binding of these metal ions to the cysteines. Oxidation or alkylation of the cysteines produces an inactive protein that cannot be reactivated by the addition of these metal ions.

We have not been able to identify any of the known conserved motifs for FMN and FAD binding (*20, 21*) in RibL. This indicates that RibL may contain a new flavin-binding site. The determination of the nature of flavin binding site must await the x-ray structure of RibL with bound FMN.

Most of the known adenylyltransferases including phosphopantetheine adenylyltransferase (*22*), nicotinate mononucleotide adenylyltransferase (NMAT) (*23*), and FAD synthetase (2) catalyze the reverse reaction (FAD + PPi → ATP + FMN). Incubation of RibL with FAD and PPi reveals that RibL does not catalyzed the reverse reaction to produce FMN and ATP (data not shown). Before our work, FAD synthetase from rat liver was the only known example of a irreversible adenylyltransferase (*24*). One reason why the RibL is not able to catalyze the reversible reaction would be if the enzyme produces two inorganic phosphates rather than PPi. A precedent for this is the MJ0145 gene product, GTP cyclohydrolase III, that was shown hydrolyzing PPi from the GTP followed by hydrolysis of the PPi into two inorganic phosphate (*25*). We used a pyrophosphate assay to confirm that PPi, not two phosphates, is the product of RibL catalyzed reaction. Based on our work, PPi inhibits the forward reaction, which is not observed in other FAD synthetases. It has been demonstrated that PPi also inhibits the activity of GCT from *Bacillus subtilis* (*26*). These authors suggest that this inhibition of GCT with PPi was due to ping-pong mechanism in which ATP binds to the enzyme and release the

PPi resulting in a covalently bond AMP. Further characterization of the enzyme, however, revealed that in fact the enzyme followed a rapid equilibrium random order mechanism (*26*). Based on studies on FAD synthetases that showed all of these enzymes also catalyze the reverse reaction and their mechanism is ordered sequential, inhibition of RibL with PPi and also the irreversibility of RibL bring up the idea that RibL could have a ping-pong mechanism. But RNA capping enzymes and DNA ligase, examples of a covalent nucleotidyl transferases, all possess a conserved lysine (KXDG) in their active site (*27*). These enzymes also have five other motifs that are common structural basis for this covalent catalysis. RibL and its homologs do not possess these conserve motifs (common structural basis) for having ping-pong mechanism suggests that RibL proceeds via a rapid equilibrium random order mechanism. In addition Hanes plots of [FMN]/*v* against [FMN] in present of different fixed concentrations of ATP, showed a series of nonparallel and non-intersecting lines indicating that RibL proceeds by a ternary-complex mechanism with substrate (ATP) inhibition (data not shown).

The kinetic constants of RibL are comparable with the FAD synthetase in rat liver that shows the K_M^{app} for FMN and ATP of 91 and 71 μM, respectively (*28*) and quite different from kinetic properties of FAD synthetase from in other organisms. For instance K_M^{app} of FMN = 1 μM, K_M^{app} of ATP = 37 μM for the *Corynebacterium ammoniagenes* enzyme (2) and K_M^{app} of FMN = 0.36 μM and V_{max}= 3.9 nmol min^{-1} mg^{-1} for human enzyme (*29*).

RibL is present in all methanogens and is distributed with lower homology among other archaea. Homologs of RibL with very low homology are present in a few bacteria and are annotated as glycerol-3-phosphate cytidylyltransferase. In *Archaeoglobus fulgidus* the MJ1179 homolog, AF1418, is clustered with riboflavin synthase (*rib*C).

Considering what is now currently known about the differences between the enzymes in the pathways for riboflavin and FAD biosynthesis in the archaea and bacteria (6-8), the data presented here further support the idea that the evolution of the biosynthetic pathways to these two coenzymes has proceeded along at least two different pathways in the organisms on earth. This idea also applies to the biosynthesis of methanopterin an analog of the bacterial coenzyme folate (*30*).

4.6 ACKNOWLEDGMENT

We would like to thank Laura Grochowski and Walter Niehaus for assistance with editing this manuscript, Kim Harich for assistance with obtaining the mass spectral data, and Keith W. Ray for obtaining the MALDI MS data for the RibL.

4.7 TABLES AND FIGURES

TABLE 4.1. Effects of the redox state on the specific activity of RibL.

All of these experiments were done in presence of 2 μg RibL, 5 mM ATP, 0.1 mM FMN, and 2.5 mM $MnCl_2$. The concentration of DTT used was 5.6 mM and mercaptoethanol (ME) was calculated to be 40 mM.

	Assay condition			
	+DTT, +Ar	+DTT, air	-DTT, air	Alkylated Cys's, +ME air
Specific activity (nmol mg^{-1} min^{-1})	40	22	3.3	0.26

TABLE 4.2. Specific activity (nmol mg^{-1} min^{-1}) comparison of RibL and its mutants with different metals.

All of these experiments were performed under standard assay condition in presence of DTT and air.

	Measured specific activity (nmol mg^{-1} min^{-1})		
Added metal	RibL-WT	RibLC126S	RibLC143S
Mg^{2+}	5.1	12	4
Co^{2+}	60	0.64	0.24

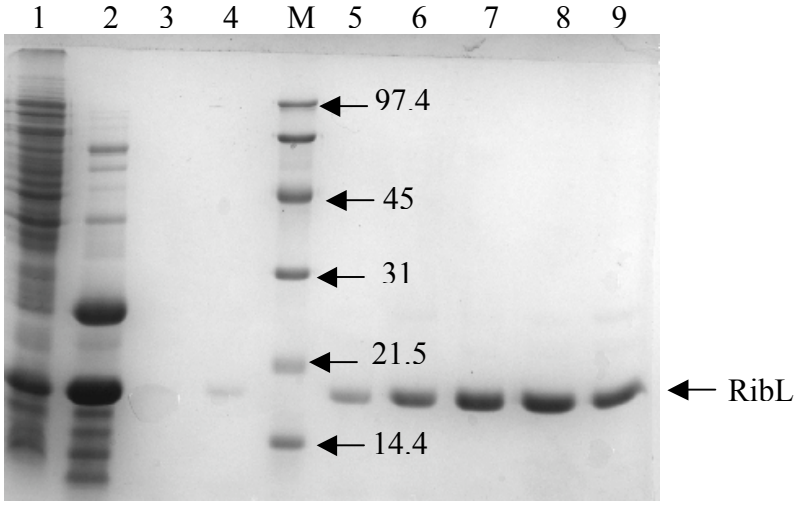

Figure 4.1 The SDS-PAGE of RibL containing samples.

The protein standard marker was run in lane marked as M. The lanes 1 and 2 show the insoluble and soluble proteins after heating the recombinant E. coli cells containing pMJ1179 at 70 °C for 10 min, respectively. The lanes 3 to 9 are consecutive MonoQ eluted fractions containing RibL.

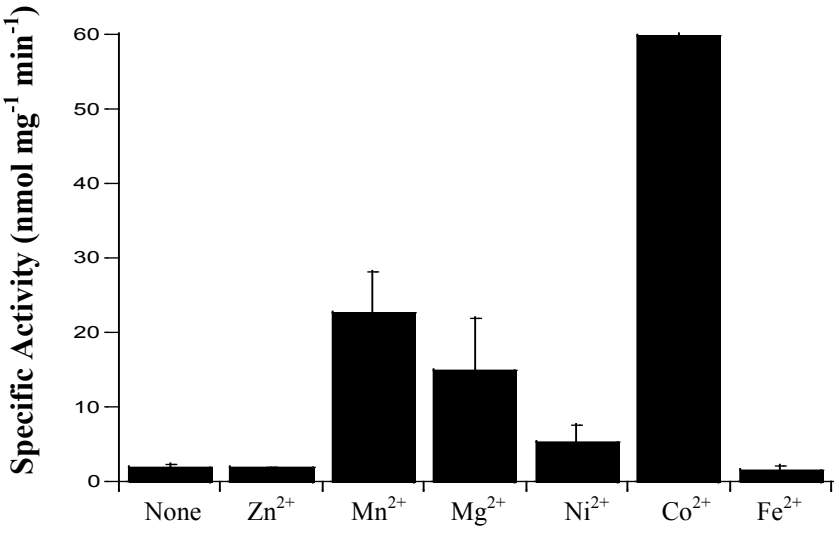

Figure 4.2 Dependency of divalent metals on the RibL catalyzed conversion of ATP and FMN to FAD and PPi.

MonoQ purified RibL (2 μg) was incubated with 5.7 mM ATP, 0.084 mM FMN and either no added metal or the indicated metals at 2.8 mM in presence of 14 mM DTT in a total volume of 35 μL of TES buffer. Only the Fe(II) assay was done under argon gas.

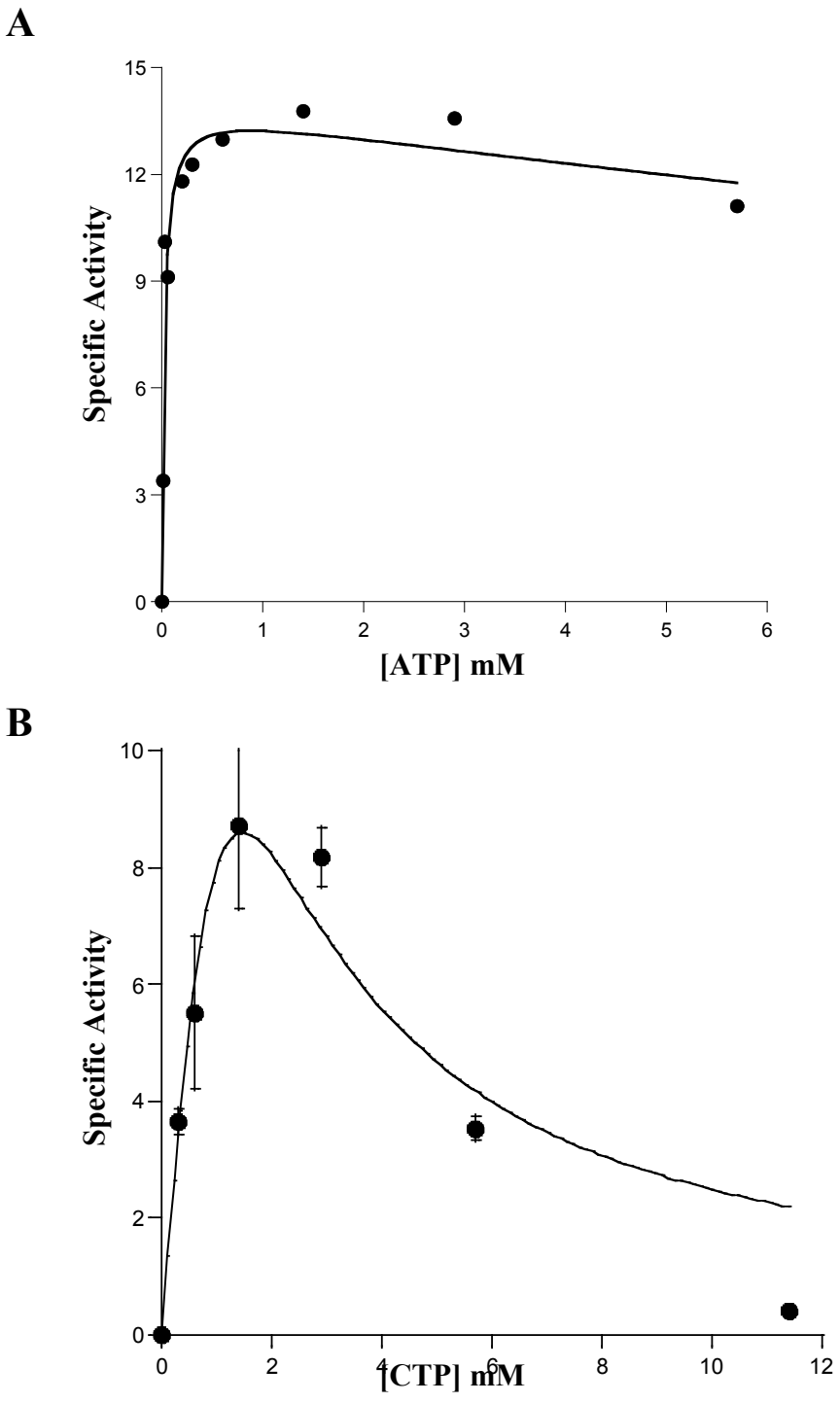

Figure 4.3 Plot of steady-state kinetic data for RibL.

Measured specific activities (nmol mg^{-1} min^{-1}) of RibL at (A) ATP concentrations of 0, 0.014, 0.03, 0.06, 0.2, 0.3, 0.6, 1.4, 2.9, 5.7 mM and (B) CTP concentration of 0.0, 0.3, 0.6, 1.4, 2.9, 5.7, 11.4 mM in presence of 0.17 mM FMN and 7 mM Mg^{2+} after 15 min incubation at 70 °C.

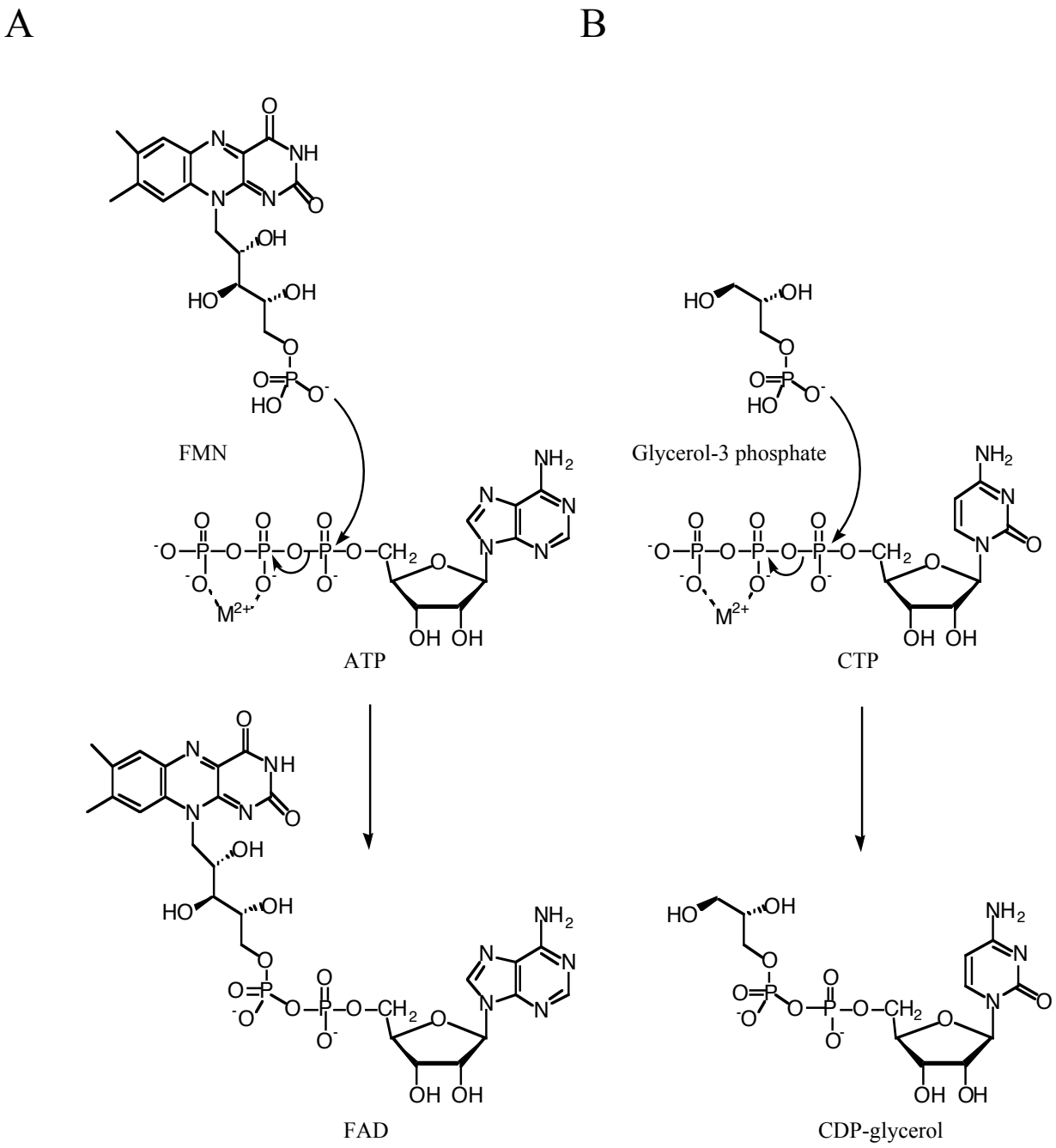

Figure 4.4 Chemical reactions that are catalyzed by (A) FAD synthetase and RibL and (B) GCT.

In all cases the phosphate group of the substrate attacks the α-phosphate of the ATP resulting in release of inorganic pyrophosphate.

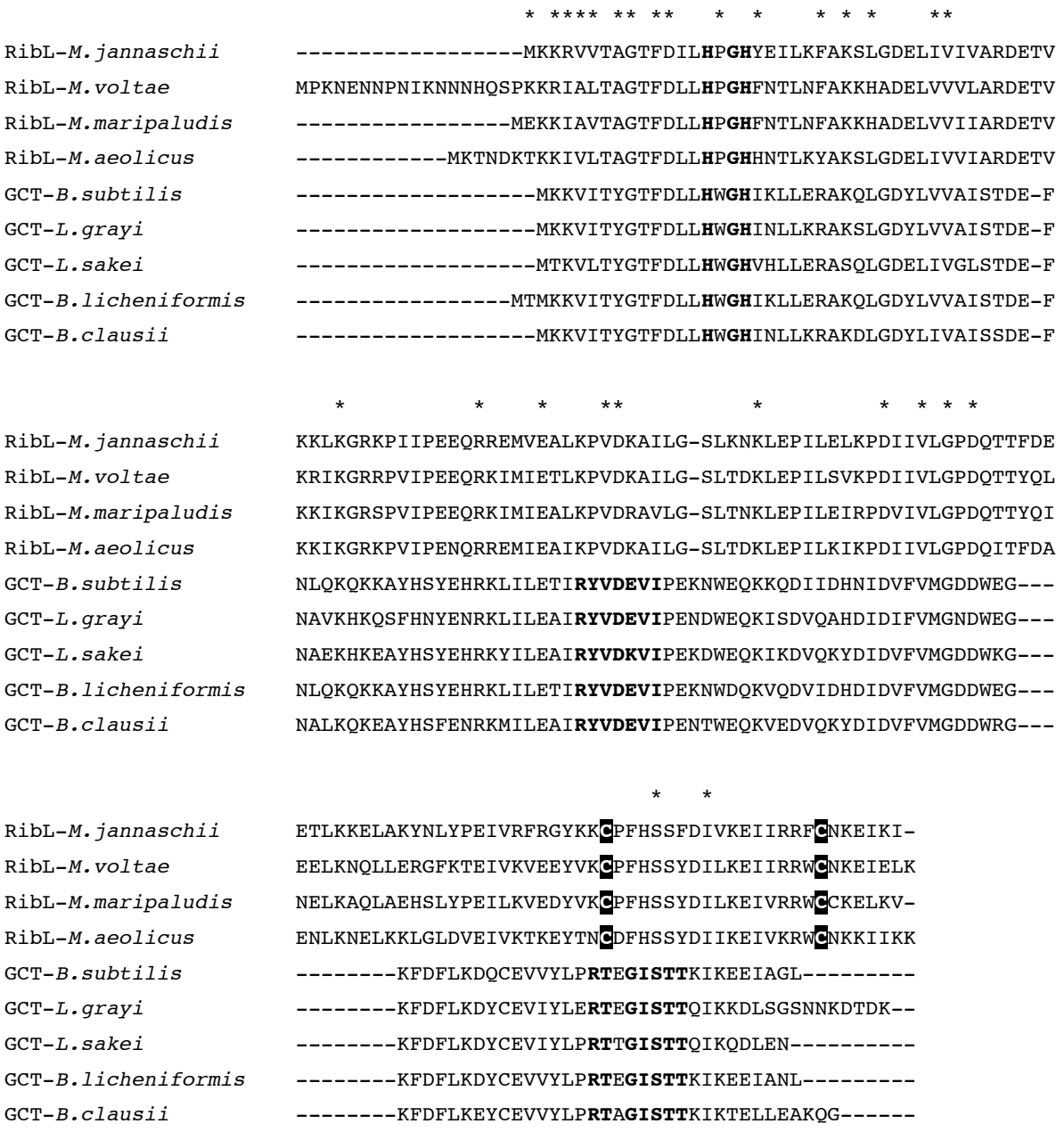

Figure 4.5 Multiple alignments of RibL and its homologs in other methanogens with some bacterial GCT sequences.

Protein sequences used to generate this multiple alignment are as follows: RibL-*M. jannaschii, Methanocaldocoaaus jannaschii*, gi:41018410; RibL-*M. voltae, Methanococcus voltae*, gi:163799362; RibL-*M. maripaludis, Methanococcus maripaludis*, gi:45358506; RibL-*M. aeolicus, Methanococcus aeolicus*, gi:150401726; GCT-*B. subtilis*, *Bacillus subtilis*,

gi:16080627; GCT-*L. grayi*, *Listeria grayi*, gi:229556270; GCT-*L. sakei*, *Lactobacillus sakei*, gi:81429187; GCT-*B. licheniformis, Bacillus licheniformis*, gi:52787498; GCT-*B. clausii, Bacillus clausii*, gi:56964865. Stars (*) indicate identical residues in both RibL homologs and GCTs. Conserved motifs are indicated in bold. The two conserved cysteines in RibL and its homologes are highlighted in black. The alignment was constructed in "The Biology WorkBench" using CLUSTALW program.

REFERENCES

(1) Manstein, D. J., and Pai, E. F. (1986) Purification and characterization of FAD synthetase from *Brevibacterium ammoniagenes*. *J. Biol. Chem. 261*, 16169-73.

(2) Efimov, I., Kuusk, V., Zhang, X., and McIntire, W. S. (1998) Proposed steady-state kinetic mechanism for *Corynebacterium ammoniagenes* FAD synthetase produced by *Escherichia coli*. *Biochemistry 37*, 9716-23.

(3) Krupa, A., Sandhya, K., Srinivasan, N., and Jonnalagadda, S. (2003) A conserved domain in prokaryotic bifunctional FAD synthetases can potentially catalyze nucleotide transfer. *Trends Biochem. Sci. 28*, 9-12.

(4) Frago, S., Velazquez-Campoy, A., and Medina, M. (2009) The Puzzle of Ligand Binding to *Corynebacterium ammoniagenes* FAD Synthetase. *J. Biol. Chem. 284*, 6610-9.

(5) Wu, M., Repetto, B., Glerum, D. M., and Tzagoloff, A. (1995) Cloning and characterization of FAD1, the structural gene for flavin adenine dinucleotide synthetase of *Saccharomyces cerevisiae*. *Mol. Cell Biol. 15*, 264-71.

(6) Mashhadi, Z., Zhang, H., Xu, H., and White, R. H. (2008) Identification and characterization of an archaeon-specific riboflavin kinase. *J. Bacteriol. 190*, 2615-8.

(7) Graupner, M., Xu, H., and White, R. H. (2002) The pyrimidine nucleotide reductase step in riboflavin and F_{420} biosynthesis in archaea proceeds by the eukaryotic route to riboflavin. *J. Bacteriol. 184*, 1952-7.

(8) Fischer, M., Romisch, W., Illarionov, B., Eisenreich, W., and Bacher, A. (2005) Structures and reaction mechanisms of riboflavin synthases of eubacterial and archaeal origin. *Biochem. Soc. Trans. 33*, 780-4.

(9) Mukhopadhyay, B., Johnson, E. F., and Wolfe, R. S. (1999) Reactor-scale cultivation of the hyperthermophilic methanarchaeon *Methanococcus jannaschii* to high cell densities. *Appl. Environ. Microbiol. 65*, 5059-65.

(10) Bult, C. J., White, O., Olsen, G. J., Zhou, L., Fleischmann, R. D., Sutton, G. G., Blake, J. A., FitzGerald, L. M., Clayton, R. A., Gocayne, J. D., Kerlavage, A. R., Dougherty, B. A., Tomb, J. F., Adams, M. D., Reich, C. I., Overbeek, R., Kirkness, E. F., Weinstock, K. G., Merrick, J. M., Glodek, A., Scott, J. L., Geoghagen, N. S., and Venter, J. C. (1996) Complete genome sequence of the methanogenic archaeon, *Methanococcus jannaschii*. *Science 273*, 1058-73.

(11) Bradford, M. M. (1976) A rapid and sensitive method for the quantitation of microgram quantities of protein utilizing the principle of protein-dye binding. *Anal. Biochem. 72*, 248-54.

(12) Deluca, C., and Kaplan, N. O. (1956) Large scale synthesis and purification of flavin adenine dinucleotide. *J. Biol. Chem. 223*, 569-76.

(13) Sandoval, F. J., Zhang, Y., and Roje, S. (2008) Flavin nucleotide metabolism in plants: monofunctional enzymes synthesize fad in plastids. *J. Biol. Chem. 283*, 30890-900.

(14) Weber, C. H., Park, Y. S., Sanker, S., Kent, C., and Ludwig, M. L. (1999) A prototypical cytidylyltransferase: CTP:glycerol-3-phosphate cytidylyltransferase from *Bacillus subtilis*. *Structure 7*, 1113-24.

(15) Leatherbarrow, R. J., Fersht, A. R., and Winter, G. (1985) Transition-state stabilization in the mechanism of tyrosyl-tRNA synthetase revealed by protein engineering. *Proc. Natl. Acad. Sci. U S A 82*, 7840-4.

(16) Frago, S., Martinez-Julvez, M., Serrano, A., and Medina, M. (2008) Structural analysis of FAD synthetase from *Corynebacterium ammoniagenes*. *BMC Microbiol. 8*, 160.
(17) Zheng, M., Aslund, F., and Storz, G. (1998) Activation of the OxyR transcription factor by reversible disulfide bond formation. *Science 279*, 1718-21.
(18) Choi, H., Kim, S., Mukhopadhyay, P., Cho, S., Woo, J., Storz, G., and Ryu, S. E. (2001) Structural basis of the redox switch in the OxyR transcription factor. *Cell 105*, 103-13.
(19) Zdanowski, K., Doughty, P., Jakimowicz, P., O'Hara, L., Buttner, M. J., Paget, M. S., and Kleanthous, C. (2006) Assignment of the zinc ligands in RsrA, a redox-sensing ZAS protein from Streptomyces coelicolor. *Biochemistry 45*, 8294-300.
(20) Dym, O., and Eisenberg, D. (2001) Sequence-structure analysis of FAD-containing proteins. *Protein Sci 10*, 1712-28.
(21) Huerta, C., Borek, D., Machius, M., Grishin, N. V., and Zhang, H. (2009) Structure and mechanism of a eukaryotic FMN adenylyltransferase. *J. Mol. Biol. 389*, 388-400.
(22) Miller, J. R., Ohren, J., Sarver, R. W., Mueller, W. T., de Dreu, P., Case, H., and Thanabal, V. (2007) Phosphopantetheine adenylyltransferase from *Escherichia coli*: investigation of the kinetic mechanism and role in regulation of coenzyme A biosynthesis. *J. Bacteriol. 189*, 8196-205.
(23) Sershon, V. C., Santarsiero, B. D., and Mesecar, A. D. (2009) Kinetic and X-ray structural evidence for negative cooperativity in substrate binding to nicotinate mononucleotide adenylyltransferase (NMAT) from *Bacillus anthracis*. *J. Mol. Biol. 385*, 867-88.
(24) Oka, M., and McCormick, D. B. (1987) Complete purification and general characterization of FAD synthetase from rat liver. *J. Biol. Chem. 262*, 7418-22.
(25) Graham, D. E., Xu, H., and White, R. H. (2002) A member of a new class of GTP cyclohydrolases produces formylaminopyrimidine nucleotide monophosphates. *Biochemistry 41*, 15074-84.
(26) Park, Y. S., Sweitzer, T. D., Dixon, J. E., and Kent, C. (1993) Expression, purification, and characterization of CTP:glycerol-3-phosphate cytidylyltransferase from *Bacillus subtilis*. *J. Biol. Chem. 268*, 16648-54.
(27) Shuman, S., and Schwer, B. (1995) RNA capping enzyme and DNA ligase: a superfamily of covalent nucleotidyl transferases. *Mol. Microbiol. 17*, 405-10.
(28) Yamada, Y., Merrill, A. H., Jr., and McCormick, D. B. (1990) Probable reaction mechanisms of flavokinase and FAD synthetase from rat liver. *Arch. Biochem. Biophys. 278*, 125-30.
(29) Galluccio, M., Brizio, C., Torchetti, E. M., Ferranti, P., Gianazza, E., Indiveri, C., and Barile, M. (2007) Over-expression in Escherichia coli, purification and characterization of isoform 2 of human FAD synthetase. *Protein Expr. Purif. 52*, 175-81.
(30) Grochowski, L. L., Xu, H., Leung, K., and White, R. H. (2007) Characterization of an Fe^{2+}-dependent archaeal-specific GTP cyclohydrolase, MptA, from *Methanocaldococcus jannaschii*. *Biochemistry 46*, 6658-67.

CHAPTER 5

Searching for Mysterious 7,8-Dihydro-D-neopterin Aldolase in *Methanocaldococcus jannaschii*

Zahra Mashhadi

Department of Biochemistry, Virginia Tech, Blacksburg, VA, 24061

5.1 ABSTRACT

Dihydroneopterin aldolase is one of the enzymes involved in biosynthesis of the coenzymes tetrahydrofolate and tetrahydromethanopterin. Tetrahydrofolate is synthesized in bacteria and lower eukaryotes *de novo*. Archaea do not have tetrahydrofolate, instead they synthesize tetrahydromethanopterin. In both pathways dihydroneopterin aldolase converts 7,8-dihydro-D-neopterin to 6-hydroxymethyl-7,8-dihydropterin. This enzyme is present in most of the organism that synthesize folate. Analyses of archaeal genomes did not reveal the presence of a gene for this aldolase. Here I have tried to identify and characterize the archaeal dihydroneopterin aldolase. The results from my work are promising and indicate that MJ1585 is the gene that encodes dihydroneopterin aldolase (DHNA) in *Methanocaldococcus jannaschii*. Further experiments are needed to prove my identification.

5.2 INTRODUCTION

Tetrahydromethanopterin (H_4MPT) is a C1 carrier coenzyme involved in methanogenic pathway in methanogens (*1*). Since the methanogenic archaea lack tetrahydrofolate (H_4folate), H_4MPT also serves as a substitute C1 carrier coenzyme for many of the enzymes where the canonical C1 carrier coenzyme folate would function (*2, 3*). The structure of the functional part of both coenzymes, H_4MPT and H_4folate, is almost identical (Fig. 5.1). The only difference in this part of their structures is methylation at C7 of the pterin in H_4MPT, which takes place at the end of the biosynthetic pathway. Although GTP serves as a precursor for the pterin in both coenzymes and the chemistry involve in the biosynthesis of the pterin ring for both coenzymes is the same, the enzymology is very different (Fig. 5.2) (*4, 5*). A review of fully sequenced and annotated genomes of methanogenic archaea revealed that homologs of the genes of folate biosynthetic enzymes were absent in the methanogens despite the fact that cell extracts of methanogens readily converted GTP to 6-hydroxymethyl-7,8-dihydropterin (H_2HMP) with 7,8-dihydro-D-neopterin 2'3'-cyclic phosphate (H_2N-cP) and 7,8-dihydro- D-neopterin (H_2neopterin) serving as intermediates (*4*).

7,8-Dihydropterin-2',3'-cyclic phosphate (H_2N-cP) is the first intermediate in this pathway and is formed by the activity of MptA, archaeal GTP cyclohydrolase (*5*). The five-member ring cyclic phosphate of H_2N-cP is then hydrolyzed into two products, 7,8-dihydropterin-2' phosphate (H_2N-2'P) and 7,8-dihydropterin-3' phosphate (H_2N-3'P) (*4*). By the activity of yet unknown phosphatase, H_2N-2'P and H_2N-3'P are converted to dihydroneopterin (H_2neopterin). The next step, which is an aldolase reaction, converts H_2neopterin to H_2HMP and glycolaldehyde, seems to share the same substrate and product as dihydroneopterin aldolase reaction in H_4folate biosynthetic pathway (Fig. 5.2).

There are two classes of aldolases based on their catalytic mechanism. Class I aldolases catalyze the aldol reaction through a protonated Schiff base that forms between substrate and a lysine residue of the enzyme that stabilizes the enolate anion of the intermediate. In class II aldolases a divalent metal, commonly Zn^{2+}, stabilizes the enolate anion of the intermediate. Dihydroneopterin aldolase (DHNA or FolB) is a unique aldolase in that it does not form a Schiff base nor does it require divalent metal for its catalytic activity (*6*). The required Schiff base is intrinsically part of the H_2neopterin structure. DHNA also has epimerase activity which catalyzes the epimerization of the C2' of H_2neopterin to form dihydromonapterin (H_2monapterin). The biological role of this epimerization is not yet known. Both the aldolase and epimerase reactions are reversible (*6*).

The ability of some organisms like *Pelasmodium palciparum* to synthesize H_4folate *de novo* but in absence of *folB* (coding for DHNA) in their genome was a mystery for long time. It ultimately was found that they possess a gene that encodes for pyruvoyltetrahydropterin synthase like protein (PTPS III). PTPS catalyzes the conversion of dihydroneopterin 3'-triphosphate (H_2N-3'PPP) to pyruvoyltetrahydropterin which is intermediate in biosynthesis of tetrahydrobiopterin and triphosphate. This PTPS paralog (PTPS III) catalyzes the conversion of dihydroneopterin 3'-triphosphate (H_2N-3'PPP) to both pyruvoyltetrahydropterin and H_2HMP (*7, 8*). These are explaining how folate synthesis can proceed.

When work on identification of archaeal DHNA was started there were no genomic leads for the non-orthologous replacements for H_2neopterin aldolase in archaea. I decided on several approaches to identify the archaeal dihydroneopterin aldolase. The first approach was to purify H_2neopterin aldolase from *M. jannaschii* cell extracts, as has been done for other proteins in our lab (*9*) and also for protein complexes in other organisms (*10*).The second approach was to

search all *M. jannaschii*'s genes annotated as aldolases and after primary sequence and predicted secondary structure analysis, select those that would be good candidates to catalyze this aldol reaction. A gene complementation experiment was the third approach that was used to identify this DHNA.

5.3 MATERIALS AND METHODS

Chemicals. 7,8-dihydro-D-neopterin, 6-hydroxymethyl 7,8-dihydro-D-neopterin and other pterins were obtained from Schircks Laboratories, Jona, Switzerland. All other chemicals were obtained from Sigma**.**

Isolation of the Native DHNA From M. jannaschii Cell Extracts. Frozen *M. jannaschii* cells (*11*) (5 g wet weight) were suspended in 30 mL of Tris-HCl buffer (25 mM tris(hydroxymethyl)aminoethane, pH 7.4,10 mM $MgCl_2$) and lysed by sonication using a Sonic Dismembrator, model 500 (Fisher Scientific). The cell lysate was clarified by centrifugation (6000 × *g,* 15 min) and separated by column chromatography. Several columns were used for the isolation of DHNA. After each step, the most active fractions were selected for the next column. The first step was performed on Q-Sepharose (45-165 μm spherical beads) column (2 × 15 cm) using a linear gradient of NaCl from 0 to 1 M in 25 mM Tris-HCl buffer, pH 7.4 with 10 mM $MgCl_2$, over 400 mL at 5 mL/min flow rate. Five mL fractions were collected. Q-Sepharose resin from GE Healthcare was used for packing the column. The eight most active fractions were combined in total volume of 40 mL. The ultrafiltration membrane (Millipore, NMWL: 3,000) was used to concentrate the combined fractions to final volume of 3.2 mL. The second step of purification was performed by anion-exchange chromatography of the concentrated mixed fraction (~3.2 mL) on a MonoQ HR column (1 × 8 cm; Amersham Bioscience) using a linear gradient of NaCl from 0 to 1 M in 25 mM Tris-HCl buffer, pH 7.2 over 55 mL at one mL/min flow rate and 1 mL fractions were collected. The four most active fractions were combined in total volume of 4 mL followed by concentration and buffer exchange with Tris-HCl buffer pH 8 by using ultrafiltration membrane (Millipore, NMWL: 3,000) to final volume of about 2 mL. This 2 mL mixture was applied to the same MonoQ column as previous step equilibrated with

Tris-HCL buffer, pH 8. The last step of purification was performed by size exclusion chromatography on a Superose 12HR column (10 mm x 300 mm) separated with aerobic buffer containing 50 mM HEPES pH 7.2, and 50 mM NaCl at 0.5 mL/min and collect 0.5 mL fractions. The three most active fractions were combined in total volume of 3 mL followed concentration by Microcon YM-3 (Millipore) to final volume of about 160 μL to apply to size exclusion column.

Analysis of Aldolase Activity. The standard HPLC assay for DHNA with H_2neopterin as substrate was performed by incubation of 20 μL of each fraction in 103 mM CHES (2-[*N*-cyclohexylamino]ethanesulfonic acid) buffer pH 8, 11.2 mM DTT, 13.8 mM EDTA, and 0.3 mM H_2neopterin in total volume of 29 μL under Ar gas at 70 ˚C for 30 min. Methanol (50 μL) was added to stop the reaction followed by centrifugation (14000*g*, 10 min). The dihydropterin reaction product and substrate were oxidized to pterins by the addition of 5 μL iodine in methanol (50 mg/mL) and the samples were incubated for 30 min at room temperature. Five μL of 1 M $NaHSO_3$ was added to reduce excess iodine. A Shimadzu HPLC system with a C18 reverse-phase column (Varian PursuitXRs, 250 × 4.6 mm, 5 μm partical size) was used for analysis of product. The elution profile included 95% sodium acetate buffer (25 mM, pH 6.0, 0.02% NaN_3) and 5% MeOH for 5 min followed by a linear gradient to 20% sodium acetate buffer and 80% MeOH over 40 min. The flow rate was 0.5 mL/min. Pterins were detected by fluorescence using an excitation wavelength of 356 nm and an emission wavelength of 450 nm. Under these conditions, neopterin and 6-hydroxymethylpterin (6-HMT) were eluted at 9.9 and 16.8 min, respectively.

Cloning and Recombinant Expression of MJ1585. The MJ1585 gene which encodes the protein identified by Swiss-Prot accession number Q58980 (*12*) was amplified by PCR from genomic DNA as described in Chapter 2 using oligonuculeotide primers synthesized by Invitrogen. The primer MJ1585Fwd, 5'-GGTCATATGGGGATTTTTATG-3' introduced *Nde*I restriction site at the 5'-end of amplified DNA and MJ1585Rev, 5'-GCTGGATCCTTATTTCCTATCTC-3' introduced *Bam*HI restriction site at the 5'-end. Purified PCR product was digested with *Nde*I and *Bam*HI restriction enzymes. DNA fragments were ligated into compatible sites in either plasmid pT7-7 or pET-19b to generate pMJ1585 and pMJ1585-His, respectively. Recombinant plasmid pMJ1585 and pMJ1585-His were transformed into *E. coli* strain K-12 Nova Blue (NB). The transformed NB cells were streaked on LBA (LB

with 100 μg/mL ampicillin) plates. Six single colonies were picked and inoculate in 5 mL LBA medium and grow overnight at 37 °C and 250 RPM to do Miniprep. The next day Miniprep was performed following the steps of Miniprep by microcentrifuge tube from QIAGEN to purify more of each plasmids, pMH1585 and pMJ1585-His. Plasmid DNA sequence was verified by sequencing.

Recombinant plasmid pMJ1585 or pMJ1585-His were used to transform *E. coli* strain BL21-Codon Plus (DE3)-RIL. Expression of MJ1585 with and without His-tag was done as described in Chapter 2. Induction of MJ1585 was confirmed by SDS-PAGE.

Isolation and Purification of MJ1585 Encoded Protein. Isolation of non His-tag protein was performed by suspending the frozen *E. coli* cell pellet (harboring pMJ1585) (~0.4 g wet weight from 200 mL of medium) in 3 mL of extraction buffer (50 mM *N*-[tris(hydroxymethyl)methyl]-2-aminoethanesulfonic acid (TES), pH 7.0, 10 mM $MgCl_2$, 20 mM DTT) and lysed by sonication followed by centrifugation (16,000*g* for 10 min). The MJ1585 coded protein was found not to remain soluble at temperatures higher than 55 °C. The resulting cell extracts from sonication were heated for 10 min at 55 °C followed by centrifugation (16,000*g* for 10 min). This process allowed for denaturing a portion of *E. coli* proteins.

Purification of His-tagged protein was performed by suspending the frozen *E. coli* cell pellet (harboring pMJ1585-His) (~0.4 g wet weight from 200 mL of medium) in 3 mL of phosphate buffer (50 mM Na_2HPO_4, 300 mM NaCl, and 10 mM imidazole) pH 8.0 and lysed by sonication followed by centrifugation (16,000*g* for 10 min). Nickel resin, Ni-NTA agarose (Qiagen) (~600 μL) was washed by phosphate buffer and combined with the soluble fraction of sonicated cells (about 4 mL) in a 15 mL plastic centrifuge tube. The tube was placed on ice on an orbital shaker for 30 min. The resin was then packed in a glass pipette and washed with phosphate buffer (2 mL). A step gradient of phosphate buffer with 20 and 500 mM imidazole was used to elute the protein. Three mL of buffer with 20 mM imidazole and 2 mL of buffer with 500 mM imidazole were added respectively and fractions of 1 mL were collected. Purification of MJ1585 coded protein was confirmed by SDS-PAGE and MS of the band in the SGS-PAGE.

Functional Complementation Experiments. The standard heat-shock *E. coli* competent cell protocol was followed to make competent cells of *E. coli folB*::kan. Briefly, the folB::Kan JW3030-2 strain was from the Keio collection (*13*) was streaked onto a LB plate containing 50 μg/mL kanamycin. One single colony was picked and used to inoculate a 5 mL LBK (LB media

with 50 μg/mL kanamycin) medium. The culture was grown overnight at 37 °C with shaking at 250 rpm. The next day 50 mL LBK was inoculated with 100 μL overnight culture and grown until they reached an absorbance of 0.6 at 600 nm. The culture was then centrifuge at 3000rpm for 5 min at 4 °C. The cells were resuspended by 25 mL ice-cold 100 mM $CaCl_2$ followed by incubation on ice for 12 min. Recentrifugation of the cells was followed by resuspending cells in 5 mL mixed ice-cold 100 mM $CaCl_2$ and 15% glycerol. Aliquots of 100 μL were transfer into microfuge tubes and quickly droped into liquid nitrogen. The competent cells were stored at -80 °C.

E. coli strain Roseltta Blue (DE 3) pLysS was used to purify its rare codon plasmid (pRARE). The QIA Prep Spin Miniprep kit using a microcentrifuge procedure was used to purify the plasmid (QIAGEN). The rare-codon plasmid which contains a chloramphenicol resistance gene was transformed into *folB*::kan competent cells as described in Chapter 2. The cells were plated on LBCK (LB with 50 μg/mL kanamycin and chloramphenicol) plates. Single colonies were picked and used to make competent cells as described above. The pMJ1585-His was then transformed to the *folB*::kan/pRARE competent cells.

E. coli folB deletant cells were transformed with PET-19b plasmid containing the MJ1585 gene, pET19b-MJ1585. The same *E. coli* cells without pET19b plasmid were used as a control. Complementation experiments were performed by streaking either transformed cells or control cells on M9 minimal media plates containing appropriate antibiotics and plus/minus IPTG. Plates were incubated for two days at 37 °C.

5.4 RESULTS AND DISCUSSION

DHNA is a key enzyme in biosynthesis of tetrahydrofolate and tetrahydromethanopterin. The conversion of H_2neopterin to H_2HMP is catalyzed by DHNA. We have no data to confirm glycolaldehyde as the other product. Although in some organisms like *P. palciparum*, the substrate (H_2neopterin-3'triphosphate) and the enzyme (PTPS III) involved in this step are different from known DHNA in bacteria, the reaction (aldol reaction) and the H_2HMP product is the same.

Despite the fact that methanogens biosynthesize H_4MPT *de novo* and their cells readily utilize GTP and convert it to 6-HMDHT, a full review of the annotated genome of methanogenic archaea revealed an absence of homologs of genes involved in biosynthesis of the pterin ring of H_4folate in bacteria. The work in our laboratory has answered some of those questions by identifying MptA and MptB, which converts GTP to H_2N-cP and H_2N-2'P (3'P), respectively (*4, 5*).

There were no gene leads to finding the DHNA based on sequence similarity. One approach to identify this enzyme was to isolate it from *M. jannaschii* cell extract. This approach was attempted several times in our laboratory over the last 6 years. Several columns including MonoQ, size exclusion, and hydroxyapatite (CHT) were used. DHNA was tracked by its activity following incubation of the fractions from each column with substrate (H_2neopterin). HPLC with a C18 reverse-phase column and a fluorescence detector set at excitation and emission wavelength of pterins was used to separate and detect the substrate and product. Every time this approach was tried it failed. The major reason was due to loss of aldolase activity. This could be due to either spreading the enzyme into so many fractions, which occurred with the hydroxyapatite column, and/or instability of the protein(s).

Comparison of the SDS-PAGE pictures of fractions eluted from each column identified two protein bands with elution patterns that were consistent with the measured aldolase activity. Electrospray mass spectroscopy (ES-MS) of the protein bands (~29 and 35 kD) and the area between those bands, which was done at University of Virginia, resulted in an extensive list of proteins (Table 5.1). Some of these proteins were already characterized (highlighted in green and referenced). Some were annotated for known reactions that are not similar to an aldol reaction (Table 5.1, highlighted in yellow). The remainders were hypothetical proteins (Table 5.1, not highlighted). After some basic sequence analysis and secondary structure prediction, some of the proteins (MJ0054, MJ0144, MJ0227, and MJ1251) were selected to test for aldolase activity. The genes were amplified and heterologously expressed in *E. coli*. The expressed proteins (purified if it was possible, if not crude extract) were tested for aldolase activity. No H_2neopterin aldolase was detected with any of these proteins.

It is very likely that DHNA purified from *M. jannaschii* cell extract is not visible on SDS gel because of the low concentration of the protein in the cell. To overcome this problem, I used more of the *M. jannaschii* cells (5 g) and repeated the purification. Q-Sepharose was the first

column used after sonicating the cells, as it was used by other groups to purify multiprotein complexes (*10*). The eight most active fractions were combined and concentrated to apply to the next column, a MonoQ with TES buffer pH 7.2. The four most active fractions from MonoQ were combined and concentrated to apply to the same MonoQ column equilibrated with TES buffer pH 8. The three most active fractions from the second MonoQ were mixed and concentrated to apply to a Superose 12 size exclusion column. The most active fractions eluted from each column were analyzed by SDS-PAGE (Fig. 5.3). We were able to identify two protein bands in SDS-PAGE with elution patterns that were consistent with the measured activity in the corresponding fractions (Fig. 5.3, showed by stars). The obtained ES-MS data showed that the upper band is elongation factor (MJ0324) and lower band consists of at least two proteins, MJ0801 and biotin synthetase (MJ0785). MJ0785 is not characterized but it is annotated as a biotin synthetase and is belong to a radical SAM family of proteins. I did not test the activity of MJ0801 encoded protein because it is a *M. jannaschii* specific protein, and is not present in any other sequenced genomes. No further work was done on these proteins.

Concurrent with the attempts to purify DHNA from *M. jannaschii*, a bioinformatics approach was also applied to try and identify the enzyme. By using the STRING (functional protein association networks) website I searched for the genes that are linked to those genes, MJ0775 (MptA), MJ0837 (MptB), MJ1427, and MJ0107 in *M. jannaschii* or any other archaea. These genes are involved in H_4MPT biosynthesis. I targeted 5 hypothetical proteins encoded by MJ0778, MJ0227, MJ0807, MJ0107, and MJ1099 that were genomically associated with those genes involved in methanopterin biosynthesis. After overexpression they were tested for aldolase activity. No H_2neopterin aldolase was detected with these proteins.

In a third approach to identify the archaeal DHNA the KEGG database was used to search for all the aldolase encoding genes in the *M. jannaschii* genome. The sequence of one member of each aldolase class was blasted against *M. jannaschii* proteins. *M. jannaschii* only had about ten proteins with primary sequence similarity to any of the forty different known aldolases that have been reported in the literature. In some cases the sequence similarity was as low as 20% to known aldolases. Several of the proteins in this list are characterized (Table 5.2, highlighted in green and referenced), some are annotated to catalyze known reactions (Table 5.2, highlighted in yellow), and one is unknown (Table 5.2, not highlighted). Among these proteins I chose MJ1585 for testing because it was annotated as an aldolase (STRING website) but the

substrate was not known. MJ1585 was heterologously expressed in *E. coli*. Temperature stability assays on sonicated cells showed that MJ1585 coded protein is not stable above 55 °C. The soluble fraction of sonicated *E. coli* cells expressing MJ1585 was incubated with H_2neopterin as substrate under Ar to keep the substrate reduced. The soluble fraction of sonicated *E. coli* cells expressing MJ0107 (a non relevant gene) was used as a control. The control was needed because *E. coli* cells possess DHNA, which is stable even at high temperatures (5 min in 100 °C) (*14*). The preliminary data showed that MJ1585 sample has much more activity compared to the control (background activity) (Fig. 5.4, A). A Ni-affinity column was used to purify the MJ1585 with the His-tag. MJ1585-His was eluted at 500 mM imidazole (Fig. 5.5). The purified protein produced two bands on a SDS-polyacrylamide gel. Based on ES-MS analysis, both upper and lower bands (Fig. 5.5, shown with star) from the purified fraction are the same (MJ1585 gene product). Activity assays of purified fraction show lots of DHNA activity but the product peak coelutes with a big hump. This fluorescent hump is caused by a complex that is formed between imidazole and iodine, which was used at the end of the incubation to oxidize product and remaining substrate. High concentration of imidazole also makes the MJ1585 gene product very unstable. The protein precipitated after only one day of storage at -4 °C. Other methods, like applying the Halo-tag, which is reported to help expression and purification of proteins, should be tested to try to improve protein stability. By having pure and stable MJ1585 protein more assays can be performed to do kinetics.

In another experiment, the plasmid containing MJ1585 (pMJ1585) was transformed into *E. coli folB*::kan cells to determine if MJ1585 can compliment the lack of *folB* gene, which codes for DHNA. The rare codon plasmid (pRARE) was also transformed into these cells due to the identification of several codons in MJ1585 gene that are not commonly used in *E. coli*. *E. coli folB*::kan with rare codon plasmid but not pMJ1585 was used as a control. Both transformed cells were plated on M9 minimal media plates with and without adding IPTG to induce expression of MJ1585. As shown in Figure 5.6 much more cells growth was seen when they harbor pMJ1585 in both added or not added IPTG.

Since H_4folate is an essential coenzyme for the cells and the most important reaction that requires this coenzyme, as a methyl transfer coenzyme is methylation of dUMP (2'-deoxyuridine-5'-phosphate) to dTMP (2'-deoxythymidine-5'-phosphate), it was expected that *E. coli folB*::kan will not grow on M9 minimal salt plates that does not supply with thymidine or

folate. To our surprise *E. coli* deletante cells grow some under this conditions, which shows that maybe *E. coli* has other genes that can catalyze the same reaction to keep the cell alive. However the complementation experiment result clearly shows that *E. coli* deletant cells have better growth by harboring the pMJ1585 (Fig. 5.6). This demonstrates that the MJ1585 gene product is able to restore folate biosynthesis in the Δ*folB* cell line. Also, results from another complementation experiment which folate was added to the M9 plates for both control and sample cells showed similar growth for both (data not shown).

MJ1585 encoded protein is annotated as an unknown aldolase. The C-terminal half of this protein has about 40% similarity to MJ0400 encoded protein which is characterized to have two functions, transaldolase and fructose-1,6-bisphosphate aldolase (*15, 16*). Activity of MJ0400 as a transaldolase on 6-deoxy-5-ketofructose-1-phosphate and L-aspartate semialdehyde produces a compound that is precursor for dihydroshikimate. The MJ1585 gene product should also be tested for F-1,6-bisphosphate aldolase activity.

To complete this work we need to produce more stable protein to work so we can characterize this aldolase. One solution might be using Halo-tag, which is clamed to cause more overexpressed protein. Also Halo-tag makes a covalent bond with the resin, which helps specifically purifying the overexpressed protein. Also homologs of MJ1585 from other methanogens can be used.

5.5 FIGURES AND TABLES

Table 5.1 The proteins identified from SDS-PAGE.

The characterized proteins are highlighted in green. The annotated proteins to known functions are highlighted in yellow. Uncharacterized proteins are not highlighted.

protein	Function	Ref.
MJ0004	2-Hydroxyglutaryl-CoA dehydratase activator	
MJ0044	IP kinase	(*17*)
MJ0054	Uncharacterized protein	
MJ0089	Putative ABC transporter permease protein	
MJ0144	FMN-binding hypothetical protein	
MJ0148	Probable tRNA pseudouridine synthase B	
MJ0179	50S ribosomal protein L2P	
MJ0186	Bifunctional ornithine acetyltransferase/N-acetylglutamate synthase protein	
MJ0188	Inosine-5'-monophosphate dehydrogenase, putative	
MJ0227	Probable acetolactate synthase large subunit	
MJ0286	Uncharacterized protein	
MJ0324	Elongation factor 1-alpha	
MJ0331	Uncharacterized protein	
MJ0501	Uncharacterized protein	
MJ0517	Uncharacterized protein	
MJ0637	Prephenate dehydratase	
MJ0671	Pyrimidine nucleotide reductase	(*18*)
MJ0734	Putative rubrerythrin	
MJ0737	Rubredoxin-like non-heme iron protein	
MJ0747	Bacteriohemerythrin; Oxygen-binding protein	
MJ0761	Uncharacterized deoxyribonuclease	
MJ0816	Uncharacterized protein	
MJ0831	Single-strand DNase	(*19*)
MJ0885	DNA dependent DNA polymerase B1	(*20*)
MJ0915	Probable L-aspartate dehydrogenase	
MJ0963	Hydantoin utilization protein B	
MJ0965	Uroporphyrinogen-III C-methyltransferase	
MJ0967	Uncharacterized protein	
MJ1038	Tryptophan synthase alpha chain	
MJ1059	Capsular polysaccharide biosynthsis protein M	
MJ1087	Mevalonate kinase	
MJ1123	Uncharacterized protein	
MJ1187	Dinitrogenase reductase activating glycohydrolase	
MJ1226	Putative cation-transporting ATPase	

MJ1236	Putative mRNA 3'-end processing factor 2	
MJ1251	Uncharacterized protein	
MJ1322	DNA double-strand break repair rad50 ATPase	
MJ1341	Uncharacterized protein	
MJ1350	Formylmethanofuran dehydrogenase, subunt C	
MJ1378	Carbamoyl-phosphate synthase large chain, N-terminal section	
MJ1427	β-RFA-P synthase	(*21*)
MJ1430	Phosphoribosyl-AMP cyclohydrolase/phosphoribosyl-ATP pyrophosphohydrolase	
MJ1465	Probable threonine synthase	
MJ1578	Probable cobalt-precorrin-4 C(11)-methyltransferase	
MJ1594	Phosphoserine phosphatase	(*22*)
MJ1598	Uncharacterized protein	
MJ1607	Uncharacterized glycosyltransferase	

Table 5.2 The proteins identified in aldolase primary sequence search.

The characterized proteins are highlighted in green. The annotated proteins for known functions are highlighted in yellow but their activity is not proven. Uncharacterized proteins are not highlighted.

Protein	Function	Ref.
MJ0400	Fructose-1,6-bisphosphate aldolase, transaldolase	(*15, 16*)
MJ1585	Uncharacterized aldolase	
MJ1038	Tryptophan synthase alpha chain	
MJ0256	Sulfopyruvate decarboxylase subunit beta	(*23*)
MJ1418	Fuculose-1-phosphate aldolase	(*24*)
MJ0633	Leucyl-tRNA synthetase	
MJ0244	Dihydrodipicolinate synthase	
MJ0277	Probable acetolactate synthase large subunit	
MJ0644	S-adenosylmethionine-2-demethylmenaquinone methyltransferase	
MJ0960	Transaldolase	(*25*)

A

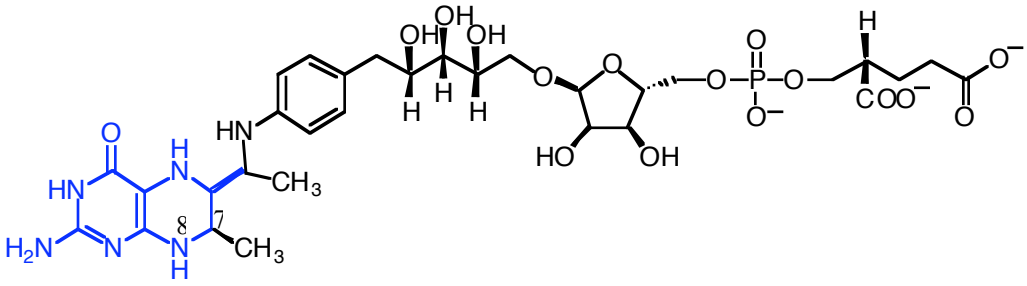

B

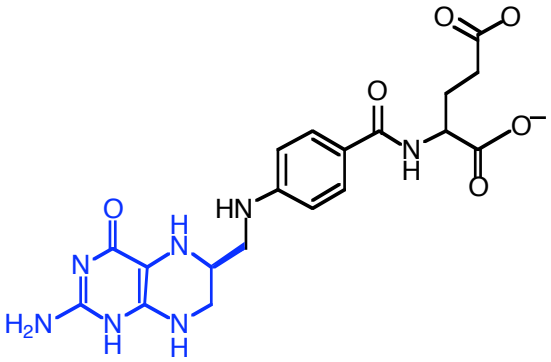

Figure 5.1. Structures of the reduced form of (A) methanopterin and (B) folate.

The pterin ring (functional core) of both coenzymes is shown in blue.

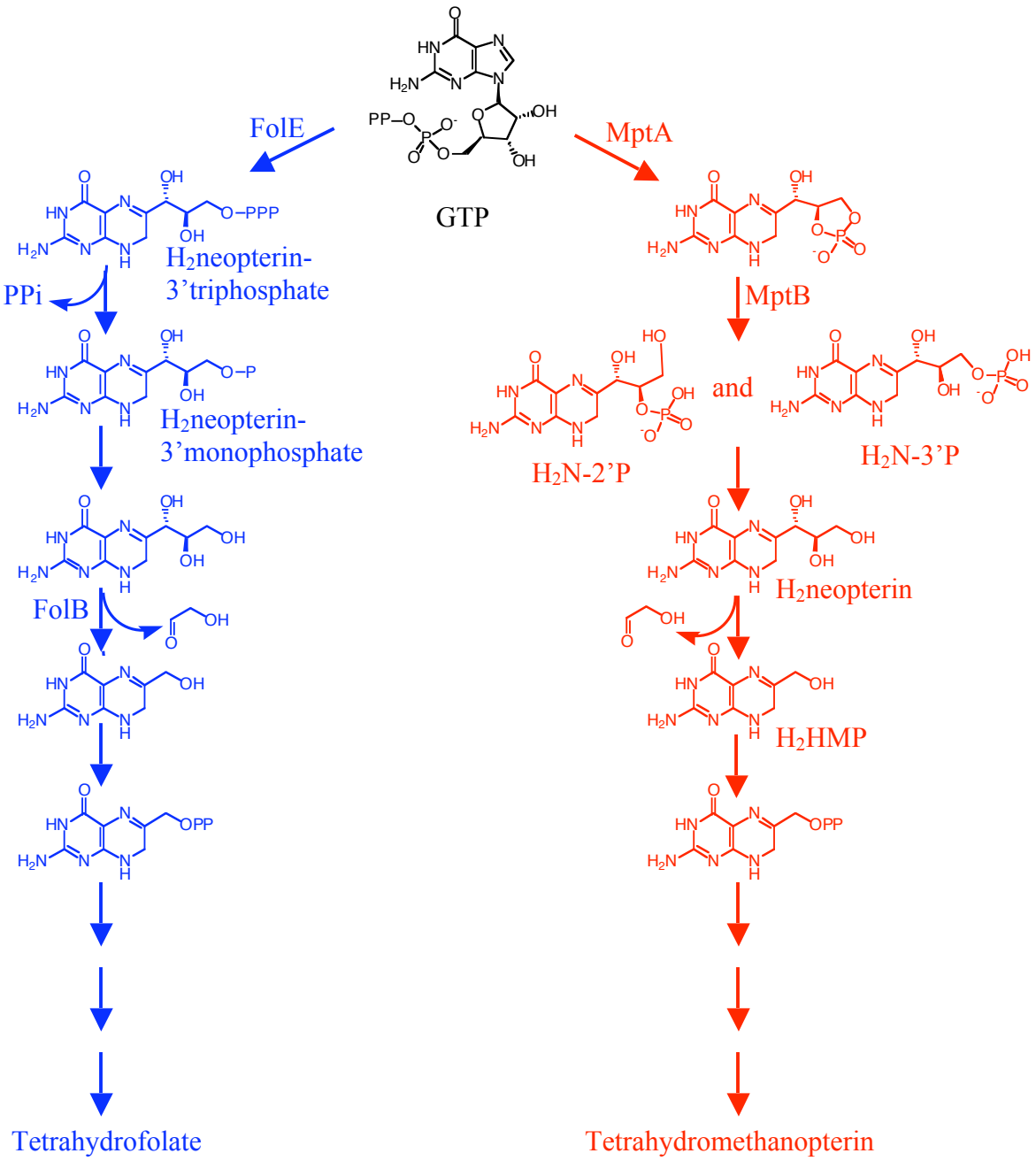

Figure 5.2. Pathways for the formation of the pterin ring in tetrahydrofolate (blue) and tetrahydromethanopterin (red) and subsequent conversion in to the final coenzymes.

A **B** **C**

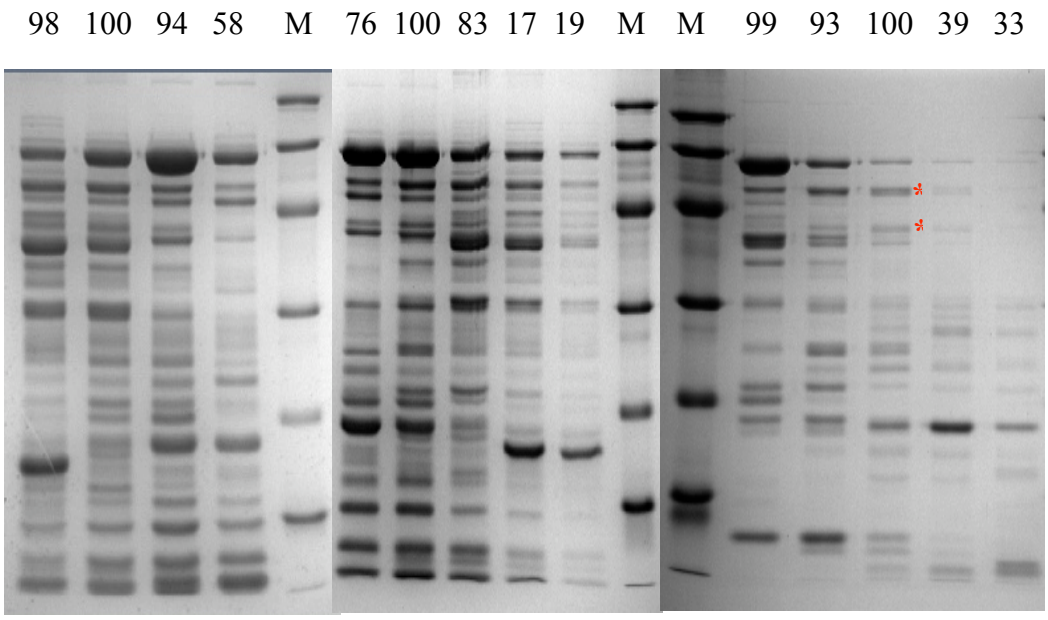

Figure 5.3 SDS-PAGE pictures of the fractions eluted from (A) MonoQ (pH 7.2), (B) MonoQ (pH 8), and (C) size exclusion chromatography columns.

In each gel picture marker lane in marked as M. The numbers on the top of each lane represent the relative activity of the respective fractions and are presented in percentage of maximum activity. Fractions in each gel are consecutive eluted fractions. ES-MS was done for the bands that are indicated with stars to the right of the bands.

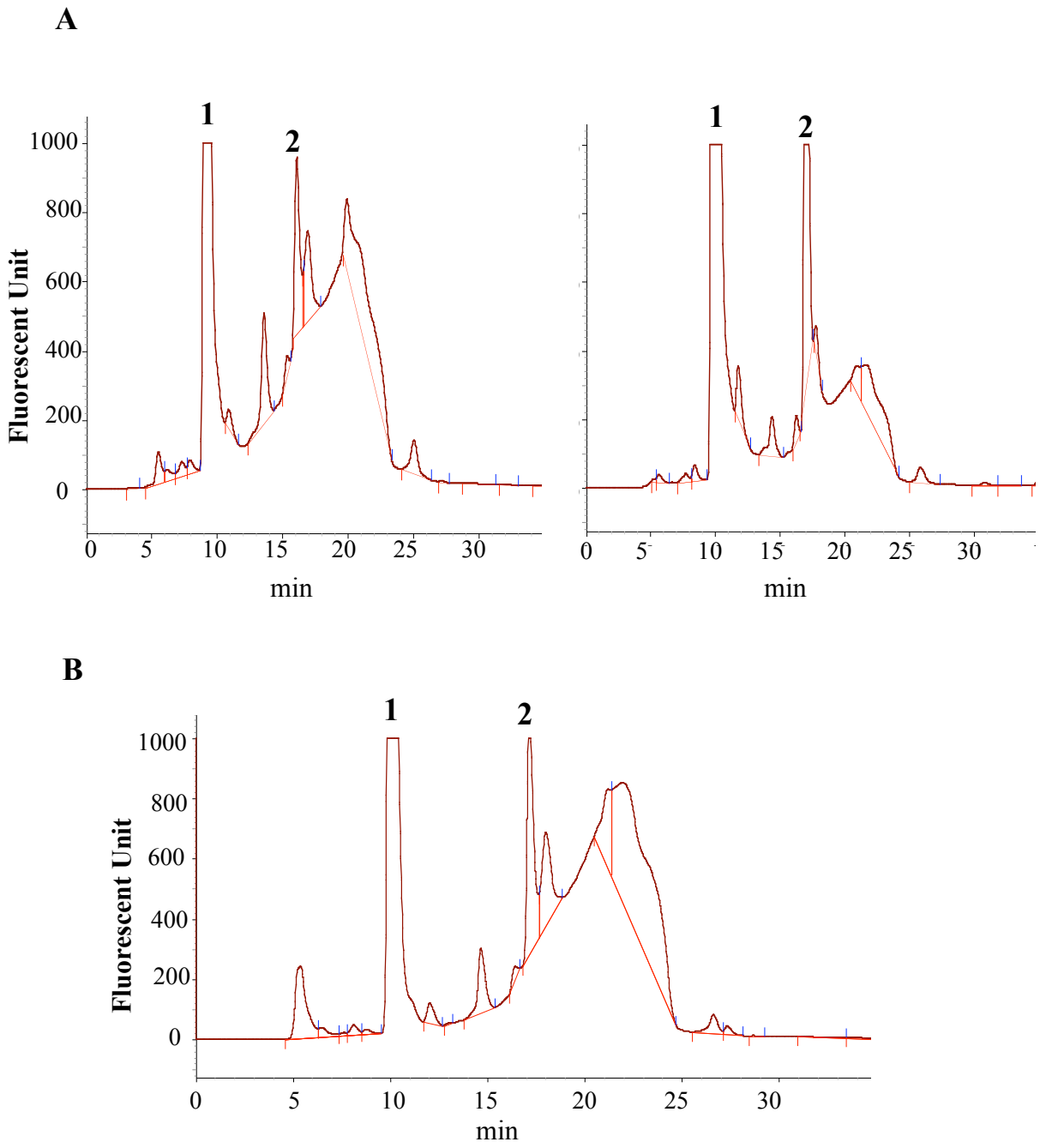

Figure 5.4 HPLC traces of the aldolase analysis assays.

(A) HPLC analysis after incubation H_2neopterin with sonicated *E. coli* cells extract that overexpressed either MJ0107, used as a control shown in the left trace or MJ1585 shown in the right trace. (B) HPLC analysis after incubation of H_2neopterin with purified His-tagged MJ1585 encoded protein. Oxidized substrate (neopterin) and oxidized product (hydroxymethylpterin) peaks are marked as 1 and 2, respectively.

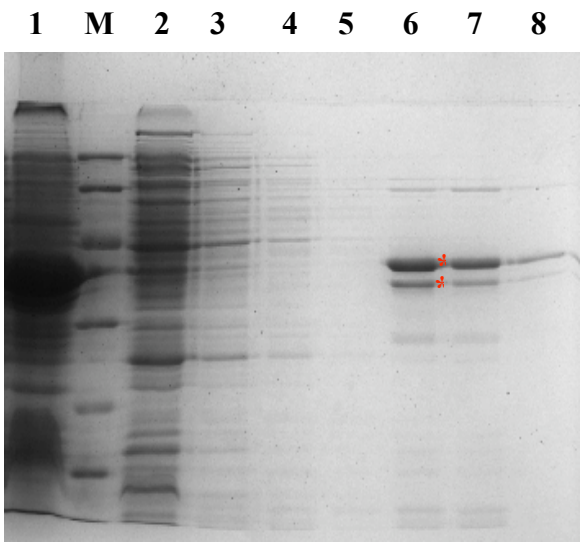

Figure 5.5 SDS-PAGE picture of the His-tagged MJ1585 fractions.

The lane with protein markers is marked as M. Pellet fraction after cell sonication is shown in lane 1. Flow through fraction, 3X wash with 20 mM imidazole, and 3X wash with 500 mM imidazole are in lanes 2, 3-5, and 6-8, respectively.

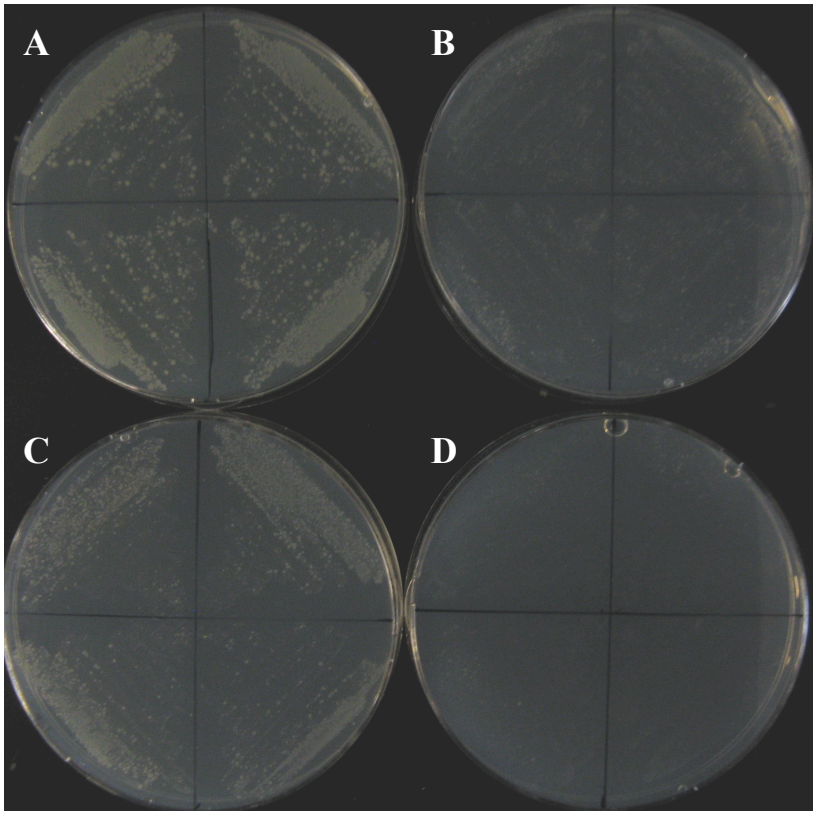

Figure 5.6 Functional complementation of the *E. coli folB* deletant by MJ1585 gene.

The *E. coli folB* deletant strain harboring either pRARE (B and D) or pRARE and pMJ1585 (A and C) on M9 minimal media plates with or without added IPTG, top (A and B) and bottom (C and D), respectively. Plates were incubated at 37 °C for two days.

REFERENCE

1. Escalante-Semerena, J. C., Rinehart, K. L., Jr., and Wolfe, R. S. (1984) Tetrahydromethanopterin, a carbon carrier in methanogenesis, *J. Biol. Chem. 259*, 9447-9455.
2. White, R. H. (1993) Structures of the modified folates in the thermophilic archaebacteria *Pyrococcus furiosus*, *Biochemistry 32*, 745-753.
3. Delle Fratte, S., White, R. H., Maras, B., Bossa, F., and Schirch, V. (1997) Purification and properties of serine hydroxymethyltransferase from *Sulfolobus solfataricus*, *J. Bacteriol. 179*, 7456-7461.
4. Mashhadi, Z., Xu, H., and White, R. H. (2009) An Fe2+-dependent cyclic phosphodiesterase catalyzes the hydrolysis of 7,8-dihydro-D-neopterin 2',3'-cyclic phosphate in methanopterin biosynthesis, *Biochemistry 48*, 9384-9392.
5. Grochowski, L. L., Xu, H., Leung, K., and White, R. H. (2007) Characterization of an Fe^{2+}-dependent archaeal-specific GTP cyclohydrolase, MptA, from *Methanocaldococcus jannaschii*, *Biochemistry 46*, 6658-6667.
6. Blaszczyk, J., Li, Y., Gan, J., Yan, H., and Ji, X. (2007) Structural basis for the aldolase and epimerase activities of *Staphylococcus aureus* dihydroneopterin aldolase, *J. Mol. Biol. 368*, 161-169.
7. Pribat, A., Jeanguenin, L., Lara-Nunez, A., Ziemak, M. J., Hyde, J. E., de Crecy-Lagard, V., and Hanson, A. D. (2009) 6-pyruvoyltetrahydropterin synthase paralogs replace the folate synthesis enzyme dihydroneopterin aldolase in diverse bacteria, *J. Bacteriol. 191*, 4158-4165.
8. Dittrich, S., Mitchell, S. L., Blagborough, A. M., Wang, Q., Wang, P., Sims, P. F., and Hyde, J. E. (2008) An atypical orthologue of 6-pyruvoyltetrahydropterin synthase can provide the missing link in the folate biosynthesis pathway of malaria parasites, *Mol. Microbiol. 67*, 609-618.
9. Graupner, M., Xu, H., and White, R. H. (2002) New class of IMP cyclohydrolases in *Methanococcus jannaschii*, *J. Bacteriol. 184*, 1471-1473.
10. Menon, A. L., Poole, F. L., 2nd, Cvetkovic, A., Trauger, S. A., Kalisiak, E., Scott, J. W., Shanmukh, S., Praissman, J., Jenney, F. E., Jr., Wikoff, W. R., Apon, J. V., Siuzdak, G., and Adams, M. W. (2009) Novel multiprotein complexes identified in the hyperthermophilic archaeon *Pyrococcus furiosus* by non-denaturing fractionation of the native proteome, *Mol. Cell. Proteomics 8*, 735-751.
11. Mukhopadhyay, B., Johnson, E. F., and Wolfe, R. S. (1999) Reactor-scale cultivation of the hyperthermophilic methanarchaeon *Methanococcus jannaschii* to high cell densities, *Appl. Environ. Microbiol. 65*, 5059-5065.
12. Bult, C. J., White, O., Olsen, G. J., Zhou, L., Fleischmann, R. D., Sutton, G. G., Blake, J. A., FitzGerald, L. M., Clayton, R. A., Gocayne, J. D., Kerlavage, A. R., Dougherty, B. A., Tomb, J. F., Adams, M. D., Reich, C. I., Overbeek, R., Kirkness, E. F., Weinstock, K. G., Merrick, J. M., Glodek, A., Scott, J. L., Geoghagen, N. S., and Venter, J. C. (1996) Complete genome sequence of the methanogenic archaeon, *Methanococcus jannaschii*, *Science 273*, 1058-1073.
13. Baba, T., Ara, T., Hasegawa, M., Takai, Y., Okumura, Y., Baba, M., Datsenko, K. A., Tomita, M., Wanner, B. L., and Mori, H. (2006) Construction of *Escherichia coli* K-12

in-frame, single-gene knockout mutants: the Keio collection, *Mol. Syst. Biol. 2*, 2006 0008.
14. Mathis, J. B., and Brown, G. M. (1970) The biosynthesis of folic acid. XI. Purification and properties of dihydroneopterin aldolase, *J. Biol. Chem. 245*, 3015-3025.
15. White, R. H. (2004) L-Aspartate semialdehyde and a 6-deoxy-5-ketohexose 1-phosphate are the precursors to the aromatic amino acids in *Methanocaldococcus jannaschii*, *Biochemistry 43*, 7618-7627.
16. Samland, A. K., Wang, M., and Sprenger, G. A. (2008) MJ0400 from *Methanocaldococcus jannaschii* exhibits fructose-1,6-bisphosphate aldolase activity, *FEMS Microbiol Lett 281*, 36-41.
17. Grochowski, L. L., Xu, H., and White, R. H. (2006) *Methanocaldococcus jannaschii* uses a modified mevalonate pathway for biosynthesis of isopentenyl diphosphate, *J. Bacteriol. 188*, 3192-3198.
18. Graupner, M., Xu, H., and White, R. H. (2002) The pyrimidine nucleotide reductase step in riboflavin and F_{420} biosynthesis in archaea proceeds by the eukaryotic route to riboflavin, *J. Bacteriol. 184*, 1952-1957.
19. Rajman, L. A., and Lovett, S. T. (2000) A thermostable single-strand DNase from *Methanococcus jannaschii* related to the RecJ recombination and repair exonuclease from *Escherichia coli*, *J. Bacteriol. 182*, 607-612.
20. Zhu, W., Reich, C. I., Olsen, G. J., Giometti, C. S., and Yates, J. R., 3rd. (2004) Shotgun proteomics of *Methanococcus jannaschii* and insights into methanogenesis, *J. Proteome Res. 3*, 538-548.
21. Scott, J. W., and Rasche, M. E. (2002) Purification, overproduction, and partial characterization of _-RFAP synthase, a key enzyme in the methanopterin biosynthesis pathway, *J. Bacteriol. 184*, 4442-4448.
22. Andronesi, O. C., Pfeifer, J. R., Al-Momani, L., Ozdirekcan, S., Rijkers, D. T., Angerstein, B., Luca, S., Koert, U., Killian, J. A., and Baldus, M. (2004) Probing membrane protein orientation and structure using fast magic-angle-spinning solid-state NMR, *J. Biomol. NMR 30*, 253-265.
23. Krum, J. G., and Ensign, S. A. (2001) Evidence that a linear megaplasmid encodes enzymes of aliphatic alkene and epoxide metabolism and coenzyme M (2-mercaptoethanesulfonate) biosynthesis in Xanthobacter strain Py2, *J. Bacteriol. 183*, 2172-2177.
24. Grochowski, L. L., Xu, H., and White, R. H. (2006) Identification of lactaldehyde dehydrogenase in *Methanocaldococcus jannaschii* and its involvement in production of lactate for F_{420} biosynthesis, *J. Bacteriol. 188*, 2836-2844.
25. Soderberg, T., and Alver, R. C. (2004) Transaldolase of *Methanocaldococcus jannaschii*, *Archaea 1*, 255-262.

CHAPTER 6

Conclusions and Outlook

Studying the biosynthetic reactions in *M. jannaschii* as a model organism for methanogens is the focus in our lab. Methanogenesis is a key component of the global carbon cycle and methanogens produce an estimated 75-85% of all methane emissions (*1, 2*). Consequently, an understanding of the chemistry and biochemistry of methanogenic coenzymes is essential for our understanding of global carbon flux. Additionally, the encoded enzymes can function as specific drug targets in those few bacteria that produce them. *M. jannaschii* genome was the first archaeal genome sequenced in 1996 (*3*). The 1.66 Mbp complete genome sequence of this archaeon is predicted to encode about 1738 proteins. Only one-third of its genes were initially assigned a role with high confidence (*3*). The metabolism of *M. jannaschii,* as well as that of other methanogens has not been studied as extensively as that of other organisms. Even after the 14 years since the sequencing the *M. jannaschii* genome, this number have not changed significantly. Based on my search of the TIGR database about 58% of the *M. jannaschii* genes are annotated as hypothetical. A pie chart of *M. jannaschii* genome function is shown in Figure 6.1 (David Graham, unpublished data). The *M. jannaschii* genome sequence revealed that about 19% of the encoded proteins are archaeal specific (*4*). Identifying and characterizing these genes may lead to the discovery of new pathways and new biological functions different from what is already known. Most genes involved in biosynthesis of the methanogenic coenzymes are in archaeal specific group. For instance both GTP cyclohydrolase III (MJ0145) (*5*) and MptA (MJ0775) (*6*) are different from GTP cyclohydrolase I and II, which were known in bacteria (*7, 8*). Also modified pathways in biosynthesis of aromatic aminoacids and purine have been reported (*9, 10*). The rest of the genes are not archaeal specific, in another words they have wider distribution than just in the archaea. Study of this group of genes in a simpler organism like *M. jannaschii* will help to annotate the genes of higher and more complex forms of life such as plants and animals.

The genome of *M. jannaschii* includes the genetic information sufficient to maintain life on simple organic matters like hydrogen, CO_2 and some minerals, which makes this organism an

excellent model to study primitive metabolism. This microorganism is a hyperthermophile and its proteins are usually stable at higher temperatures (>70 °C), which make working with these proteins easier and thus more productive. To study the function of these proteins, they can be heterologosly overexpressed in *E. coli*. Heat stability of *M. jannaschii* protein is a big advantage for their purification. Typically a heating step of the *E. coli* cell extract at 70 °C or 80 °C follow by a MonoQ, result in 90 to 95% pure overexpressed protein which can be used in enzyme assays and crystallization for further structural analysis.

Another reason to study the methabolism of *M. jannaschii* is our desire to uncover the nature of the chemical reactions that were occurring in the oceans after the early earth's surface cooled down enough to have hot liquid oceans where life could evolve (>3.8 billion years). These chemical reactions would represent those prebiotic reactions that would have been specifically used in the first organism. There is very little or no detailed information of the chemistry involved remaining in the geological records. Study on the first organism that lived on earth is either difficult or impossible with current technologies. To identify these reactions, we must extrapolate back from present-day biochemistry by studying organisms that would be likely to still function with some of this original ancient anaerobe metabolism. The study of the origin of life is also made difficult since we do not know the exact nature of the first living system(s). But this first form of life, whatever it was, should be hypertermophilic and also should be able to sustain life only on simple organic compounds and minerals. It is clear that whatever the chemistry involved in the first organism was, it did not include the many pathways that are currently associated with living systems such as glycolysis or the citric acid cycle which are always used to extrapolate back to the Last Universal Common Ancestor (LUCA). Important examples of compounds in early life that reside in contemporary organisms would include all the different cofactors/coenzymes. Evidence that microbial methanogenesis is an ancient process continues to increase. Recent geochemical evidence from the carbon isotope analysis of methane trapped in quartz fluid inclusions supports the presence of the biological production of methane at >3.46 Gigayear (Gyr =10^9 years) ago in the Archaean era (*11*). This is supported by the fact that > 50% of the genes in archaeal genomes have no assigned function.

Work with *M. jannaschii* has uncovered several examples of previously unrecognized metabolism that give us new insights into primitive metabolism may look like (*12*). My work particularly discovered new enzymes involved in the biosynthesis of coenzymes,

tetrahydromethanopterin and FAD, in *M. jannaschii*. The research in our laboratory shows that in the archaea the first two enzymes used for the biosynthesis of methanopterin, MptA and MptB (Chapter 2), and the first two enzymes involved in coenzyme F_{420} and riboflavin biosynthesis, ArfA and ArfB, all begin from the nucleotide GTP and require Fe(II) to function (*5, 6, 13, 14*). The oxygenation of the atmosphere resulted in the loss of the soluble Fe(II) as insoluble Fe(III), and the green oceans became blue as we see them today. On the basis of the high availability of Fe(II) in these early oceans, the first reactions used for the cleavage of GTP or GTP-like molecules were likely Fe(II) dependent. Discoveries in our laboratory have more than doubled the number of known examples of enzymes using Fe(II) to carry out this type of hydrolytic reaction.

It has been shown that *M. jannaschii* utilizes modified pathways even for the biosynthesis of widely distributed coenzymes such as FMN and FAD from those known pathways in other organism. My discoveries in this pathway, identification of first example of CTP-dependent riboflavin kinase and also a novel air sensitive archaeal FAD synthetase, as part of my Ph.D. projects has emphasized this fact. In either case, methanogenic coenzymes or more common coenzymes, establishing the enzymes/genes involved in these pathways has and will continue to contribute to the assignment of gene function - an important endeavor in this post genomics age (*15*).

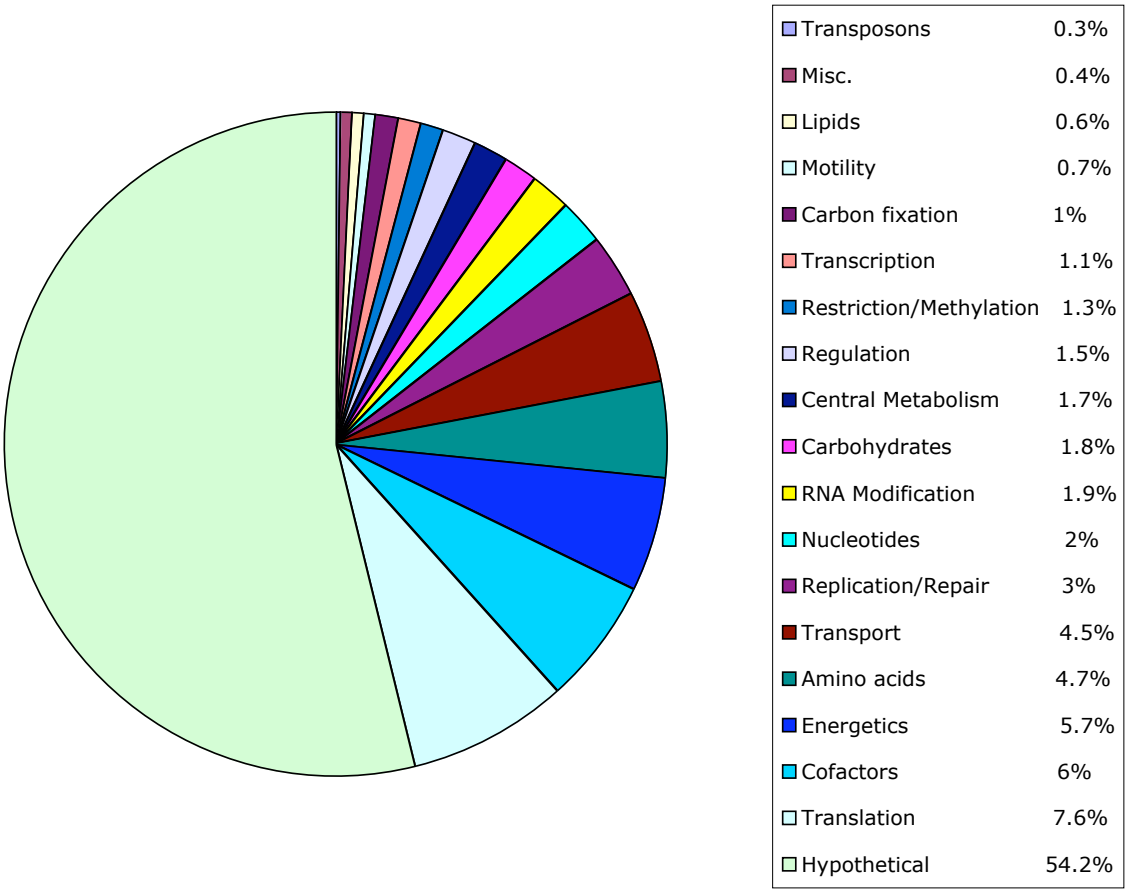

Figure 6.1 *M. jannaschii* gene functions.

The *M. jannaschii* genes that are predicted to produce protein (1738) are used to make this chart. Each slide of the pie represents genes that are involved in individual pathways or processes in the cell and they are color-coded. Indicated percentages are percentage of total genes.

REFERENCES

(1) Zinder, S. H. (1993) Physiological Ecology of Methanogens, in *Methanogenesis Ecology, Physiology, Biochemistry & Genetics* (Ferry, J. G., Ed.) pp 128-206, Chapman & Hall, New York.

(2) Fenchel, T., King, G. M., and Blackburn, T. H. (1988) *Bacterial Biogeochemistry The Ecophysiology of Mineral Cycling*, Academic Press, San Diego.

(3) Bult, C. J., White, O., Olsen, G. J., Zhou, L., Fleischmann, R. D., Sutton, G. G., Blake, J. A., FitzGerald, L. M., Clayton, R. A., Gocayne, J. D., Kerlavage, A. R., Dougherty, B. A., Tomb, J. F., Adams, M. D., Reich, C. I., Overbeek, R., Kirkness, E. F., Weinstock, K. G., Merrick, J. M., Glodek, A., Scott, J. L., Geoghagen, N. S., and Venter, J. C. (1996) Complete genome sequence of the methanogenic archaeon, *Methanococcus jannaschii*. *Science 273*, 1058-73.

(4) Graham, D. E., Overbeek, R., Olsen, G. J., and Woese, C. R. (2000) An archaeal genomic signature. *Proc. Natl. Acad. Sci. U S A 97*, 3304-8.

(5) Graham, D. E., Xu, H., and White, R. H. (2002) A member of a new class of GTP cyclohydrolases produces formylaminopyrimidine nucleotide monophosphates. *Biochemistry 41*, 15074-84.

(6) Grochowski, L. L., Xu, H., Leung, K., and White, R. H. (2007) Characterization of an Fe^{2+}-dependent archaeal-specific GTP cyclohydrolase, MptA, from *Methanocaldococcus jannaschii*. *Biochemistry 46*, 6658-67.

(7) Foor, F., and Brown, G. M. (1975) Purification and properties of guanosine triphosphate cyclohydrolase II from *Escherichia coli*. *J. Biol. Chem. 250*, 3545-51.

(8) Bracher, A., Eisenreich, W., Schramek, N., Ritz, H., Gotze, E., Herrmann, A., Gutlich, M., and Bacher, A. (1998) Biosynthesis of pteridines. NMR studies on the reaction mechanisms of GTP cyclohydrolase I, pyruvoyltetrahydropterin synthase, and sepiapterin reductase. *J. Biol. Chem. 273*, 28132-41.

(9) White, R. H. (2004) L-Aspartate semialdehyde and a 6-deoxy-5-ketohexose 1-phosphate are the precursors to the aromatic amino acids in *Methanocaldococcus jannaschii*. *Biochemistry 43*, 7618-27.

(10) Ownby, K., Xu, H., and White, R. H. (2005) A *Methanocaldococcus jannaschii* archaeal signature gene encodes for a 5-formaminoimidazole-4-carboxamide-1-_-D-ribofuranosyl 5'-monophosphate synthetase. A new enzyme in purine biosynthesis. *J. Biol. Chem. 280*, 10881-7.

(11) Ueno, Y., Yamada, K., Yoshida, N., Maruyama, S., and Isozaki, Y. (2006) Evidence from fluid inclusions for microbial methanogenesis in the early Archaean era. *Nature 440*, 516-9.

(12) Grochowski, L. L., and White, R. H. (2007) Promiscuous Anaerobes: New and Unconventional Metabolism in Methanogenic Archaea. *Ann. N. Y. Acad. Sci. 1125*, 190-214.

(13) Mashhadi, Z., Xu, H., and White, R. H. (2009) An Fe^{2+}-dependent cyclic phosphodiesterase catalyzes the hydrolysis of 7,8-dihydro-D-neopterin 2',3'-cyclic phosphate in methanopterin biosynthesis. *Biochemistry 48*, 9384-92.

(14) Grochowski, L. L., Xu, H., and White, R. H. (2009) An iron(II) dependent formamide hydrolase catalyzes the second step in the archaeal biosynthetic pathway to riboflavin and 7,8-didemethyl-8-hydroxy-5-deazariboflavin. *Biochemistry 48*, 4181-8.

(15) White, R. H. (2006) The Difficult Road from Sequence to Function. *J. Bacteriol. 188*, 3431-3432.